A COMPARATIVE STUDY OF LINEAR TECHNIQUES ACTIVE VIBRATION CONTROL H-INFINITY AND ADAPTIVE FILTERS ON A FLEXIBLE STRUCTURE OF ONE DEGREE OF FREEDOM

EFRAÍN GUILLERMO MARIOTTE PARRA B.Sc.

Dynamics, Control and Robotics, DicBOT Research Group

UNIVERSIDAD INDUSTRIAL DE SANTANDER
DEPARTMENT OF PHYSICAL-MECHANICAL ENGINEERING
MASTER OF MECHANICAL ENGINEERING
BUCARAMANGA
2015

A COMPARATIVE STUDY OF LINEAR TECHNIQUES ACTIVE VIBRATION CONTROL H-INFINITY AND ADAPTIVE FILTERS ON A FLEXIBLE STRUCTURE OF ONE DEGREE OF FREEDOM

EFRAíN GUILLERMO MARIOTTE PARRA, B.Sc.

Master Research Project

Submitted to the Graduate Committee of the School of Mechanical Engineering

Director JABID E. QUIROGA MÉNDEZ, M.Sc.

Co-Director CARLOS BORRÁS PINILLA, Ph.D.

Dynamics, Control and Robotics, DicBOT Research Group

UNIVERSIDAD INDUSTRIAL DE SANTANDER
DEPARTMENT OF PHYSICAL-MECHANICAL ENGINEERING
MASTER OF MECHANICAL ENGINEERING
BUCARAMANGA
2015

Dedicatory

To Pablo for being the engine of my relentless craving for life. Without you, I would not have any reason to do anything. To Heidy, for being my match. To my mother, for whom I always feel gratefulness for your unconditional love.

Acknowledgment

To Farides for helping me untangle the wires of ideas so that anyone can read this book. To Andres for his patience and unconditional support of a true friend. To Alvaro for being the best one and my friend.

CONTENTS

Page

LIST OF FIGURES

Page

LIST OF ANNEXES

ABSTRACT

TITLE: COMPARATIVE STUDY OF LINEAR TECHNIQUES ACTIVE VIBRATION CONTROL H-INFINITY AND ADAPTIVE FILTERS ON A FLEXIBLE STRUCTURE OF ONE DEGREE OF FREEDOM *

AUTHOR: EFRAÍN GUILLERMO MARIOTTE PARRA **

KEY WORDS: Active Vibration Control (AVC), Adaptive Control, Robust Control, Flexible Structure, Finite Impulse Response (FIR) filter, H_∞ and µ-synthesis Robust Controller, Filtered-x Least Mean Square (FxLMS), Recursive Least Square (RLS)

DESCRIPTION:

The present study compared the designs of controllers based on Robust Control and Adaptive Control methodologies applied in Active Vibration Control (AVC). The AVC systems were implemented in a three-cart plant. The comparison was performed using as a decision criterion the trade-off relationship between the generalization of the solution and the magnitude of the disturbance rejection against the computational cost and control effort.

The Robust H_∞ controller and the µ-synthesis Robust Controller were applied considering two parameters of uncertainty. The designed controllers were confronted using colored noise bandwidth. Simulations in Matlab environment showed an improved performance of Robust controller synthesized by the technique of mixed-µ.

Adaptive Control methodologies were used as an adaptive System Identification (SI) for every propagation path of each disturbance. The SI generated Finite Impulse Response (FIR) filters that modeled the dynamic responses of every path. Control simulations were performed on these models adopting feedforward and feedback filter designs. Filters were compared beneath periodic disturbances. Real time simulations in Matlab environment displayed more efficient results when using Recursive Least Square (RLS) filter.

The best controllers out of the comparisons carried out previously were confronted by changing the parameters of the plant: the bandwidth of the frequency response was increased.

Finally, the advantages of employing each controller are presented. As a result, the Adaptive Filter rejects better periodic disturbances than the Robust Controller, which rejects better non-periodic disturbances.

* Magister degree work
**Physical-Mechanical Engineering Department, School of Mechanical Engineering. Director: Jabid Quiroga Méndez M.Sc. Codirector: Carlos Borrás Pinilla PhD

RESUMEN

TÍTULO: ESTUDIO COMPARATIVO DE LAS TÉCNICAS LINEALES DE CONTROL ACTIVO DE VIBRACIONES H-INFINITO Y FILTROS ADAPTATIVOS PARA UNA ESTRUCTURA FLEXIBLE DE UN GRADO DE LIBERTAD*****

AUTOR: EFRAÍN GUILLERMO MARIOTTE PARRA ******

PALABRAS CLAVES: Control Activo de Vibraciones (Active Vibration Control, AVC), Control Adaptativo, Control Robusto, Estructura Flexible, Filtro de Respuesta Finita al impulso (Finite Impulse Response, FIR), Controlador H_∞ y μ-Synthesis, Mínimos cuadrados (*Least Mean Square*, LMS), *Recursive Least Square*, RLS.

DESCRIPCIÓN:

En el presente estudio se compararon los diseños de los controladores basados en las metodologías de Control Robusto y de Control Adaptativo aplicado al Control Activo de Vibración (AVC). EL sistema AVC fue implementado en una planta de tres masas con un grado de libertad. La comparación se realizó utilizando como criterio de decisión la relación de trade-off entre la generalización de la solución y la magnitud del rechazo de las perturbaciones contra el costo de cálculo y el esfuerzo en el control aplicado.

Los Controladores Robustos H_∞ y μ-sintetizado son diseñados considerando incertidumbres paramétricas. Dichos controladores se contrastaron usando ruido coloreado. Las simulaciones realizadas el ambiente de Matlab muestran mejor rendimiento al controlador robusto sintetizado usando la técnica mixed-μ.

Se aplicó la metodología de Control Adaptativo para realizar Identificación del Sistema (SI) en cada camino de propagación de las perturbaciones estudiadas. La identificación del Sistema configuró filtros de Respuesta Finita al Impulso (FIR) que modelaron las respuestas dinámicas de dichos caminos. Las simulaciones fueron realizadas usando diseños de filtros en Feedforward y Feedback. Los Filtros fueron comparados empleando perturbaciones periódicas. Simulaciones en tiempo real en el ambiente de Matlab mostraron mejores resultados al filtro RLS.

Los controladores resultantes de cada comparación previamente realizada se contrastaron aplicándolos a la planta con un ancho de banda más grande. Finalmente, las ventajas de emplear cada controlador son expuestas. Como resultado, Filtro Adaptativo rechaza mejor perturbaciones periódicas que el Controlador Robusto, el cual rechaza mejor las perturbaciones no-periódicas

* Proyecto de grado de Maestría

** Facultad de Ingenierías Físico-Mecánicas, Escuela de Ingeniería Mecánica. Director: M.Sc. Jabid Quiroga Méndez., Codirector: PhD Carlos Borrás Pinilla.

INTRODUCTION

Nowadays, the problem of acoustic noise is more evident as the number of machines (engines, turbines, fans and compressors) increases in the transportation and manufacturing industries. This noise is generated by vibrations of flexible structures. Those machines' perpetual movements generate periodic vibrations. There are two ways to eliminate this noise: through canceling the vibration with a robust flexible structure or by placing acoustic actuators. A strong relationship between these two methods is denoted in order to present an unified solution. The traditional way of damping vibration is passive by using mufflers or dampers. These elements tend to increase the rigidity of the structure by decreasing the cutoff frequency of the plant, thus eliminating the vibration to the range of "high frequency"; however, they are robust, costly or ineffective in many cases at "low frequencies", where it is possible the operating point of the machine can be located.

Active Vibration Control (AVC) uses an electromechanical or electroacoustic system which cancels the unwanted emissions, such as the accelerations resulting from positioning servo system, based on the principle of superposition of waves. Specifically, a secondary vibration of equal magnitude is produced in opposite phase, which is added to the first vibration canceling the initial one. These systems are developed to increase the precision in measurement and manufacturing systems, to promote technologies that require it, as in the case of lab-on-a-chip technology. In general, this type of positioning mechanism systems have several degrees of freedom creating mixed accelerations with amplitudes and frequencies varying in time (changing operating points), making such systems difficult to control. Adaptive methods provide a greater range of frequencies to be controlled. The problem of vibration control is delimited to low frequency ranges where the system behaves linearly and simulation is still valid. It is necessary, since the control system behaves based on the simulation of the actual model. If the simulation does not have the same response as the real model, the control will not be the appropriated one.

Figure 1. Scheme of a positioning servo system (Robotic arm)

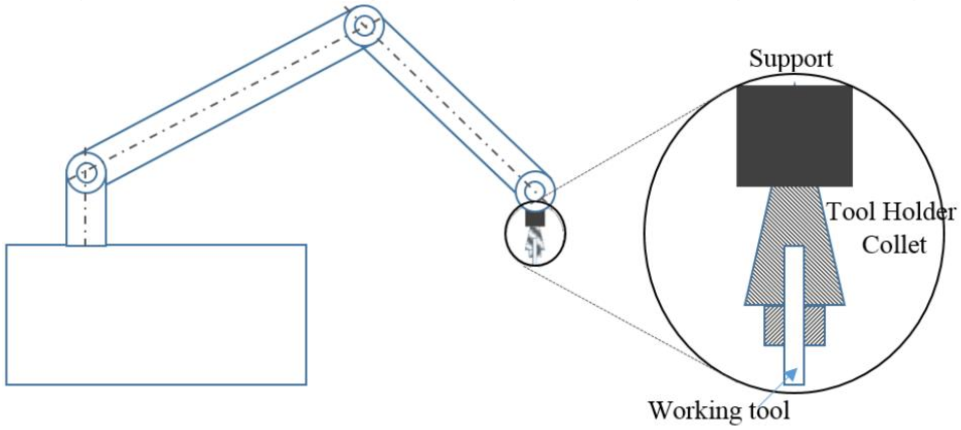

This investigation was proposed to solve the AVC linear problem, which is applicable to electromechanical systems for high precision positioning with several degrees of freedom. The types of accelerations at the end of the positioning mechanism are observed as periodic vibrations caused by the servo motors oscillation frequencies; impulsive acceleration due to changes of direction in the positioning without slowing; and non-periodic vibrations, simulated as white noise caused by agents external to the operation of the machine and the sensor noise of the control system. The case study of this investigation is the model of an AVC system at the end of the chain of servo systems, where it performs the main operation of the machine, as shown in

Figure 1. Firstly, the AVC system will observe all accelerations previously raised. Finally, it will reject these disturbances in order to not affect the activity of the machine. The AVC system is a structure of one Degree of Freedom (DOF) to facilitate simulation. The structure consists of one mass connected to the reference framework by springs, modeled as a spring and damper system in parallel, the scheme is shown in figure 2.

Figure 2. Scheme of the studied Plant

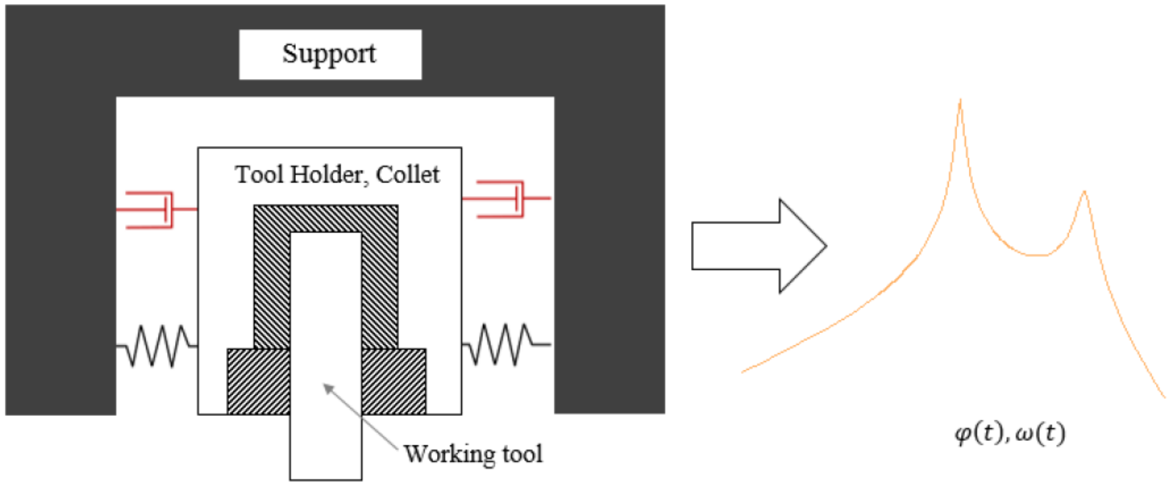

The disturbance rejection is an application of both, the Robust Control and the Adaptive Control using electromechanical systems. In the case of Robust Control “worst-case” principle is used. The H-infinity norm, that is the maximum possible amplitude value for a given disturbance in the system, was implemented to find an objective function so minimize both, the maximum amplitude value and the use of control, to reject this disturbance. Unlike Feedback control, the Robust Control design process does not required a precise knowledge about the Plant. This gives the versatility to control the plant under various operating points within a preset range allowed in the design. The uncertainties may be caused whether by the linearization of the model or by the uncertain values of the Plant parameters. The design of the ∞-norm can be posed as an optimization problem using the system ∞-norm as a cost function. The ∞-norm is the “worst-case” gain of the system and therefore provides a favorable match to engineering specifications, which are typically given in terms of bounds on errors and controls. The small-gain theorem states that, for unstructured perturbation, robust stability depends on the ∞-norm of the closed loop system from the perturbation input to the perturbation output. The minimization of the closed loop ∞-norm, therefore, can also be used as a means of maximizing robustness [10].

For Adaptive Control Filter design, there are more uncertainties about the possible operating points of the Plant. This is why; it is looked for the controller to be more autonomous due to possible drastic changes in the lifetime of the machine. To solve this, the control system was designed with a System Identification of the Plant. This system used also an Adaptive Filter to pull out the filter modeling of the Plant through the use of white noise. The Adaptive Filter algorithm seeks to reduce the error between the reference signal, the disturbance to be rejected, and the signal generated for the task. Linear algorithms such as LMS (Least Mean Square) and (RLS) Recursive Least Square are used to search for improved controlled response of the rejection of system disturbances [11, 12, 13, 15].

1. OBJECTIVES

1.1. GENERAL OBJECTIVE

- Theoretical study was performed on linear Active Vibration Control (AVC) of a flexible structure with one degree of freedom (Studied Plant), to reject periodic vibrations using Adaptive Filters and Robust Control, looking for an improved performance based on the trade-off relationship between the generalization of the solution and the disturbance attenuation.

1.2. SPECIFIC OBJECTIVES

- Simulation of the plant studied and the implementation of the AVC were programed in the Matlab environment considering the uncertainties of the model, and the use of Robust Control toolbox and the Digital Signal Processing (DSP) toolbox.
- Robust Control was implemented in the Studied Plant simulation to eliminate disturbances on mass 2, see Figure 8 and 9. Using H_∞, complex μ-Synthesis and Mixed μ-Synthesis techniques. A comparative study was made based on “worst-case” scenario analysis.
- AVC was implemented by means of three adaptive filters to simulate the Studied Plant: 1) a feedforward Filtered-X Least Mean Square (FxLMS); 2) an Adaptive Feedforward filter, using the algorithm Recursive Least Square (RLS), and modeling the propagation path of “Feedback Compensation”; and 3) Feedback FxLMS-based filter. Performance comparison was made based on the trade-off relationship between the generalization of the solution

versus the computational cost and the amount of attenuation of the disturbance.

- The performances of the Robust Controller and Adaptive Filter were confronted by applying them to the Studied Plant.

2. BACKGROUND

2.1. ACTIVE VIBRATION CONTROL AVC

AVC has long been applied, in particular to ships. Mallock (1905), reported about vibration on steam ship by synchronization of two engines in opposite phase, and Allen (1945), on roll stabilization by buoyancy control with activated fins, auxiliary rudders with variable angle of attack protruding laterally from the ship hull into water. Active damping of aircraft skin vibration was proposed in 1942, providing multichannel Feedback Control with displacement sensor and electromagnetic actuators, mainly in order to prevent fatigue damage. Early publications can also be found on the AVC in mechanical wave filters where a desire longitudinal wave mode in a bar is superimposed by an interfering a detrimental flexural wave mode, the latter can be damped by pair of piezoelectric patches on either side of the bar which are connected through an electrical resistor [24].

Damping and stiffness control in mechanical junction can be achieved by dry friction control where the pressing force is controlled by a piezoelectric actuator, in Feedback or Feedforward Control, typically by a nonlinear algorithm, e.g., a Neural Network. Active Control technology has been applied for improved vibration isolation of tables for optical experiments, scanning microscopes, vibrations sensitive semiconductor manufacturing, and active compensation systems for electromagnetic stray-fields which is important, e.g., for high-resolution electron microscope. [24]

The Active Control of sound or vibration involves the introduction of a number of controlled “Secondary” interferences destructively with the field caused by the original primary noise [11, 12, 14]. The extent of which such destructive interference is possible depends of the geometric arrangement of the primary and secondary source and their environment, and on the spectrum of the field produced by the primary source. In broad terms, considerable cancellation of the primary field can be achieved if the primary and secondary source are positioned within half of a wavelength of each other at the frequency of interest. Active methods of control are thus best at attenuating low frequency sound, which complements more conventional passive methods of control since these tends to work best at high frequencies [14].

One form of primary sound or vibration fields which is particular importance in practice is that produced by rotating machines. The waveform primary field in these cases is nearly periodic, and since it is generally possible to directly observe the action of the machine producing the original disturbance, the fundamental frequency of the excitation is generally known. Each secondary source can be driven at each harmonic via controller which adjusts the amplitude and face of references signal whose frequency is arranged to be a multiple of this known fundamental frequency. It is often desirable to design these controllers adaptive, because the frequency or spatial distribution of the primary field changes with time, and the controller is required to track these changes. A more difficult adaptive task has to be performed when the response of the system to be controlled to a given secondary excitation also varies with time. In this case the algorithm which simultaneous performs identification and control must be implemented [14].

2.2. ROBUST CONTROL

The purpose of Robust Control is to design a controller that guarantee the stability and desired performance of a system, despite system non-linearity, unmodeled dynamics, disturbance, and changes of parameters at different operating points. $\mathcal{H}_\infty$ control design and μ-synthesis are the most popular Robust Control techniques [23]. There are many applications in Robust Control field. A three-cart problem with two uncertainties and two outputs, with disturbance rejection in a mechanical path is used as a case of study in [16]. In [17] System Identification and controller design for a level control plant with non-linearity, time delay and change of parameters is provided using different operating points. The purpose of this study is determinate the influence of these uncertainties in the controller design and operation.

In [21] is recognized the parametric uncertainties inherent to the design or construction of a flexible robot manipulator, modeling them as unstructured uncertainties, improving the designing of the AVC system. In [1] the AVC is studied using robust stability control with a delayed Feedback to compensate the unmodeled dynamics of a flexible robot manipulator.

[3] presents a procedure for design and tuning of reduced orders H_∞ feedforward compensators for active vibration control systems subject to wide band disturbances for a three-cart problem, this paper also considers the use of an identification system for propagation paths. H_∞ Robust Controller and the controller order reduction technique are applied. In [9] the mixed µ-synthesis robust performance's design is studied for a two-mass two-spring system with stiffness uncertainty and time delay's uncertainty.

In [8] the design methodologies and architectures of the robust controllers H_∞ and µ-Synthesis are studied for different plants characterized by parametric uncertainties such as stiffness and damping, unmodeled delay's and actuator's force uncertainties.

2.3. ADAPTIVE CONTROL

Since the characteristic of the acoustic noise source and the environment are time varying, the frequency content, amplitude, phase, and sound velocity of the undesired noise are non-stationary. An Active Noise Control (ANC) system must therefore be adaptive in order to cope with these variations. Adaptive Filters adjust their coefficients to minimize an error signal, and can be design as Finite Impulse Response (FIR) or Infinite Impulse Response (IIR). The most common form of adaptive filter is the FIR filter using the Least-Mean-Square (LMS). The development of improved Digital Signal Processing (DSP) hardware allows these more sophisticated algorithms to be implemented in real time to improve system performance, obtaining large amounts of noise reduction in a small package, particularly at low frequencies [18, 19].

Adaptive Feedforward broadband is used in AVC when a measure of the disturbance is available. The additive feedback coupling between the compensator system and the measurement of the disturbance was studied, concluding that the absence of this feedback propagation path caused an error in the Adaptive Control [20]. On the other hand, this feedback coupling may destabilize the system. Simultaneous use of an Adaptive Feedback compensator and Feedforward compensation to disturbance rejection was proposed [2]. The action of the Feedback loop adds a new design specification for the stability conditions to the adaptive Feedforward compensation. In [18] the DSP algorithm was reviewed for ANC, and is studied the DSP broadband Feedforward Control and the Adaptive Feedback Control, with the purpose of showing the differences in implementation between the Feedforward and Feedback schemes. In [4, 5] the adaptive sinusoidal disturbance rejection in linear discrete time systems was studied using an approach based on the parameterizing the set of stabilizing controllers applying the Youla-Kucera Parametrization. In [6, 7] a theoretical framework for stochastic modeling of FxLMS-Based ANC was proposed to model without using conventional simplifying assumptions regarding the physical plant to be controlled. In [25] a stochastic analysis of FxLMS-based Internal Model Control (IMC) Feedback ANC system was conducted when a primary noise is band-limited white noise. In [22] the algorithms and DSP implementation was studied to adaptive filtering for AVC system.

For the studied Active Control it is possible to find a generalized solution to AVC for several types of vibrations at the same time without sacrificing the attenuation using the most common controllers in both control cases.

3. BASIC CONCEPTS

3.1. DISTURBANCE REJECTION ANALYSIS

The control system must maintain the output close to the desire value in the presence of the disturbances. Disturbances are inputs beyond the control of the designer and are usually inputs that tend to drive the output away from its desired value. Disturbance inputs consist of an infinite variety of types, which complicates the analysis of disturbance rejection. A set of “Typical” disturbance are therefore defined. The system response, subject to these disturbances is used to characterize the disturbance rejection of the system.

Disturbance inputs often exist for short period of time. Wind guts on antennas, meteor strikes on spacecrafts, and sticking of a motor shaft are all examples of a short duration disturbances. Short-duration disturbances can be approximated by impulse functions.

Constant and step disturbance are also commonly encountered. Gravity on an airplane, engine torque on helicopter, and solar pressure on geosynchronous satellite are examples of constant or nearly constant disturbances. Step disturbance are encountered when a load is placed on a motor, a robot picks up an object, and when a satellite experiences solar pressure upon departing

Earth’s shadow. The steady-state analysis of step and constant disturbance is identical. The analysis of step disturbance requires, in addition, the computation of transient response.

Sinusoidal disturbance such waves acting on a ship, acoustic waves acting on a structure (Earthquake acting on a building), and vibrations caused by rotating machinery frequently appear in control applications. Disturbance can often be characterized as existing only within a given frequency band. The frequency response (From the disturbance input to the reference output) provides a very useful tool for evaluating the effects of sinusoidal or band-limited disturbance.

Disturbances are often best modeled as random processes. A simple random process that is often employed in disturbance rejection analysis is white noise. Examples of white noise disturbance are turbulence acting on a jetliner, choppy seas acting on a ship, and measurement noise in a closed loop control system. White noise is an idealization of a zero mean random input with a short correlation time (True white noise does not exist in nature). When colored white noise disturbance are more appropriate, this colored noise disturbances can then be accomplished by analyzing the combination of the plant and the shaping filter subject to a white noise disturbance.

The specification of the disturbances in particular application proves to be one of the more difficult task in control design. The disturbance rejection of a control system can be evaluated by applying a representative disturbance input to the system and finding the resulting tracking problem error and control input. The frequency response of the closed loop system can also be used to quantify the disturbance rejection.

3.2. COST FUNCTION

The performance of a control system can be quantified in many applications by a cost function. A cost function is, in general, a real-valued, non-negative function of the system, or the time histories of the state, the reference output, and control inputs, subject to a given set of initial conditions and inputs. The cost (the real number resulting from the application of the cost function) can be used to evaluate the performance of a system, where superior performance is indicated by a smaller cost. The cost can also be based to compare the performance of multiple controller design; that is, the decision on which of several alternative design is superior can be made by comparing their cost. The controller that minimizes the cost, over all possible design or a set of possible candidates' designs, is known as an optimal controller. The selection of a cost function for practical application is a useful art in control design. The cost function given is based on norms.

3.2.1. Norms

The norm, denoted $\|*\|_p$, is a real-valued function of the element of a linear space $\mathcal{B}$. A linear space is a set where any linear combination of element is also an element of the set, and can be composed of vectors, signals, systems or other possible collection of elements. A norm has the following properties

$$\|x\|_p \geq 0$$

$$\|x\|_p = 0 \; if \; and \; only \; if \; x = 0$$

$$\alpha\|x\|_p = |\alpha|\|x\|_p$$

$$\|x + y\|_p \leq \|x\|_p + \|y\|_p$$

where $x, y \in \mathcal{B}$ and α is an scalar. Intuitively, norms provide a measure of the size of the vector, signal or system. Norms can also be used to denote the distance between two vectors, two signals, or two systems.

3.2.2. Quadratic Cost Function

The goals of the control system are to drive the output errors to zero[1], and to do this while using a reasonable amount of control. A typically control design represents a compromise between keeping the output errors small and keeping the control small. The cost function should therefore, include a measure of both the size of the output errors and the size of the control.

$$J = \int_0^{t_f} y^T(t)Y(t)y(t)dt = \|y(t)\|_{Y(t)}^2$$

Where the reference output is assumed to include both: the output errors and the control inputs. This cost functions is quadratic since it is a quadratic function of the reference output. The weighting function $Y(t)$ is a positive definite matrix,

[1] the output errors include both the errors between the outputs and the reference inputs, and any state or linear combination of state that the control system is tasked with driving to zero

selected to quantify the relative importance of the various outputs errors and control inputs. The parameter t_f is the final time, which can be infinity if the control system is intended to operate indefinitely.

3.2.3. Cost Function for Systems with Random Inputs

The state and control trajectories become random processes when the system is subject to random disturbance inputs. The quadratic cost function, as defined above, are then random variables instead of the desirable real values. The expected value of the signal can be used to provide a real measure of performance:

$$J = E\left[\int_0^{t_f} y^T(t)\boldsymbol{Y}(t)y(t)dt\right] = \int_0^{t_f} E[y^T(t)\boldsymbol{Y}(t)y(t)]dt$$

In applications where the random inputs are stationary, the system operates long enough that the initial transient can be ignored, the weighting matrix is time invariant and the closed-loop system is stable, the cost,

$$\int_0^{t_f} E[y^T(t)\boldsymbol{Y}(t)y(t)]dt$$

is proportional to the cost with a time-varying weighting matrix.

3.2.4. The System ∞-Norm Cost Function

The maximum gain of a generic system over all frequencies is given by the system ∞-norm:

$$\|\boldsymbol{G}\|_\infty = \sup_\omega \bar{\sigma}|\boldsymbol{G}(j\omega)|$$

Where $\sup_\omega$ is the supremum operator and $\bar{\sigma}$ is the maximum singular value, $\boldsymbol{G}$ is the transfer function of the generic system, this cost function is particularly applicable to the design of the system where the performance is specified by bounds of the output error and the control, and reasonable bounds can be generated for sinusoidal disturbance inputs. The ∞-norm also finds applications in robustness analysis. The ∞-norm is imprinted as the maximum system gain over the given time interval.

3.3. ROBUSTNESS

Mathematical model uses physics, chemistry, aerodynamics and so on, in order to produce an equation that describes the plant. A number of assumptions are typical made during this process in order to yield a simple model. Examples include ignoring friction between moving parts, and ignoring vibration on a motor shaft. This assumptions are justified by the need of simple design models and difficult encountered in generating over more accurate models, for example, the friction between moving parts may be difficult to determine and may change episodically, creating errors in an initial accurate model. For these reasons, a mathematical model is never a perfect representation of the physical object.

The control system engineer should be assured that a design will function acceptably before committing implementation. Such assurance can be obtained by analyzing control system stability and performance with respect to a range of plant models that is expected to encompass the actual plant. This type of analysis is termed robustness analysis.

The analysis of robustness requires that the discrepancy between the mathematical model of the plant and the actual plant be quantified. Since a perfect mathematical model of the plat is not available, this discrepancy can not be uniquely defined. Instead, a set of mathematical models is defined which includes the actual plants dynamics. This set is specified by a nominal plant and a set of perturbations termed admissible perturbations. The admissible perturbations are typically assumed to be bound, where the bound is dependent of the uncertainty of the model.

A controller that works adequately for all admissible perturbations is termed robust. There are two types of Robustness, robust stability and robust performance. A control system is said to be robustly stable if it is stable for all admissible perturbations. A control system is said to perform robustly if it satisfies the performance specification for all admissible perturbations. Note that stability and performance robustness depends on the controller, the nominal model, and the set of disturbances. Performance robustness also depends on the performance specifications.

3.3.1. Unstructured Uncertainty

Uncertainty can be modeled as a perturbation of the nominal plant. This perturbation is an error bound transfer function, where bounded is defined in terms of the system ∞ norm. This type of plant uncertainty is termed unstructured since not detailed model of the disturbance (the unknown transfer function) is employed.

3.3.2. Unstructured Uncertainty Models

An unstructured perturbation can be connected to the plant in a number of ways, each generating a unique set of possible plant models. Five basic connections of the perturbation to the nominal plant model are presented: additive perturbation, input multiplicative perturbation, output-multiplicative perturbation, input Feedback perturbation, and output Feedback perturbation. And additive unstructured uncertainty models the actual plant as equal to the nominal plant plus a perturbation:

$$\boldsymbol{G}(s) = \boldsymbol{G_0}(s) + \boldsymbol{\Delta_a}(s)$$

Where $\boldsymbol{\Delta_0}(s)$ denotes the additive perturbation. An input-multiplicative uncertainty models the actual plant as the nominal plant plus a series of combinations of the perturbation and the nominal plant (the perturbation appears on the input to the nominal plant):

$$\boldsymbol{G}(s) = \boldsymbol{G_0}(s)[\mathbf{I} + \boldsymbol{\Delta_i}(s)]$$

Where $\boldsymbol{\Delta_i}(s)$ denotes the input multiplicative perturbation. An output-multiplicative uncertainty models the actual plant as the nominal plant plus a series of combinations of the nominal plant and the perturbation (the perturbation appears on the output of the nominal plant):

$$\boldsymbol{G}(s) = [\mathbf{I} + \boldsymbol{\Delta_0}(s)]\boldsymbol{G_0}(s)$$

Where $\mathbf{\Delta_0}(s)$ denotes the output-multiplicative perturbation. An input Feedback uncertainty models the actual plant as the nominal plant in series with the perturbation in a Feedback loop (the Feedback loop appears in the input of the nominal plant):

$$\boldsymbol{G}(s) = \boldsymbol{G_0}(s)\left[\mathbf{I} + \mathbf{\Delta}_{\boldsymbol{fi}}(s)\right]^{-\mathbf{1}}$$

Where $\mathbf{\Delta}_{\boldsymbol{fi}}(s)$ denotes the input Feedback perturbation. An output Feedback loop uncertainty models the actual plant as the nominal plant in series with the perturbation in a Feedback loop (the Feedback loop appears on the output to the nominal plant):

$$\boldsymbol{G}(s) = \left[\mathbf{I} + \mathbf{\Delta}_{\boldsymbol{f0}}(s)\right]^{-\mathbf{1}}\boldsymbol{G_0}(s)$$

Where $\mathbf{\Delta}_{\boldsymbol{f0}}(s)$ denotes the output Feedback perturbation. Block diagrams of these five uncertainty models, appearing in a Feedback system are given in figure 3.

The uncertainty models are used to represent various types of uncertainty in the plant. the additive perturbation represents unknown dynamics operating in parallel with the plant. The multiplicative perturbation represents unknown dynamics operating in series with the plant. The Feedback perturbations are used primarily to represent uncertainty in the gain and phase of the plant (or the control loop if a feedback control is applied to the plant).

Figure 3 Unstructured uncertainties in the plant model: a) additive uncertainty; b) input-multiplicative uncertainty; c) output-multiplicative uncertainty; d) input-Feedback uncertainty; e) output-Feedback uncertainty

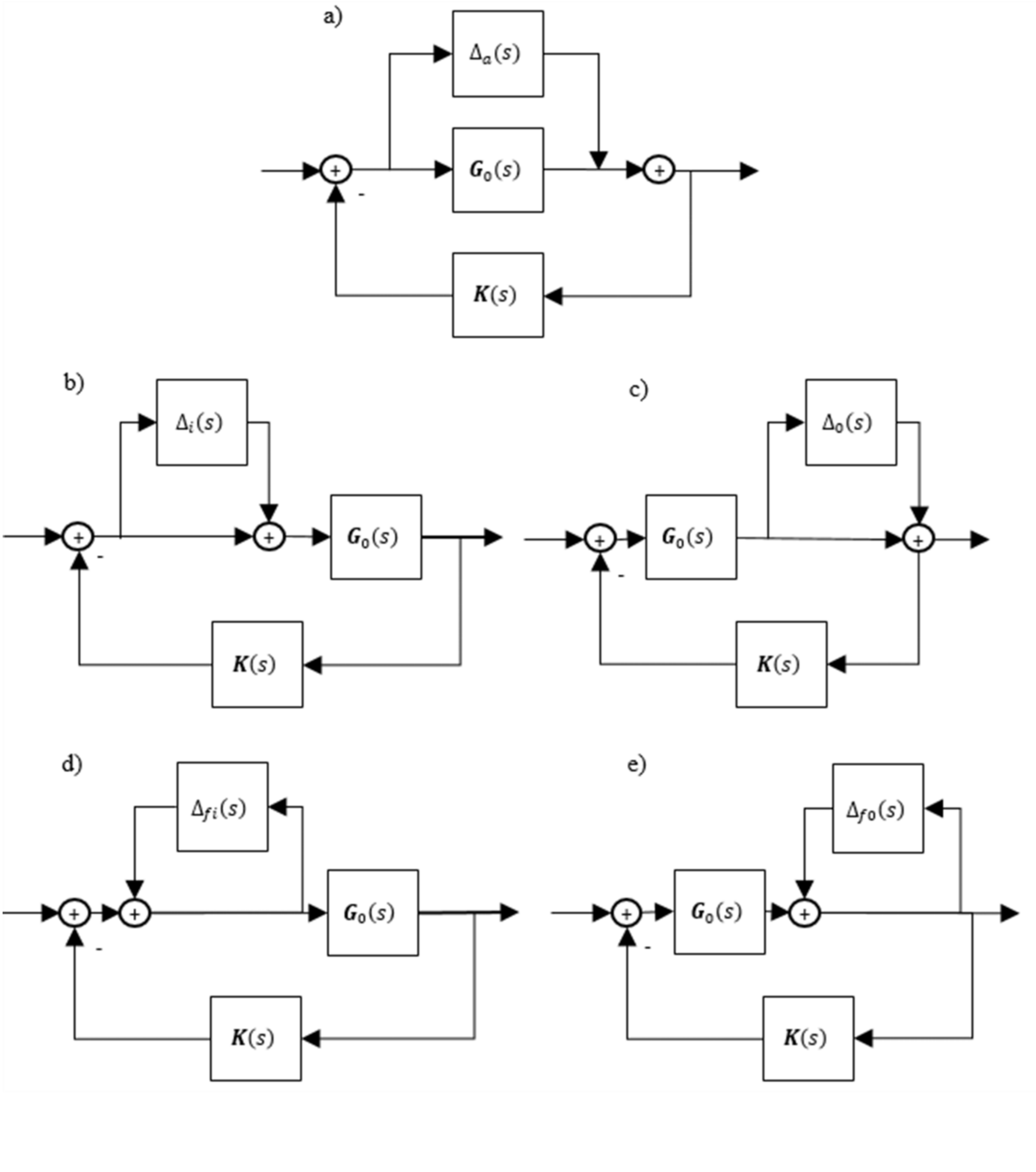

Stability robustness or performance can be evaluated when the disturbances in these models are bounded:

$$\bar{\sigma}\{\mathbf{\Delta}'(j\omega)\} \leq \Delta_{max}(j\omega)$$

Where $\bar{\sigma}$ is the maximum singular value, and $\{\mathbf{\Delta}'(j\omega)\}$ can be any of the disturbances described above.

3.3.3. Stability Robustness Analysis

A general Feedback system, where the perturbation is bounded $\Delta_{\infty} \leq 1$ is internally stable for all possible perturbations provided the nominal closed loop system is stable and

$$\left\|N_{y_d w_d}\right\| = \sup_{\omega}\{\bar{\sigma}[N_{y_d w_d}(j\omega)]\} \leq 1$$

Where $N_{y_d w_d}$ is the nominal closed loop system response from the augmented perturbation input to the augmented perturbation output. This results known as the small-gain theorem and provides a test for robust stability with respect to the bound perturbation.

3.3.4. Structured Uncertainty

Structured uncertainties arise when the plant is subject to multiple perturbations. Multiple perturbations occurs when the plants contains a number of uncertain parameters, or when the plant contains multiple unstructured uncertainties. For example, the plant model may be well specified except for two uncertainties constants, which are modeled as a nominal value plus a perturbation. The structured uncertainty is a very general way of modeling uncertainty, structured uncertainties also arise when the perturbation is restricted to be purely real or when other constraints on the perturbation are present.

A plant subject to structured uncertainty can be placed in standard form analogous that used for unstructured uncertainty. The standard form of the structured uncertainty model has the individual perturbation normalized to 1 and placed in a feedback loop around the nominal plant. The standard form of the structured uncertainty model is shown in Figure 4. The structured perturbation $\Delta(s)$ is a block diagram transfer function:

$$\mathbf{\Delta}(s) = \begin{bmatrix} \Delta_1(s) & 0 & 0 & 0 \\ 0 & \Delta_2(s) & \cdots & 0 \\ \vdots & \vdots & \ddots & \vdots \\ 0 & 0 & \cdots & \Delta_n(s) \end{bmatrix}$$

Where n is the number of perturbations and the blocks $\Delta_i(s) \in \boldsymbol{C}^{l_i \times n_i}$ represents the individual perturbations applied to the plant. An individual block can represent an uncertain in a parameter (Scalar perturbation) or an unstructured uncertainty. The set of all transfer functions matrices with this block diagram form is denoted $\bar{\Delta}$ The structured perturbation is normalized so that its infinity norm is bound by 1: $||\Delta||_\infty \leq 1$.

Figure 4 Standard form of the structured uncertainty model

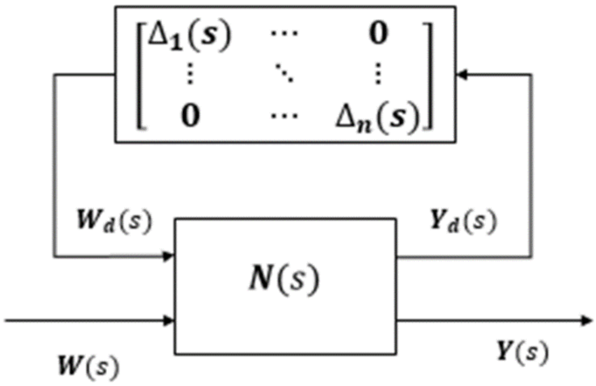

3.3.5. Structured Singular Value and Stability Robustness

The stability of a system subject to a structural uncertainty is determinate by analyzing the Feedback system in Figure 5. The nominal closed-loop system is assumed to be stable. Stability may be evaluated by determining the “size” of the smallest perturbation the results in a pole with a non-negative real part. A perturbation that results in such a pole is termed a destabilizing perturbation.

The Structured Singular Value is defined as follows:

$$\mu_{\bar{\Delta}}(N) = \frac{1}{\min\limits_{\Delta \in \bar{\Delta}} \bar{\sigma}(\Delta)\ such\ that\ det(\boldsymbol{I} + \boldsymbol{N\Delta}) = 0}$$

$$\mu_{\bar{\Delta}}(N) = 0\ if\ det(\boldsymbol{I} + \boldsymbol{N\Delta}) \neq 0\ for\ all\ \Delta \in \bar{\Delta}$$

The Structured Singular Value (SSV) is, in general, a real-valued function of a complex matrix N, which depends on the structure of the perturbation as defined by $\bar{\Delta}$

The stability robustness criterion for a system with structured uncertainty is summarized as follow: a general Feedback system, as given in Figure 4, is internally stable for all possible perturbations:

$$\Delta(j\omega) \in \bar{\Delta}\ and\ \|\Delta\|_{\infty} \leq 1$$

if and only if the nominal closed-loop system is internally stable and

$$\sup_{\omega}\{\bar{\sigma}[N_{y_d w_d}(j\omega)]\} \leq 1$$

Figure 5. Diagonal scaling of the plant: (a) the Feedback perturbation; (b) diagonal scaling added to the plant and the perturbation; (c) diagonal scaling leaves the diagonal perturbation unchanged

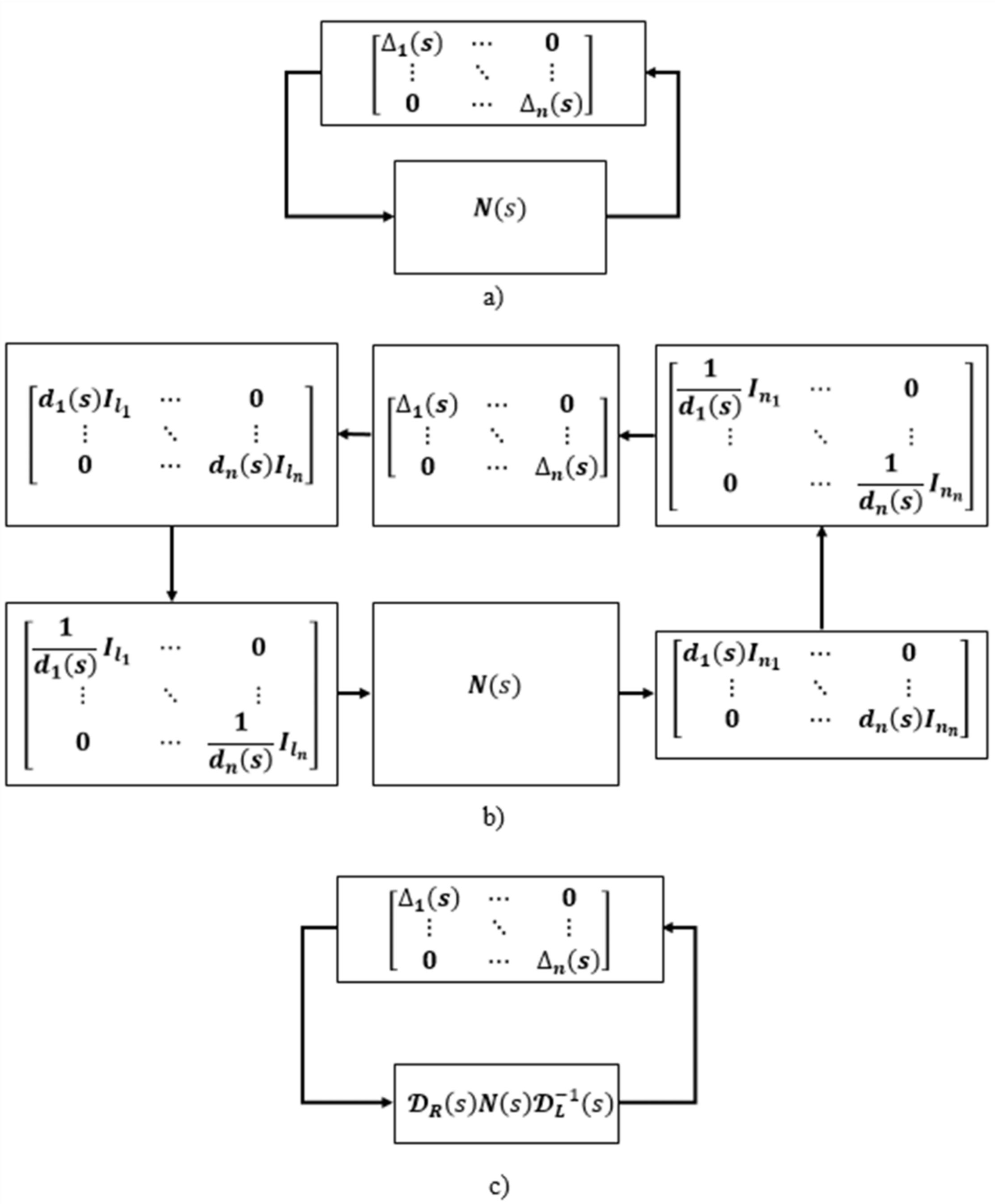

The SSV of a transfer function $N(s)$ is the inverse of the smallest perturbation that, when placed in the Feedback loop, yields a closed-loop pole located at s.

The closed loop poles of this system are not changed by the inclusion of the diagonals matrices $\mathfrak{D}_L(s)$ and $\mathfrak{D}_R(s)$ and their inverses:

$$\mathfrak{D}_L(s)=\begin{bmatrix} \mathrm{d}_1(s)\boldsymbol{I}_{l_1} & 0 & 0 & 0 \\ 0 & \mathrm{d}_2(s)\boldsymbol{I}_{l_2} & \cdots & 0 \\ \vdots & \vdots & \ddots & \vdots \\ 0 & 0 & \cdots & \mathrm{d}_n(s)\boldsymbol{I}_{l_n} \end{bmatrix}$$

$$\mathfrak{D}_R(s)=\begin{bmatrix} \mathrm{d}_1(s)\boldsymbol{I}_{r_1} & 0 & 0 & 0 \\ 0 & \mathrm{d}_2(s)\boldsymbol{I}_{r_2} & \cdots & 0 \\ \vdots & \vdots & \ddots & \vdots \\ 0 & 0 & \cdots & \mathrm{d}_n(s)\boldsymbol{I}_{r_n} \end{bmatrix}$$

The uncertainty blocks have their dimensions $\Delta_i(s) \in \boldsymbol{C}^{l_i \times r_i}$ and the identity matrices have the dimensions$\boldsymbol{I}_{r_i} \in \mathbb{R}^{r_i \times r_i}$. These dimensions match up with the perturbation blocks to yield.

Since the maximum singular value is changed by inclusions of the scaling matrices, and this result is valid for all diagonal scaling matrices (with the given block structure) and for all s, then:

$$\mu_{\bar{\Delta}}(N)=\min_{\substack{\{d_1,d_2,\ldots,d_n\} \\ d_i \in (0,\infty)}} \bar{\sigma}(\boldsymbol{\mathfrak{D}_R}(s)\boldsymbol{N}\boldsymbol{\mathfrak{D}_L}(s)^{-1})$$

The parameters d_i are called D-scale. This bound is valid for all complex D-scales, and as special case, for all real $\mathfrak{D}$ scale. For the case of complex perturbations, the phase shift of the perturbation is arbitrary, and any phase shift (including sign changed) imparted by $\mathfrak{D}$ -scales has no effect on the bound. Therefore, the minimization above can be performed over the set of possible real $\mathfrak{D}$ -scale without lose generality.

The perturbed closed-loop transfer function is dependent on both the nominal closed-loop transfer function and the perturbation. The conditions for performance robustness can be precisely stated in terms of these transfer functions.

$$\sup_{\omega} = \{\mu_{\bar{\Delta}}[\boldsymbol{N}_{y_d w_d}(s)]\} \leq 1$$

3.4. THE PROBLEM OF THE $\mathcal{H}_\infty$ CONTROLLER

The $\mathcal{H}_\infty$ output Feedback controller (or simply the $\mathcal{H}_\infty$ controller) utilizes partial state measurement, corrupted by disturbances, to generate the control. The suboptimal $\mathcal{H}_\infty$ control problem is defined by the plant and cost function. The plant is given by the following state model:

$$\dot{x} = \boldsymbol{A}\boldsymbol{x}(t) + [\boldsymbol{B_u} \quad \boldsymbol{B_w}] \begin{bmatrix} \boldsymbol{u}(t) \\ \boldsymbol{v}(t) \end{bmatrix}$$

$$\begin{bmatrix} \boldsymbol{m}(t) \\ \boldsymbol{y}(t) \end{bmatrix} = \begin{bmatrix} \boldsymbol{C_m} \\ \boldsymbol{C_y} \end{bmatrix} \boldsymbol{x}(t) + \begin{bmatrix} 0 & \boldsymbol{D_{mw}} \\ \boldsymbol{D_{yu}} & 0 \end{bmatrix} \begin{bmatrix} \boldsymbol{u}(t) \\ \boldsymbol{y}(t) \end{bmatrix}$$

Where the $x(t)$ is a vector that represents the states of the plant, $\boldsymbol{u}(t)$ is a vectors that represents the control signals, the disturbance signals are $\boldsymbol{w}(t)$, $\boldsymbol{m}(t)$ is the vector that represents the measured signals, and $\boldsymbol{y}(t)$ is the vector that represents the the references outputs. Matrices that represents the weights $\boldsymbol{B_u}$ to the control, $\boldsymbol{B_w}$ to the disturbance signals, $\boldsymbol{C_m}$ to the measurements, $\boldsymbol{C_y}$ to the reference output, and the weights for the paths $\boldsymbol{D_{mw}}$ from the disturbance signals to the measurements, and $\boldsymbol{D_{yu}}$ from the control signal to the reference outputs. The matrices $\boldsymbol{B_w}$and $\boldsymbol{D_{mw}}$ are assumed to satisfy the following conditions:

$$\boldsymbol{D}_{mw}\,\boldsymbol{B}_{w}^{T} = 0;$$

$$\boldsymbol{D}_{mw}\,\boldsymbol{D}_{mw}^{T} = \boldsymbol{I}$$

These conditions require that the disturbance entering the plant and the measurement are distinct and the output equation of the plant be scaled to normalize the measurement noise. The matrices $\boldsymbol{C}_y$ and $\boldsymbol{D}_{yu}$ are assumed to satisfy the following conditions:

$$\boldsymbol{D}_{yu}^{T}\,\boldsymbol{C}_{y} = \boldsymbol{0};$$

$$\boldsymbol{D}_{yu}^{T}\,\boldsymbol{D}_{yu} = \boldsymbol{I}.$$

These conditions require that the reference output consist of an output dependent only on the state and a distinct output depend only on the control input. The plant is assumed to be controllable from the control input and observable from the measured output. These conditions guarantee that the plant can be stabilized using output Feedback, a necessity when operating over infinite time intervals and always desirable. These conditions guarantee the existence of a steady-state $\mathcal{H}_\infty$ suboptimal output Feedback for sufficiently large performance bounds.

The suboptimal $\mathcal{H}_\infty$ control problem is to find a Feedback controller for the above plant such that the ∞-norm of the closed-loop system is bounded:

$$\left\|G_{yw}\right\|_{\infty,[0,t_f]} = \sup_{\|w(t)\|_{2,[0,t_f]}} \frac{\|y(t)\|_{2,[0,t_f]}}{\|w(t)\|_{2,[0,t_f]}} < \gamma$$

The closed-loop system is also required to be internally stable when the final time is infinite. The solution of the optimal $\mathcal{H}_\infty$ control problem (minimizing the closed-loop ∞-norm) is calculated using the Structured Singular Value.

The steady-state $\mathcal{H}_\infty$ controller is the solution to the following suboptimal control problem: find a linear, time-invariant controller system, described in Laplace domain as follows:

$$\boldsymbol{u}(s) = \boldsymbol{K}(s)\boldsymbol{m}(s)$$

that internally stabilizes the closed-loop system and bounds the ∞-norm of the closed loop-system:

$$\left\|G_{yw}\right\|_{\infty,} < \gamma$$

The steady-state $\mathcal{H}_\infty$ suboptimal control can be obtained by combining the existence results for the full information controller and the output estimator, we find as follows: A solution exists for $\mathcal{H}_\infty$ suboptimal control problem if and only if the following conditions are satisfied:

1. There is a positive semidefinite solution of the algebraic Ricatti equation

$$\boldsymbol{PA} + \boldsymbol{A^T P} - \boldsymbol{P}(\boldsymbol{B_u}\,\boldsymbol{B_u^T} - \boldsymbol{\gamma^{-2}}\,\boldsymbol{B_w B_w^T})\boldsymbol{P} + \boldsymbol{C_y^T C_y} = 0$$

Such $\boldsymbol{A} - \boldsymbol{P}(\boldsymbol{B_u}\,\boldsymbol{B_u^T} - \boldsymbol{\gamma^{-2}}\,\boldsymbol{B_w B_w^T})\boldsymbol{P}$ is stable (i.e., has only eigenvalues with negative real parts).

2. There is a positive semidefinite solution of the algebraic Ricatti equation

$$\boldsymbol{AQ} + \boldsymbol{QA^T} - \boldsymbol{Q}(\boldsymbol{C_m^T}\,\boldsymbol{C_m} - \boldsymbol{\gamma^{-2} C_y^T C_y})\boldsymbol{Q} + \boldsymbol{B_w B_w^T} = \boldsymbol{0}$$

Such that: $\boldsymbol{A} - \boldsymbol{Q}(\boldsymbol{C_m^T}\,\boldsymbol{C_m} - \boldsymbol{\gamma^{-2} C_y^T C_y})\boldsymbol{Q}$ is stable.

3. the spectral radius of the product of these Ricatti solutions is bounded:

$$\rho\,(\boldsymbol{PQ}) < \boldsymbol{\gamma}^{2}$$

The suboptimal full information controller is then given by

$$\boldsymbol{u}(t) = -\boldsymbol{B}_{\boldsymbol{u}}^{\boldsymbol{T}}\boldsymbol{P}\boldsymbol{x}(t) = -\boldsymbol{K}\boldsymbol{x}(t).$$

The suboptimal $\mathcal{H}_{\infty}$ estimator gain can be written in terms of the Ricatti equation solution:

$$\boldsymbol{G}(t) = \boldsymbol{Q}(t)\boldsymbol{C}_{\boldsymbol{m}}^{\boldsymbol{T}}$$

3.5. THE PROBLEM OF THE µ-SYNTHESIS CONTROLLER

Robust performance can be analyzed using the SSV for system containing both structured and unstructured perturbation. The direct computation of the SSV is intractable in all but the simplest case. The µ-synthesis design methodology attempts to minimize the supremum of the closed-loop system's SSV:

$$J = \mu_{\bar{\Delta}}(N) = \sup_{\substack{\{d_1, d_2, \dots, d_n\} \\ d_i \in (o, \infty)}} \bar{\sigma}(\boldsymbol{\mathfrak{D}_R}(j\omega)\boldsymbol{N}(j\omega)\boldsymbol{\mathfrak{D}_L}(j\omega)^{-1}).$$

Direct minimization of this cost function is typically not tractable. As an alternative, it is reasonable to minimize the upper bound of the SSV. D-K iteration seeks to overcome this problem by alternatively performing ∞-norm optimization and D-Scale optimization.

The D-K iteration algorithm is summarized as follow:

1. Model the Plant. The plant model should include disturbance inputs, control inputs, reference outputs, measured outputs, and perturbations. Append the performance block to the uncertainty matrix.
2. Generate a control system to minimize the ∞-norm of the transfer function from the augmented perturbation input to the augmented perturbation output.
3. Compute the Structured Singular Value for the closed-loop system (with both uncertainty and performance blocks). Save the D-Scale used in computing the SSV.
4. Fit a low-order transfer function to each frequency-dependent D-Scale.
5. Append this transfer function to the plant. The rational transfer function approximation for the D-scales and the inverse D-scales are append to the nominal close-loop system. This is typically accomplished by generating state models for the D-scales and the inverse D-scales, and appending these states models to the nominal closed-loop system.
6. For this augmented plant, generate a controller to minimize the ∞-norm of the transfer function from the augmented perturbation input to the augmented perturbation output.
7. Return to step 4, until the SSV of the closed-loop system fails to improve

This algorithm has typically been found to converge to a minimum cost in a few iterations. The D-K iteration algorithm is not guarantee to converge to the global minimum of the cost function. Further, this global minimum is not guaranteed to equal the global minimum of the cost function, except when the number of performance and perturbation blocks is less than or equal to 3.

3.6. ADAPTIVE FILTER

Adaptive filtering involves the changing of filter parameters (coefficients) over time, to adapt to changing signal characteristics. Over the past three decades, digital signal processors have made great advances in increasing speed and complexity, and reducing power consumption. As a result, real-time adaptive filtering algorithms are quickly becoming practical and essential for the future of communications, both wired and wireless.

3.6.1. Adaptive Filtering Methodology

Adaptive Filters self-learn using the error signal as the objective function. As the signal into the filter continues, the Adaptive Filter coefficients adjust themselves to achieve the desired result, such as identifying an unknown filter or canceling noise in the input signal. In figure 6, the shaded box represents the Adaptive Filter, comprising the Adaptive Filter and the adaptive Recursive Least Squares (RLS) algorithm.

Figure 6. Block Diagram Defining General Adaptive Filter Algorithm Inputs and Outputs

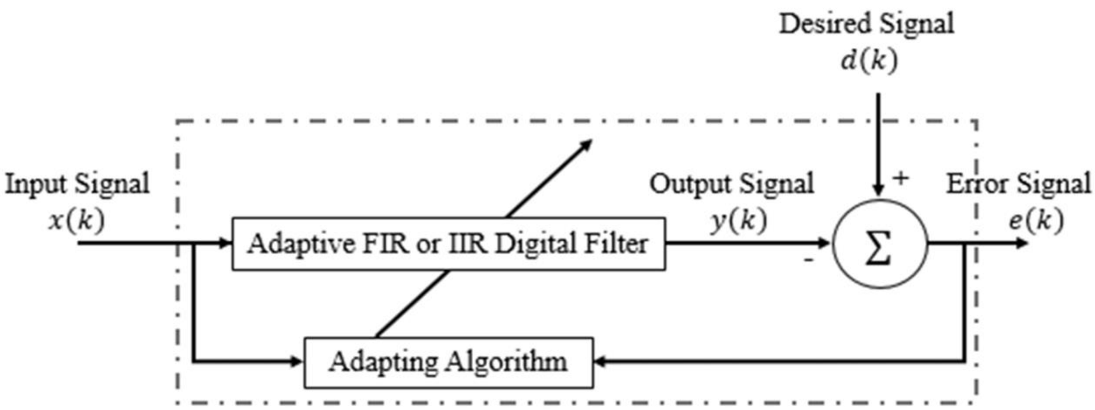

3.7. SYSTEM IDENTIFICATION

One common Adaptive Filter application is to use adaptive filters to identify an unknown system, such as the response of an unknown communications channel or the frequency response of an auditorium, to pick fairly divergent applications. Other applications include echo cancellation and channel identification.

In figure 7, the unknown system is placed in parallel with the Adaptive Filter. This layout represents just one of many possible structures. The shaded area contains the Adaptive Filter system.

Clearly, when $e(k)$ is very small, the Adaptive Filter response is close to the response of the unknown system. In this case the same input feeds both the Adaptive Filter and the Unknown System.

Figure 7. Using an Adaptive Filter to Identify an Unknown System

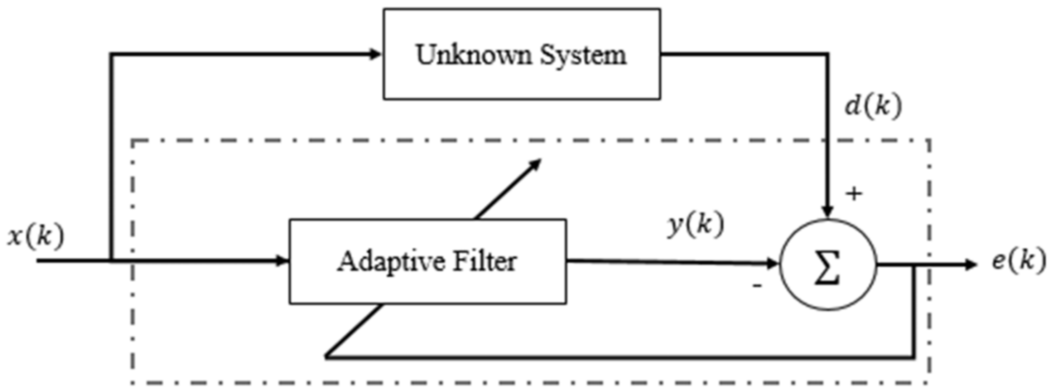

4. ROBUST CONTROL DESIGN

The active mass driver's model shown in Figure 8 provides a faithful test bed for the abstraction shown in Figure 2, for this reason this model was chosen as the Studied Plant. In this chapter, the AVC design applied on the Studied Plant using Robust Control methodology is described. The design was applied on a flexible structure with two uncertain parameters with real parts, unmodeled delay, unmeasurable disturbances, two noisy measurements, one control signal, and one performance output. First, parametric uncertainties were fully identified at several operating points considering physical constraints. Then, the three-cart's physical system dynamics was described. The $\mathcal{H}_\infty$ controller was proposed to reject the disturbance. The unstructured uncertainties were released from the parametric uncertainties and their effects on the system performance were studied. The mixed μ-synthesis and DK iteration were used to improve Robust performance.

4.1. PARAMETRIC UNCERTAINTIES

The model of the Studied Plant consists of five metal plates connected by springs, the first and last plates are the supports and each of them are equipped with one inertial actuator. The first will excite the structure (disturbance) and the second will create vibrational forces which can counteract the effect of these vibrational disturbances.

Figure 8. Modeled Real Plant

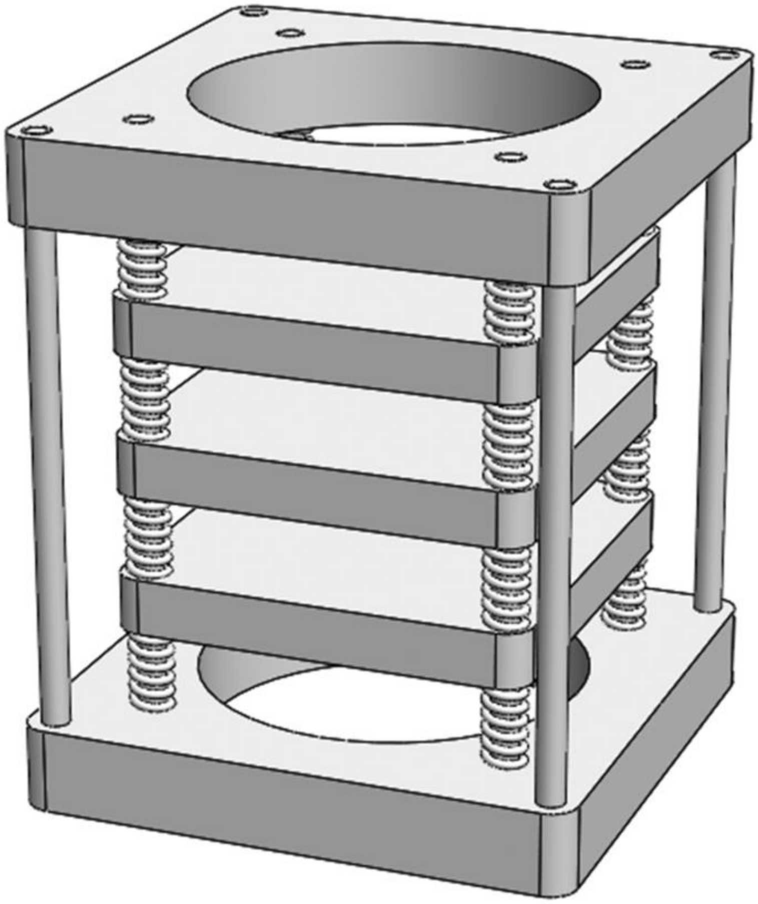

The Plant was simplified to a two dimensional scheme. The simplified plant was obtained and expressed in Space-State representation. This representation is called the Nominal Plant Model (see Figure 9). In this simplification, all four parallel springs are assumed all with the same constant, and they are modeled as one spring and one dash pot in parallel.

Figure 9. A three-cart simplified model, the spring constant $\boldsymbol{k}$ and damping ratio b are uncertainties

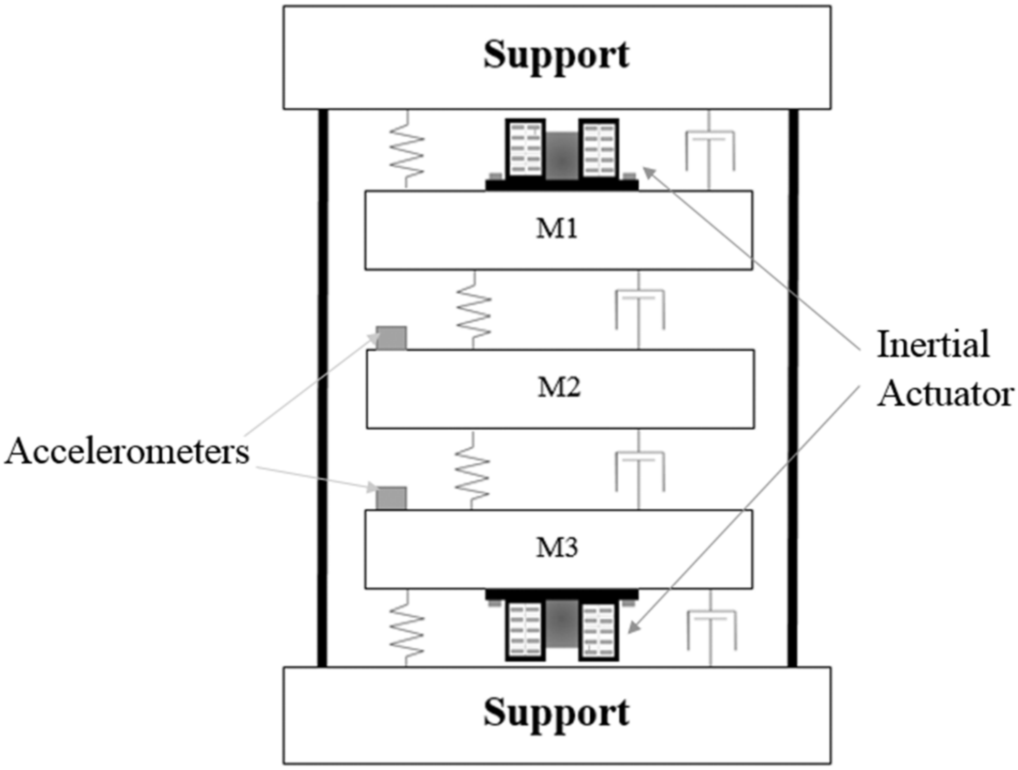

$$k_{simp} = \sum_{1}^{4} k_i \pm \varepsilon \tag{1}$$

The error of model simplification is assumed about 10 % of the real value at low frequencies. This error may be caused by uncertainty in the manufacturing process, also because of the uncertainty in the linear model. Equations of energy balance were used to model the movement of the masses, equations (2) and (3):

$$x_{max} * f_b * \bar{V} = \left(\frac{1}{2} k_{simp} (x_{max})^2 - \frac{1}{2} m (V_{max})^2\right) \tag{2}$$

$$f_b = \frac{0.95}{2x_{max}\bar{V}} k_{simp}(x_{max})^2 = \frac{0{,}475 x_{max} k_{simp}}{\bar{V}} \left(-\frac{1}{2} m (V_{max})^2\right) \quad (3)$$

Where x is the displacement of the mass, V is the velocity of the mass, k is the simplified spring constant, and f_b is the damping coefficient. Masses are constrained in displacement and speed to emulate the real plant. The damping coefficient is a parametric uncertainty caused by the uncertainty of the spring constant, and it is assumed with a low value due to the worst case model to control is a pure mass-spring system. This is because, the system will not lose energy by friction but by the superposition of the vibrations (the AVC situation), making more difficult the design of the controller. The parametric uncertainties were calculated with the upper and lower bound for the parameters $k \; and \; f_b$.

$$\begin{gathered} k \in [k_{lower-bound} \quad k_{upper-bound}] \\ f_b \in \left[f_{b_{lower-bound}} \quad f_{b_{upper-bound}}\right] \end{gathered} \quad (4)$$

4.2. THREE-CART MIMO DYNAMICS

The dynamic of the Mass-Spring-Dash pot (MSD) system shown in Figure 9 is described by:

$$\begin{cases} \dot{\boldsymbol{x}}(t) = \boldsymbol{A}\boldsymbol{x}(t) + \boldsymbol{B_1} f_s + \boldsymbol{B_2} d_s(t) \\ \boldsymbol{m}(t) = \boldsymbol{C_2}\boldsymbol{x}(t) + \boldsymbol{D_{22}}\boldsymbol{w_0}(t) + \boldsymbol{D_{21}}\boldsymbol{u}(t) \\ \boldsymbol{y}(t) = \boldsymbol{C_1}\boldsymbol{x}(t) + \boldsymbol{D_{11}}\boldsymbol{u}(t) \end{cases} \quad (5)$$

Where

$$\boldsymbol{x}(t) = [\boldsymbol{x_1}(t) \quad \boldsymbol{x_2}(t) \quad \boldsymbol{x_3}(t) \quad \boldsymbol{v_1}(t) \quad \boldsymbol{v_2}(t) \quad \boldsymbol{v_3}(t)]^{\boldsymbol{T}} \quad (6)$$

$$w_0 = [d_s(t) \quad v_1 \quad v_2]^T \tag{7}$$

$$\boldsymbol{y}(t) = \boldsymbol{C_1}\boldsymbol{x}(t) + \boldsymbol{D_{11}}\boldsymbol{u}(\mathrm{t}) \tag{8}$$

The State dynamic matrix is described by:

$$\boldsymbol{A} = \begin{bmatrix} \boldsymbol{0_{3\times3}} & I_{3\times3} \\ \boldsymbol{A_{21}} & \boldsymbol{A_{22}} \end{bmatrix} \tag{9}$$

Where

$$\boldsymbol{A_{21}} = \begin{bmatrix} -\frac{k_1 + k_2}{m_1} & \frac{k_2}{m_1} & 0 \\ \frac{k_2}{m_2} & -\frac{k_2 + k_3}{m_2} & \frac{k_2}{m_2} \\ 0 & \frac{k_3 + k_4}{m_3} & -\frac{k_4}{m_3} \end{bmatrix}$$

(10)

$$\boldsymbol{A_{22}} = \begin{bmatrix} -\frac{b_1 + b_2}{m_1} & \frac{b_2}{m_1} & 0 \\ \frac{b_2}{m_2} & -\frac{b_2 + b_3}{m_2} & \frac{b_2}{m_2} \\ 0 & \frac{b_3 + b_4}{m_3} & -\frac{b_4}{m_3} \end{bmatrix}$$

$$\boldsymbol{B_1} = \begin{bmatrix} \boldsymbol{0_{3\times1}} \\ \boldsymbol{0} \\ \boldsymbol{0} \\ \frac{\boldsymbol{1}}{\boldsymbol{m_3}} \end{bmatrix} \quad \boldsymbol{B_2} = \begin{bmatrix} \boldsymbol{0_{3\times1}} \\ \frac{\boldsymbol{1}}{\boldsymbol{m_1}} \\ \boldsymbol{0} \\ \boldsymbol{0} \end{bmatrix} \quad \boldsymbol{B} = [\boldsymbol{B_1} \quad \boldsymbol{B_2}] \tag{11}$$

$$\boldsymbol{C_{11}} = [0 \quad 1 \quad 0 \quad 0 \quad 0 \quad 0]; \boldsymbol{C_{21}} = \boldsymbol{A}(\boldsymbol{5},:); \boldsymbol{C_{31}} = \boldsymbol{A}(\boldsymbol{6},:); \boldsymbol{C} = \begin{bmatrix} \boldsymbol{C_{11}} \\ \boldsymbol{C_{21}} \\ \boldsymbol{C_{31}} \end{bmatrix} \tag{12}$$

$$\boldsymbol{D_{11}} = [\boldsymbol{0_{2\times1}}]; \boldsymbol{D_{12}} = [\boldsymbol{0_{2\times3}}];\ \boldsymbol{D_{21}} = [\boldsymbol{0_{2\times1}}]; \boldsymbol{D_{22}} = \begin{bmatrix} 0 & 1 & 0 \\ 0 & 0 & 1 \end{bmatrix};$$

$$\boldsymbol{D} = \begin{bmatrix} \boldsymbol{D_{11}} & \boldsymbol{D_{12}} \\ \boldsymbol{D_{21}} & \boldsymbol{D_{22}} \end{bmatrix} \tag{13}$$

The k_i are the spring constants; b_i are the damping coefficients; $m_i, x_i and\ v_i$ are the mass, position and speed of mass $i = 1,..,3$, respectively; f_s is the control force signal, d_s is the disturbance source.

The MIMO system includes one disturbance random input force $w(t)$ acting on mass m_1 and two accelerometers on masses m_2, m_3. The control force $u(t)$ drive the inertial actuator with an unmodeled delay upon the mass m_1. The disturbance force $d_s(t)$ is an independent stationary stochastic process generated by applying continuous-time white noise $\xi(t)$ with zero mean in a low-pass filter. The low pass filter, $W_{dist}(s) = P_{dist}/(s + P_{dist})$, has a pole in P_{dist}. This is caused by the low cross frequency of real mechanical system, as follows:

$$d_S(s) = W_{dist}(s)\xi(s) \tag{14}$$

The overall State-Space representation includes the disturbance dynamics via one augmented state variables $x_{[7,1]}$. For the current case, the following parameters in (5) are known and fixed (the units are omitted): $\sqrt{k/_m} = 2$

The $\boldsymbol{y}(t)$ vector represents the position of mass $m_2(x_{m_2})$ and acceleration on masses $m_2(a_{m_2})$ and $m_3(a_{m_3})$:

$$\begin{cases} y_1(t) = x_2(t) \\ y_2(t) = \ddot{x}_2(t) \\ y_3(t) = \ddot{x}_3(t) \end{cases} \tag{15}$$

All Feedback loops use two measurements $z(t)$

$$\begin{cases} z_1(t) = \ddot{x}_2(t) + \nu_1(t) \\ z_2(t) = \ddot{x}_3(t) + \nu_2(t) \end{cases} \tag{16}$$

In Equation (16), $\nu_1(t)$ and $\nu_2(t)$ are white noise caused by the sensor's dynamics and they are defined by $E\nu_i(t) = 0, E(\nu(t)\nu(\tau)) = 10^{-16}\delta(t-\tau)$, where $\nu(\tau) = [\nu_1(t) \quad \nu_2(t)]^T$

The frequency response of the nominal plant can be observed in Figure 10, also the two poles of a_{m_2} which have to be diminished by the controller. On the other hand, the pole at 2 rad/s in a_{m_3} is an obstacle to obtain the desired performance in the robust design, because a greater control effort is produced at this frequency. For this reason the a_{m_3} signal was chosen as a performance output because it is a measure of the control effort.

Additionally, there is unmodeled delay τ in control channel caused by the delay between the actuator force and its action on mass m_1, so neglecting τ produces an error about $e^{-s\tau-1}$. The transport delay of 0.5 s [22] in the system is modeled by a weight function that operates as a high pass filter. On the other hand, the inertia of the masses and springs causes a transport delay in the plant.

Figure 10. Frequency response of the nominal model

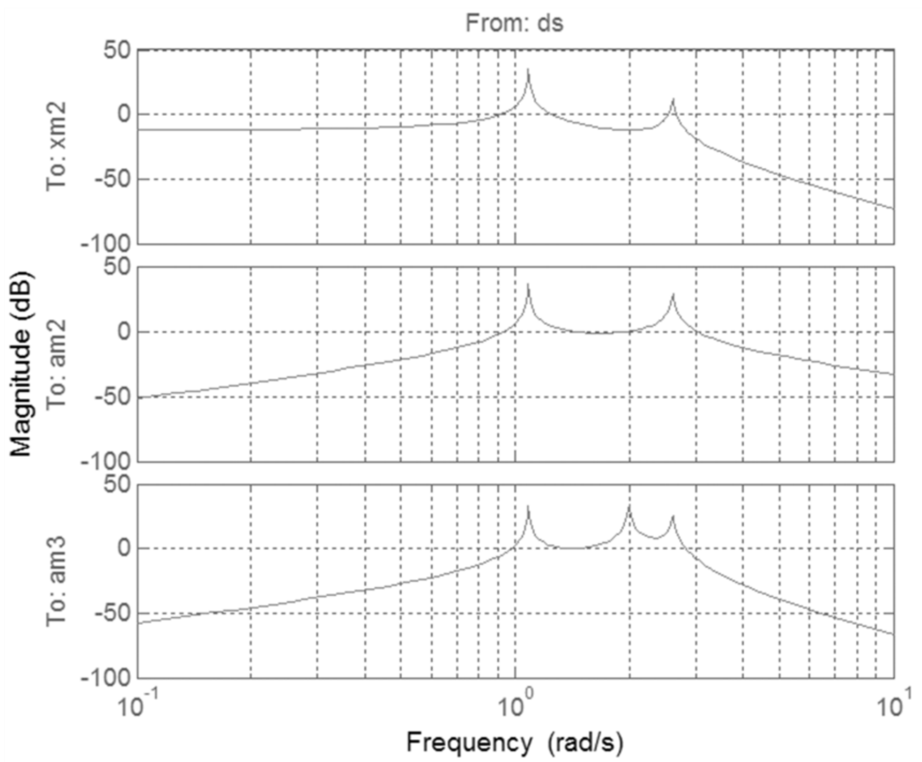

Figure 11. Comparative Bode plot of the Unmodeled Dynamics vs Plant input delay

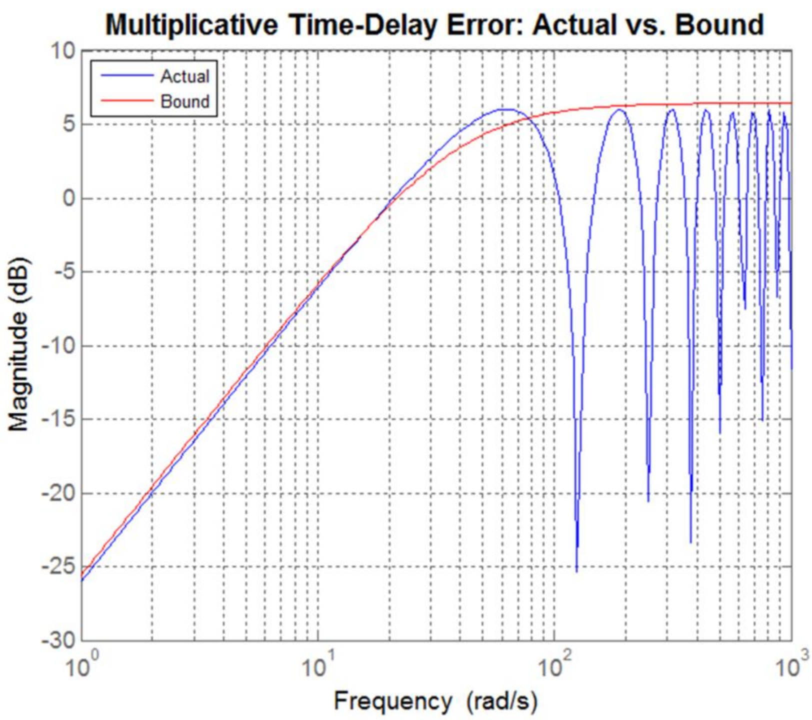

This delay is named after Unmodeled Dynamics due to the delay was not taken into account in the State-Space representation. Matlab software models this delay using a digital highpass filter as part of the structure of the representation. Modeled as a complement of the structure, the design of the robust controller does not take the delay in count. To consider this Unmodeled Delay, it was modeled using a transfer function of a highpass filter with a similar behavior to the delay model using the Matlab digital filter. The weight function of Unmodeled Dynamics is a transfer function that models the inertia of the Studied Plant. The differences between Time-Delay response of the actual plant, modeled as a digital filter, and the frequency response of the Unmodeled Dynamic weight (17) are shown in Figure 11.

$$w_{unmod}(s) = \frac{2{,}1s}{s+40} \tag{17}$$

4.2.1. Inertial Actuator Modeling

The model of the inertial actuator is a first order low pass filter that penalizes high frequencies content in the control signal and limits the band pass:

$$Act_{nominal} = \frac{1}{\left(\frac{s}{50}+1\right)} \tag{18}$$

The constraints of the actuator are established by a System Identification (SI) process. Variations between the actuator model and the physical device can be modeled as a family of actuator models. The resulting family of models embraces a nominal model with an amount of uncertainty that is frequency dependent, (see Figure 12).

Figure 12. Comparative Bode plot of the actuator nominal model vs 20 randomly sampled models

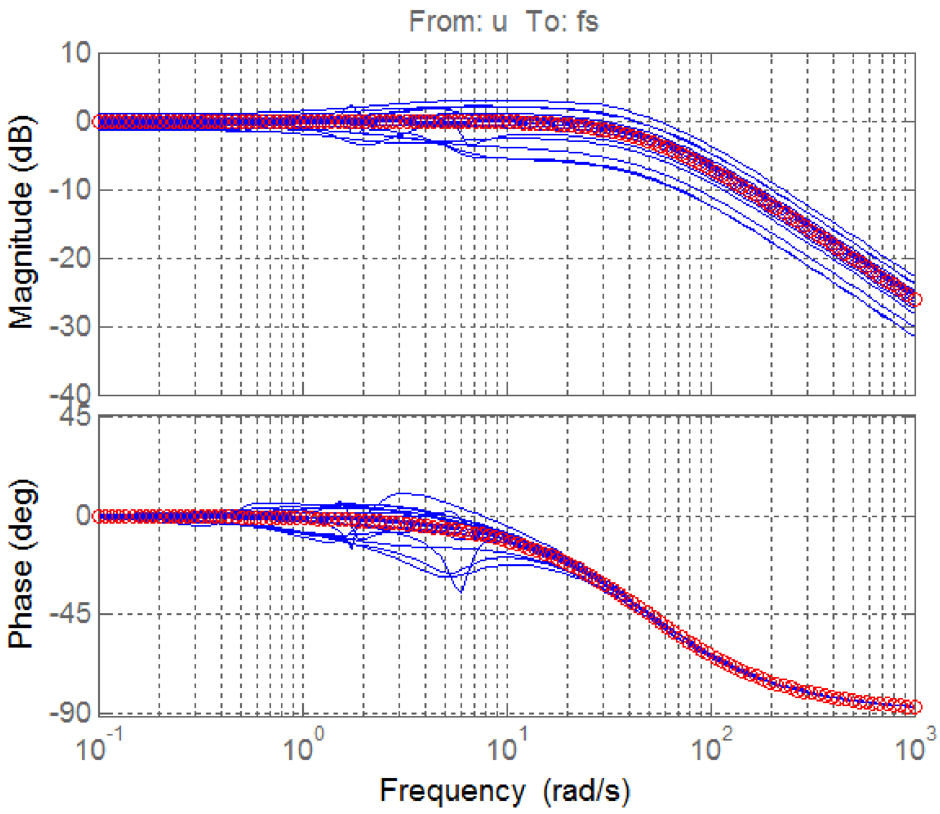

At low frequency, the frequency responses of the models are similar to the nominal actuator. In turn, the variations of the frequency responses increase as the frequency increases. The weighting function, W_{act} , reflects this behavior and it is used to modulate the amount of uncertainty as a function of frequency. The resulting model of the actuator is an uncertain State-Space model.

4.3. $\mathcal{H}_\infty$ ROBUST CONTROLLER DESIGN

The generalized plant is obtained connecting all dynamic models and signal, as shown in Figure 13. Linear Fractional Transformation (LFT) of the plant is obtained using Matlab software. The optimal controller is found solving the two Ricatti equations to the LFT model [17].

Figure 13. MIMO weights for robust synthesis

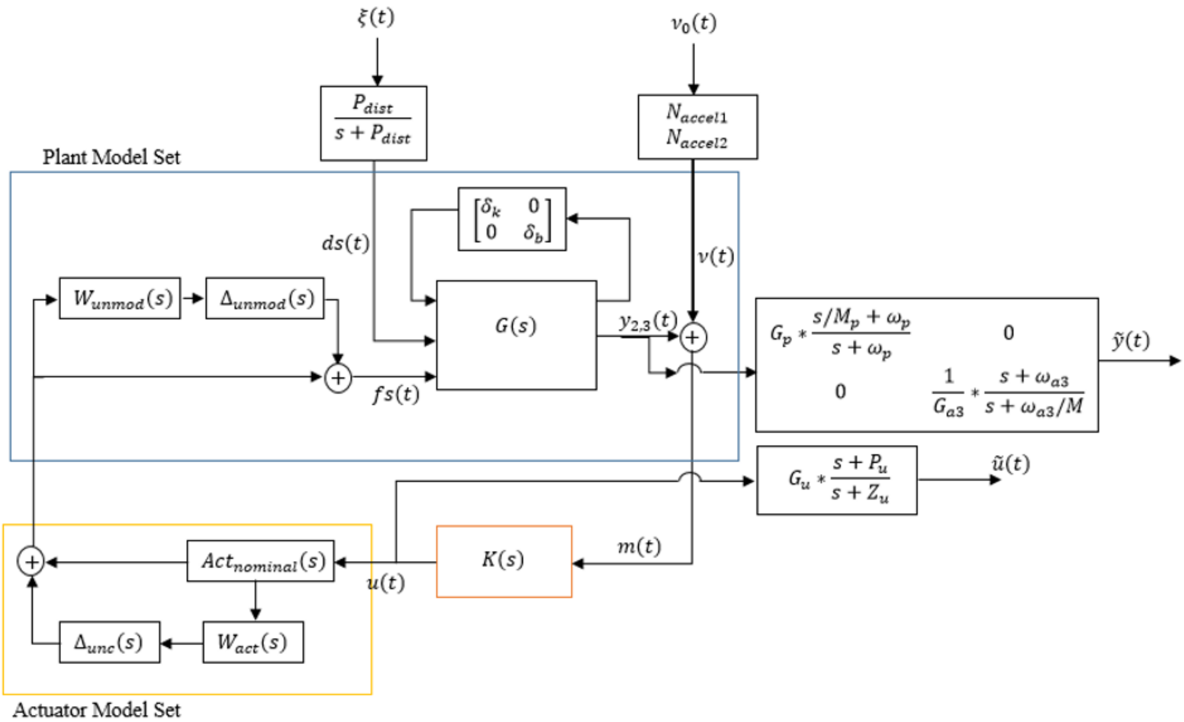

4.3.1. Nominal Model and Structured Uncertainties

The parametric uncertainties, gain and time delay determined by modeling, are converted into unstructured uncertainties for $\mathcal{H}_\infty$ controller design. Equation (19) expresses the transfer function of the generalized plant considering the uncertainties raised so far in (4) and (17) as a transformation of the nominal plant.

$$\boldsymbol{G_u} = \boldsymbol{K_p e^{-\tau s} G_0}(s) \tag{19}$$

These parametric uncertainties can be converted into the multiplicative uncertainty general form of:

$$\forall G_u(s) \in \Omega \; G_u = (1 + \Delta(s)W_t(s)G_n(s)) \tag{20}$$

Where Ω is the family of plants, $G_n(s)$ is the nominal plant, G_u is the generalized plant.

In this case, $W_t(s)$ is a stable transfer function indicating the upper bound of the uncertainty and $\Delta(s)$ indicates the normalized uncertainty, $\|\Delta(s)\|_\infty \leq 1$. In this general representation, $\Delta(s)W_t(s)$ represents the deviation of the model system by the uncertainties present in gain and time delay. The parameters uncertainties of (4) are represented by:

$$k_L \leq k_{nom} \leq k_H \Longrightarrow k = k_{nom} + (\sigma_k)\delta_k;\; \delta_k \leq 1 \tag{21}$$

$$b_L \leq b_{nom} \leq b_H \Longrightarrow b = b_{nom} + (\sigma_b)\delta_b;\; \delta_b \leq 1 \tag{22}$$

In (20), the delay is replaced by a multiplicative uncertainty simplifying the controller design. In Figure 14 is observed the differences between the nominal plant model and a family of plants generated randomly.

Figure 14. Bode Plot for nominal and 20 samples of uncertainties

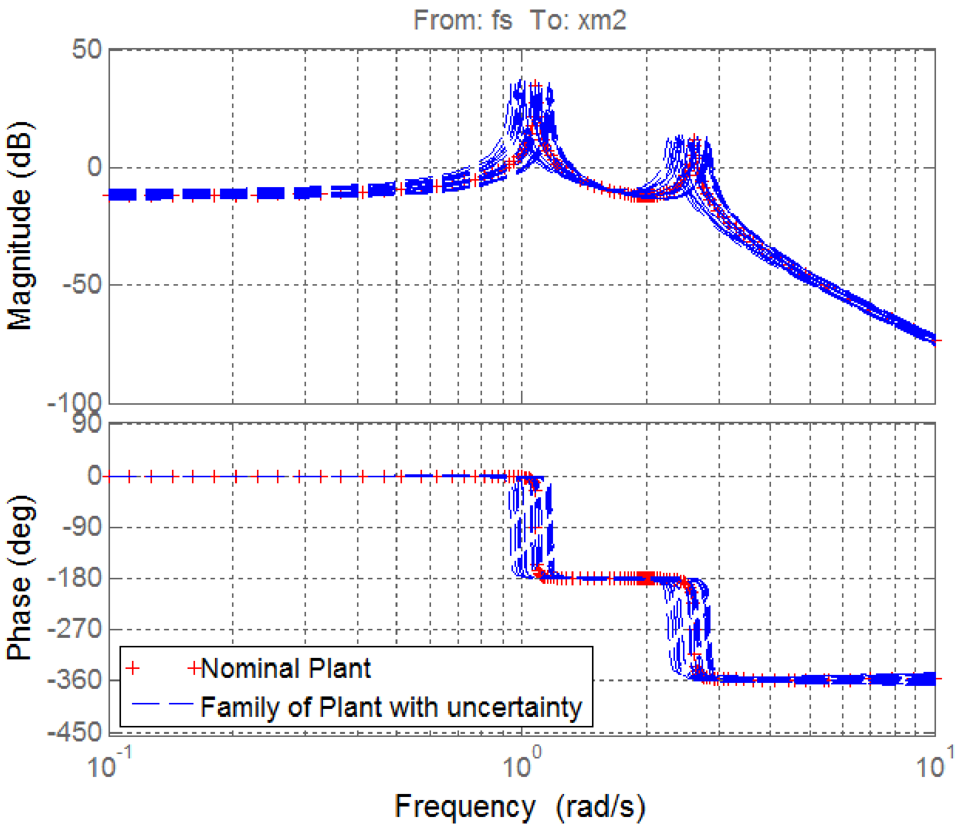

4.3.2. Scaling

The signal references, the disturbance input, and the control signals are normalized in time and frequency domains. The performance of the resulting controller depends on this weighting. The control is penalized by a factor of 1 at low frequencies and by a factor of 10 at high frequencies with cross frequency of 100 rad/s. The Control Weight $\boldsymbol{W_u}$ is expressed by (23)

$$\boldsymbol{W_u} = \frac{\boldsymbol{G_u} * (s + P_u)}{(s + Z_u)} \tag{23}$$

The models of each sensor are constant transfer functions, where each constant determinates the sensor accuracy.$\boldsymbol{N_{accel1}}$ is the accelerometer on mass $\boldsymbol{m_2}$ and $\boldsymbol{N_{accel2}}$ is the accelerometer on mass $\boldsymbol{m_3}$. The sensor weighted function $\boldsymbol{W_n}(\boldsymbol{s})$ is (24)

$$W_n = [\boldsymbol{N_{accel1}} \quad \boldsymbol{N_{accel2}}]^T \tag{24}$$

The Control Weight and the sensor weighted function, together with the Unmodeled Dynamic's weight (17) and the actuator (18), limit the bandwidth of the closed loop system by penalizing large high-frequencies control signals. The weight functions (17), (18), and (23), (24) are the same in any of the subsequent designs.

4.3.3. The Limitation Imposed on the Performance

The bandwidth of the sensitivity function is assumed to be the system bandwidth. The increase of the bandwidth produces a faster response of the system and a large peak on the sensitivity function. Otherwise, decreasing this bandwidth causes a reduction of the phase margin and a more sensitivity to the noise and parameters variations. Therefore, it is proposed (25) and (26) which are the tradeoff between the mentioned problems above and the reference disturbance rejection problem. The weight functions (25) and (26) are applied in the output vector $\boldsymbol{y}(t)$.

$$W_p = \frac{G_p * (s/M_p + \omega_p)}{(s + \omega_p)} \tag{25}$$

$$W_{ac_3} = \frac{1}{G_{a_3}} * \frac{(s + \omega_{a_3})}{(s + \omega_{a_3}/M)} \tag{26}$$

In (25), $\boldsymbol{M_p}$ is the maximum value of the sensitivity function in all frequencies, $\boldsymbol{\omega_p}$ is the bandwidth from the normalized disturbance to the $\boldsymbol{m_{a_2}}$ and $\boldsymbol{\omega_{a_3}}$ is the bandwidth from the disturbance source ($\boldsymbol{d_s}$) to $\boldsymbol{m_{a_3}}$. The transfer function of the actuator works as a low pass filter (See figure 13). In addition, the transfer functions, that represent the propagation paths of the accelerations from the inertial actuator to masses 2 and 3 $\boldsymbol{a_{m_2}}$ and $\boldsymbol{a_{m_3}}$ respectively), work also as low pass filters. Therefore, transfer functions (25) and (26) represent the goal of disturbance rejection. They attenuate disturbances only below 10 rad/s, because beyond this value transfer functions studied have a frequency response below -70dB.

The comparison of the close-loop targets response using the weight function (25) and (26) with the open loop response can be observed in Figure 15.

Figure 15. Bode plot comparison between closed-loop target and the open-loop response

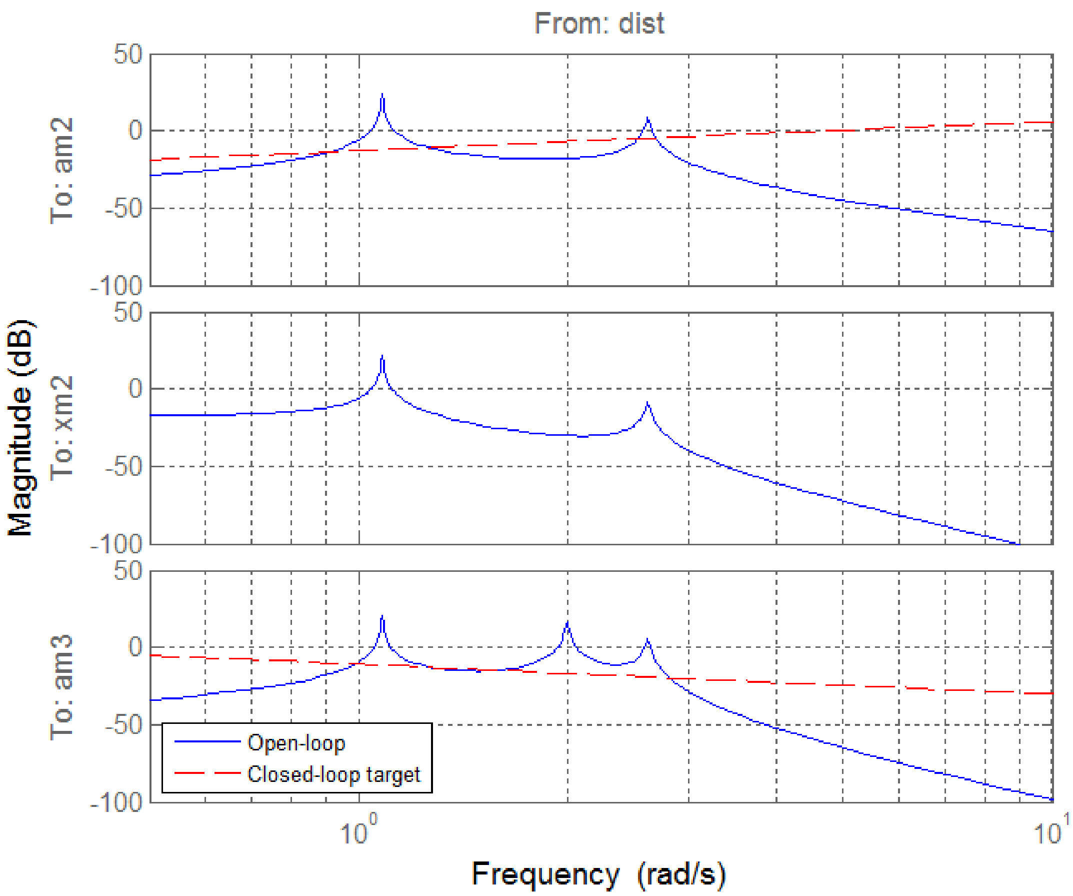

4.4. CONTROLLER DESIGN

The suboptimal $\mathcal{H}_\infty$ control problem is to find a Feedback controller for the generalized plant such that the ∞-norm of the closed-loop system. Bode plot comparison between closed-loop target and the open-loop response is bound:

$$\left\|G_{yw}\right\|_{\infty,[0,t_f]} = \sup_{\|\omega(t)\|_{2,[0,t_f]}} \frac{\|y(t)\|_{2,[0,t_f]}}{\|w(t)\|_{2,[0,t_f]}} < \gamma \tag{27}$$

Figure 16. N-Δ Block Diagram

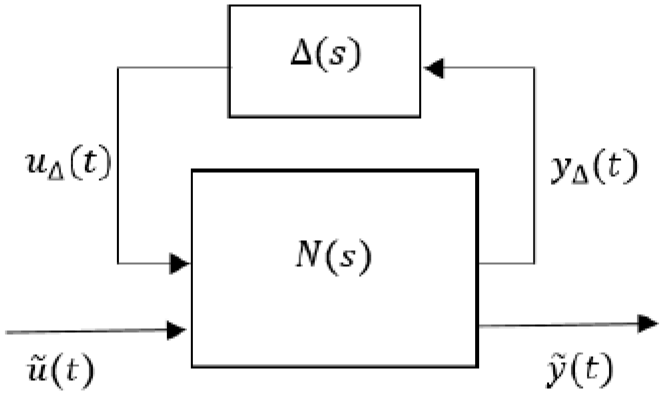

This is a suboptimal solution; an optimal solution is obtained by minimization of the closed loop system ∞-norm. Where $\boldsymbol{\gamma}$ are the performance bounds imposed to the design. The block diagram of Figure 13 is used to obtain generalized plant N in Figure 16 and the LFT model.

For the block diagram of Figure 13 the LFT is derived via the generalized plant. The minimization of the Maximum Singular Value of the generalized plant N is solved numerically by using the $\mathcal{H}_\infty$ Robust Control Toolbox in MATLAB. The outcome of this problem is a controller with the same order of the generalized plant with a Space-State representation of 13 states, 1 output (control), and 2 inputs $\boldsymbol{a_{m_2}}$ and $\boldsymbol{a_{m_3}}$. The frequency response of the closed loop system with the controller proposed and the modeled uncertainties are shown in Figure 17. The influence of the pole at 2 rad/s is noted in the actuator force frequency response (see Figure 17). The attenuation of high frequencies responses caused by the low bandwidth of actuator model is presented in the same figure.

Figure 17. Bode plot of the open loop system and compare to the close loop response with the controller

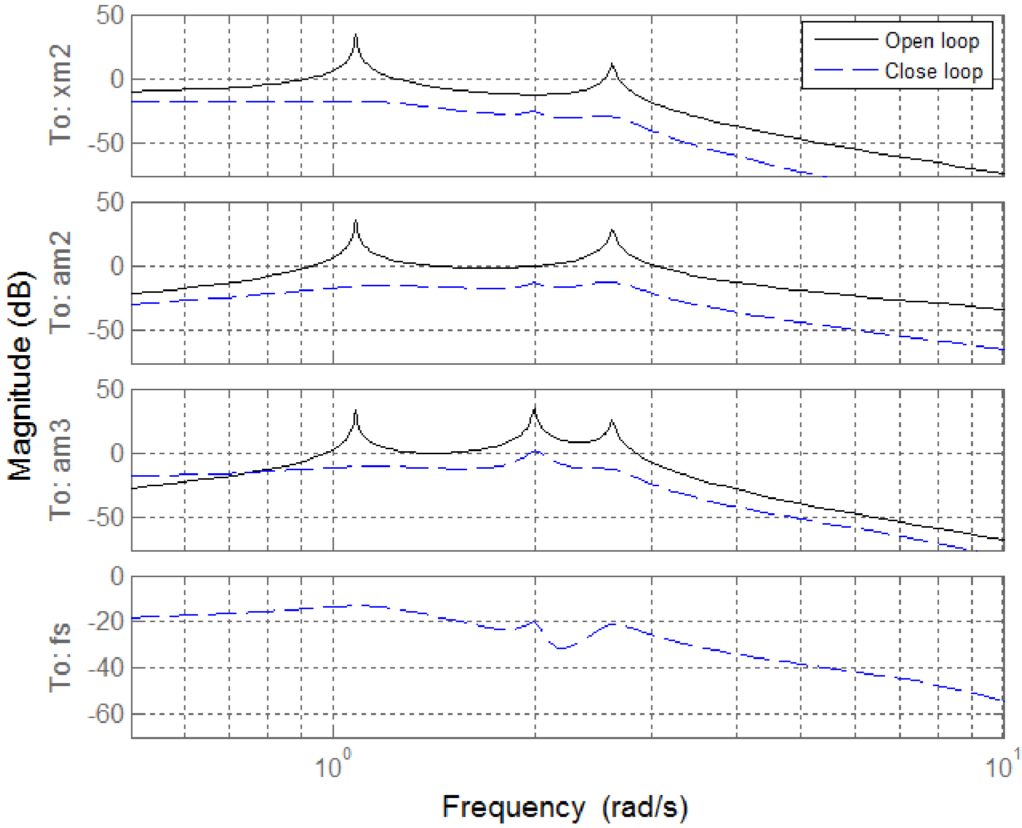

4.4.1. Robust Stability and Performance

The peak gain of the close-loop system is 0.3461. Therefore, the robust stability is guaranteed and the system is stable even in the worst condition.

Although the system has reached the robust stability, the controller cannot estimate-control correctly all possible states within the range prescribed by the weighting functions. This means that the driver is unable to model the bounded uncertainties. This situation can lead to produce a controller gain of 6.23 at 1.95 rad/seconds.

4.5. μ-SYNTHESIS AND DK-ITERATION

The minimization of the maximum Structured Singular Value (SSV), not the ∞ norm which is the maximum singular value, is a mathematically precise method to generate controllers that meet robust performance specifications. Robust Performance can be analyzed using the SSV as given by the cost function. $\mathcal{D}-\mathcal{K}$ Iteration seeks to overcome the problem of minimization of SSV by alternatively performing ∞-norm optimization and D-scale optimization.

The controller based on μ-synthesis is obtained using the controller cost function (26) as an objective function to minimize the control effort. The resulting controller has a $\mathbf{35^{th}}$ order with a μ value of 1.2538 and the system gain only models 89.4% of the uncertainties. The complex μ -synthesis process performed considers the uncertainties $\boldsymbol{k}$ and $\boldsymbol{f_b}$ as complex variables. This process was not able to reduce the μ value below the unit, giving no an acceptable Robust performance. This occurs because the variation range is too large for the performance desired, considering the number of measured signals and output references. This situation may also happen because the DK-scaling considers the parametric uncertainties, stiffness and damping, as complex variables which penalize the optimization process.

Figure 18. Bode plot comparison between open loop system and the close loop response with the robust controller

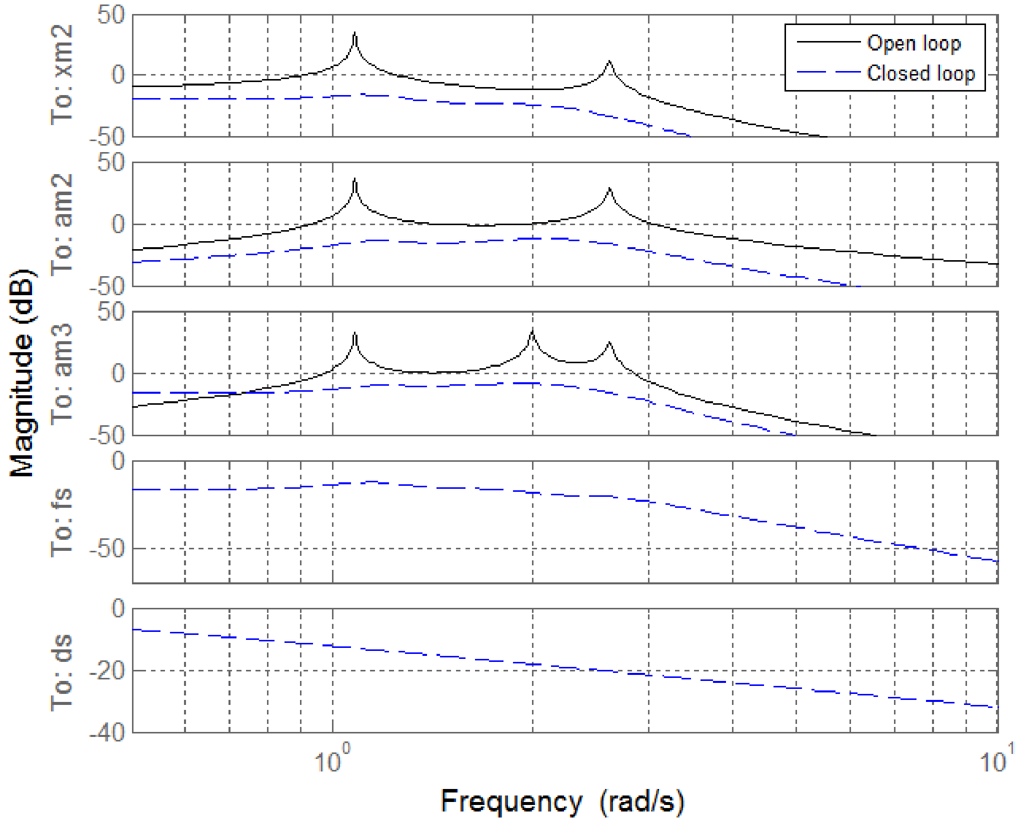

The frequency response of the closed loop system is shown in Figure 18. The influences of the poles in the open loop frequency responses at $\boldsymbol{a}_{m_2}$ and $\boldsymbol{a}_{m_3}$ are attenuated by the controller.

4.6. MIXED µ-SYNTHESIS

In the interest of improving the Robust performance to a desire value a Mixed-µ synthesis is used. Mixed-µ synthesis considers real part uncertain parameters directly in the synthesis process. A scaling function was applied to the DK-iteration process. After this process, the order associated with the complex uncertainties was settled of $\mathbf{5}^{th}$ and $\mathbf{6}^{th}$ order for the uncertain real-valued parameters both used in Mixed-µ synthesis.

The controller obtained from the Mixed µ-Synthesis is a State-Space model with 1 output, 2 inputs, and 87 states, with the µ value of 0.8271. The close loop response with the mixed-µ controller is shown in Figure 19. The frequency response of the actuator force slightly increase its magnitude around the poles of $\boldsymbol{a}_{m_2}$ and $\boldsymbol{a}_{m_3}$ without surpass the 0 dB magnitude, reaching a desired Robust performance.

Figure 19. Bode plot comparison between closed-loop target and the close loop response with the Mixed-µ controller

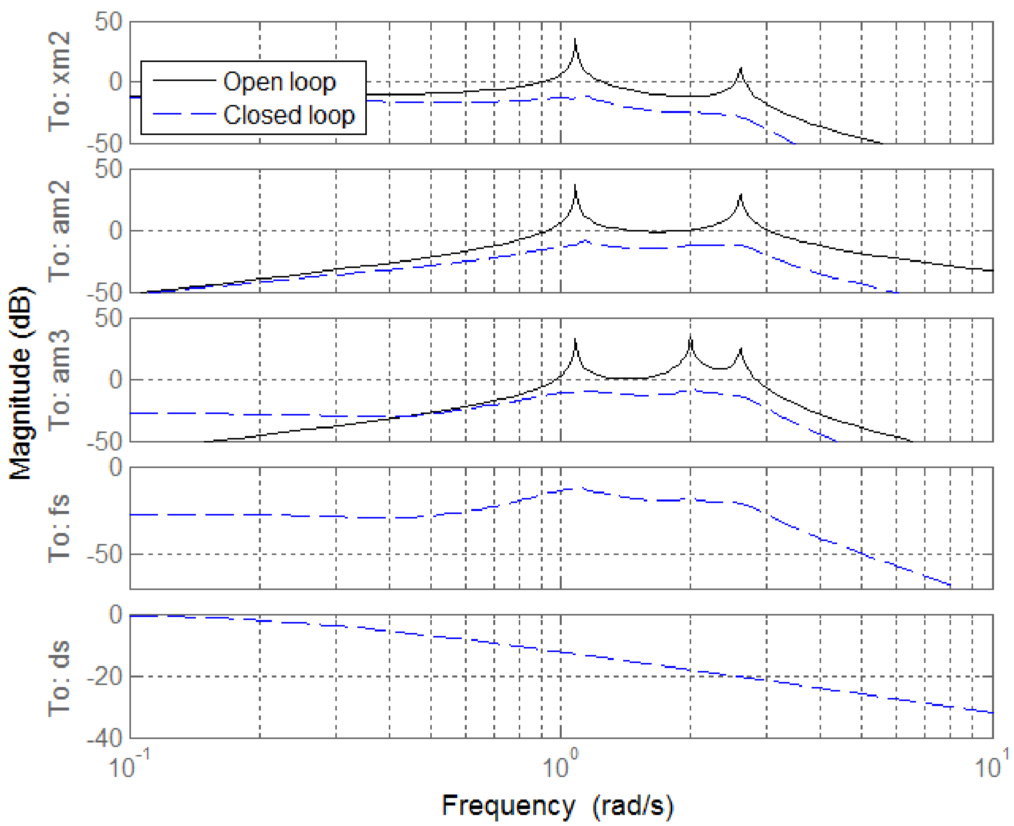

4.7. DISTURBANCE REJECTION SIMULATIONS

To compare the disturbance rejection performance white noise is injected into the low-pass $\boldsymbol{W_{dist}}$ filter to simulate the input disturbance $(\boldsymbol{f_s})$. The disturbance rejection simulation in Matlab environment of the Complex and mixed μ-synthesis controller in closed loop with the system are presented in Figure 20.

Figure 20. Disturbance rejection response

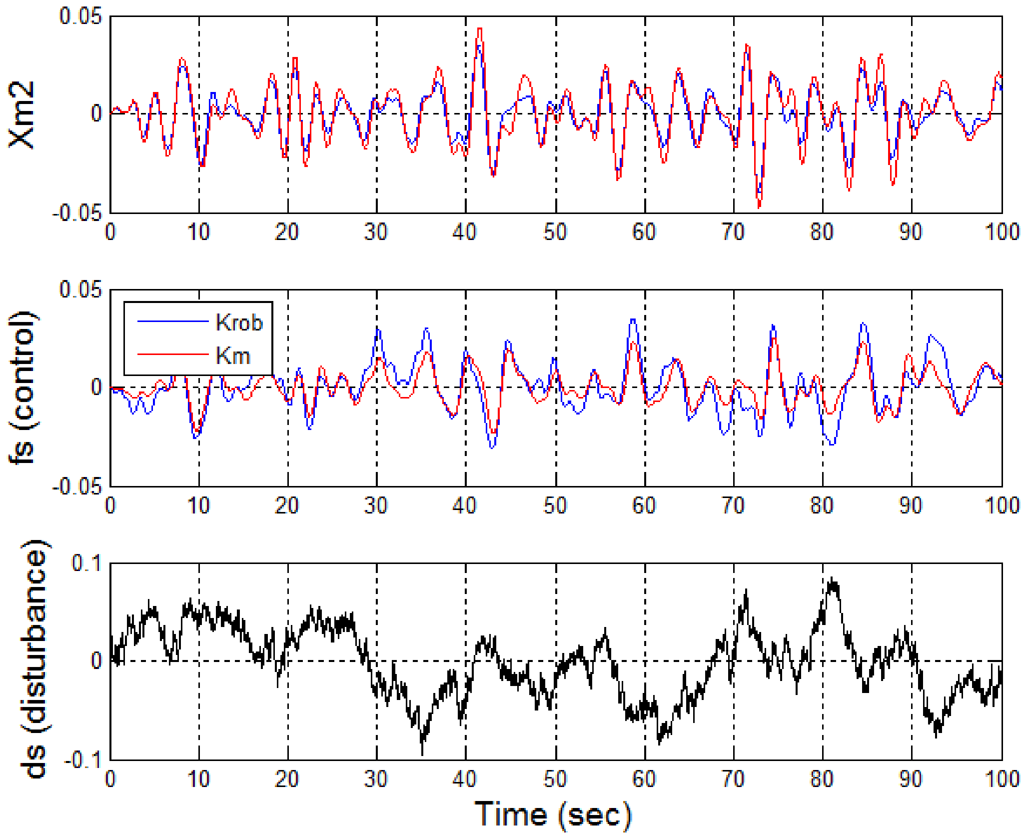

The mixed-μ controller weighted the real part of the uncertainties, stiffness and damping, producing less control than the Complex μ-Synthetized. This is what makes different Robust performances of Complex μ-Synthesis from Mixed-μ Synthesis. The “worst-case” disturbance rejection scenario is shown in Figure

21. The system presents the desired performance with both controllers. However, the mixed-µ controller has also the advantage in the disturbance rejection at x_{m_2} , and the controller force f_s is lower, showing the desired robust performance.

Figure 21. Disturbance rejection response of the worst-case

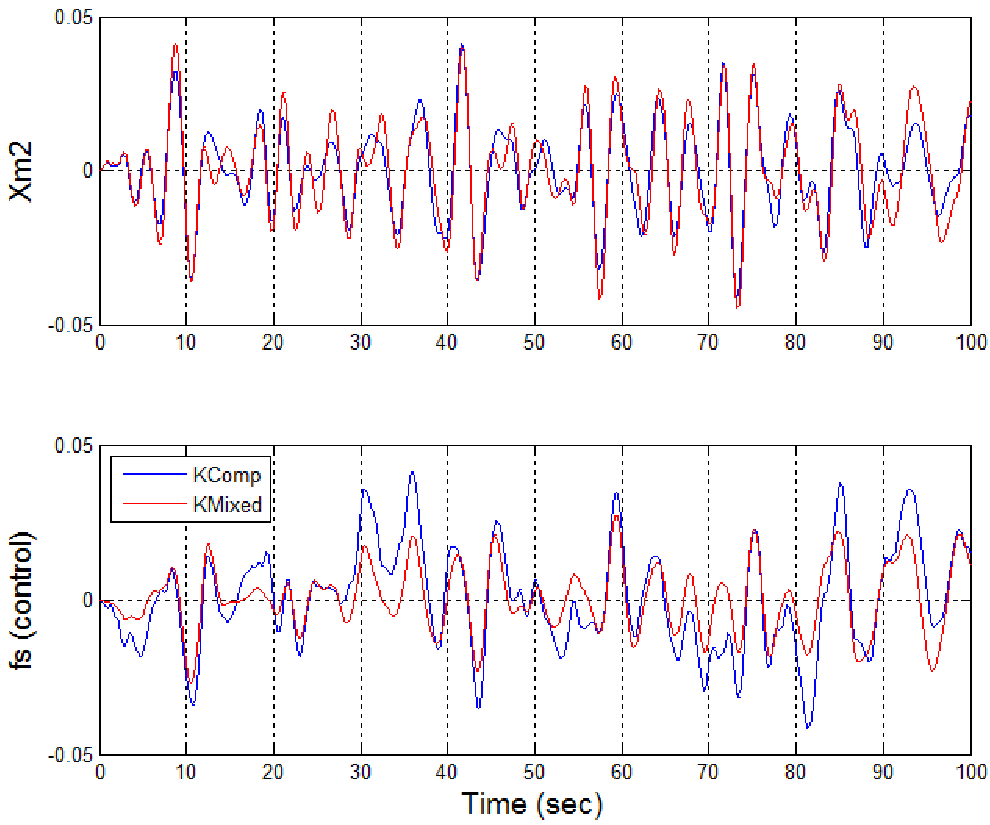

The order reduction is applied to the Mixed-µ controller to decrease the computational cost. In order to reduce the controller order, The Robust Control toolbox of Matlab was used to evaluate the performance of every controller, from the 87^{th} order controller to the first order controller. In Figure 22 the results are shown:

Figure 22. Robust performance as a function of controller order

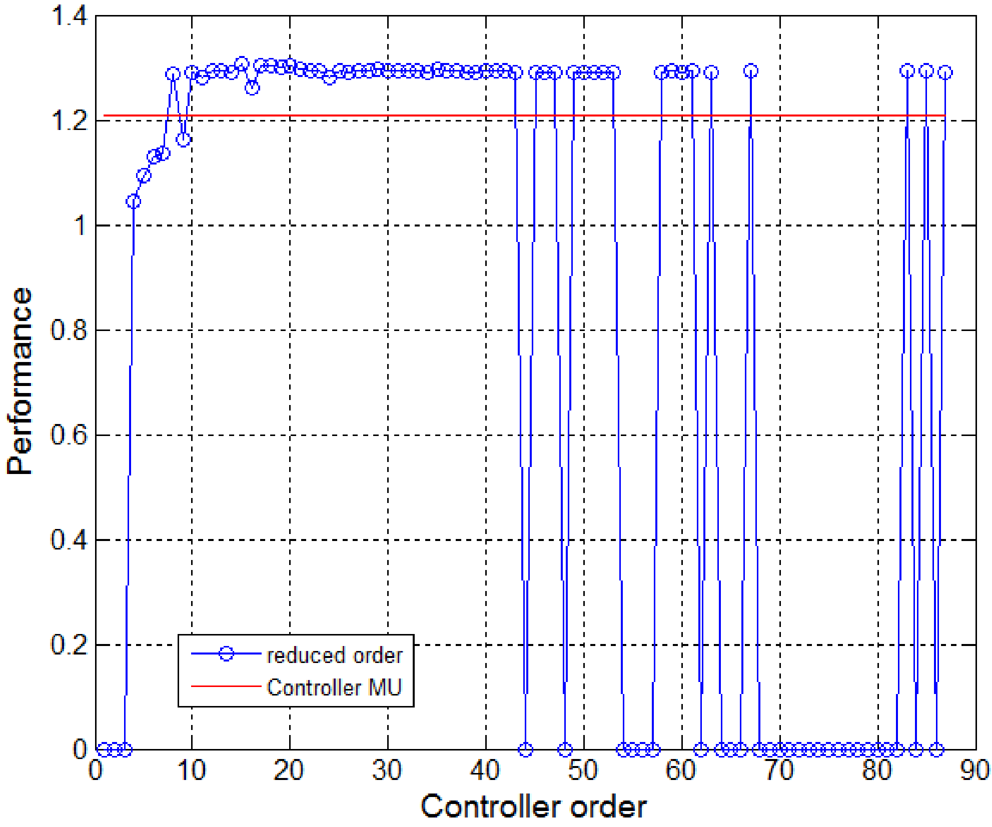

As shown in Figure 22, the $\mathbf{8}^{th}$ order controller presents the desired Robust performance with a reasonable computational cost for a non-adaptive controller with a maximum gain of 0, 9796. In Figure 23, the differences in disturbance rejection of the closed loop system using both, the $\mathbf{87}^{th}$ order controller and the $\mathbf{8}^{th}$ order controller, are shown when white noise is injected to the closed loop generalized plant via $\boldsymbol{W}_{dist}$.

Figure 23. Disturbance rejection comparison 87th and 8th controller order

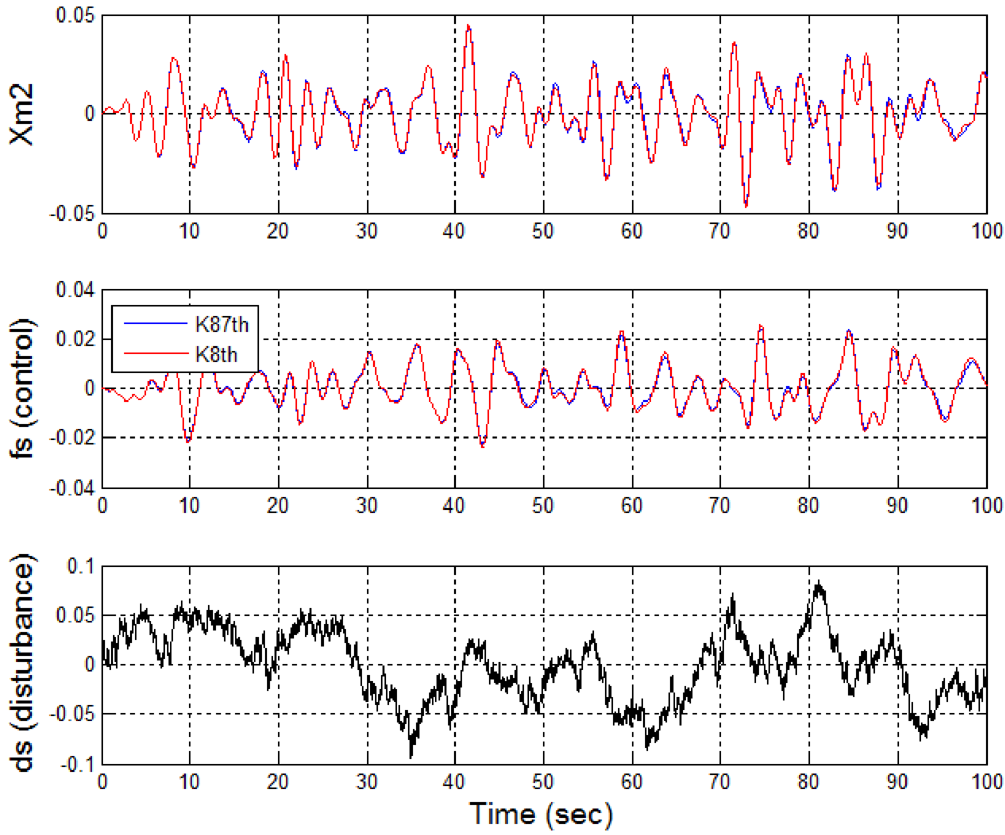

4.8. PRELIMINARY CONCLUSIONS

In this study a design of a Robust controller is accomplished providing Robust stability and Robust performance.

- The desired Robust performance is obtained through proposed weight functions for parametric uncertainties, delay and inertial actuator uncertainty, besides the reduction of the frequency response of the propagation paths to mass accelerations of the Studied Plant.

- By using $\mathcal{H}_{\infty}$ controller for the Studied Plant, a cost function of 6.23 was achieved. In this case, it was considered to reduce the range of uncertainties of the model or, to decrease the signal range to reject. None of them was an option for this design. A mixed-mu complex synthesis was used to obtain an improved Robust performance.

- Furthermore, the μ-synthesis provided a more competent Robust performance in disturbance rejections at the same conditions of uncertainty. In this study is recommended the $\mathcal{H}_\infty$ Controller for systems with low range parametric uncertainties or designs with only stability requirements.
- Also, the complex μ-Synthesis procedure, when the modeled uncertainties are real-valued and they are considered as complex variables, produces a controller which uses more effort trying to compensate the imaginary value of the uncertainties.

5. ADAPTIVE CONTROLLER DESIGN

Within this Chapter, Active Vibration Control (AVC) for a three-cart problem is studied. A comparison of Adaptive Filters is implemented using the Filtered-x Least Mean Square (FxLMS) algorithm and Recursive Least Square (RLS) algorithm, when a correlated measurement of the disturbance is available. The proposed RLS compensator considers a Feedback coupling between the compensator and the measure of the disturbance. The secondary propagation path of the plant was estimated using System Identification (SI) Normalized LMS (NLMS) algorithm. The internal “positive” coupling is considered as a Finite Impulse Response (FIR) filter estimated by the Real Plant parameters. The propagation paths are fully identified as a group of transfer functions in series considering the electrical domain and mechanical domain. Simulations using DSP system toolbox of Matlab had shown a superior performance of RLS algorithm with a reasonable computer cost.

5.1. THREE-CART DYNAMICS WITH INERTIAL ACTUATOR

Figure 24 represents an AVC system using a vibration measurement correlated with the disturbance and an inertial actuator for reducing the residual acceleration. The system consists of five metallic plates connected by springs. The plates M1 and M3 are equipped with inertial actuators. M1 serves as disturbance generator (inertial actuator 1 in figure 24) and M3 serves for disturbance compensation (inertial actuator 2 in Figure 24). The system is equipped with a measure of the residual acceleration (on plate M2) and a measure of the disturbance being sensed by an accelerometer on plate M1.

Figure 24. Scheme of the Plant, AVC system

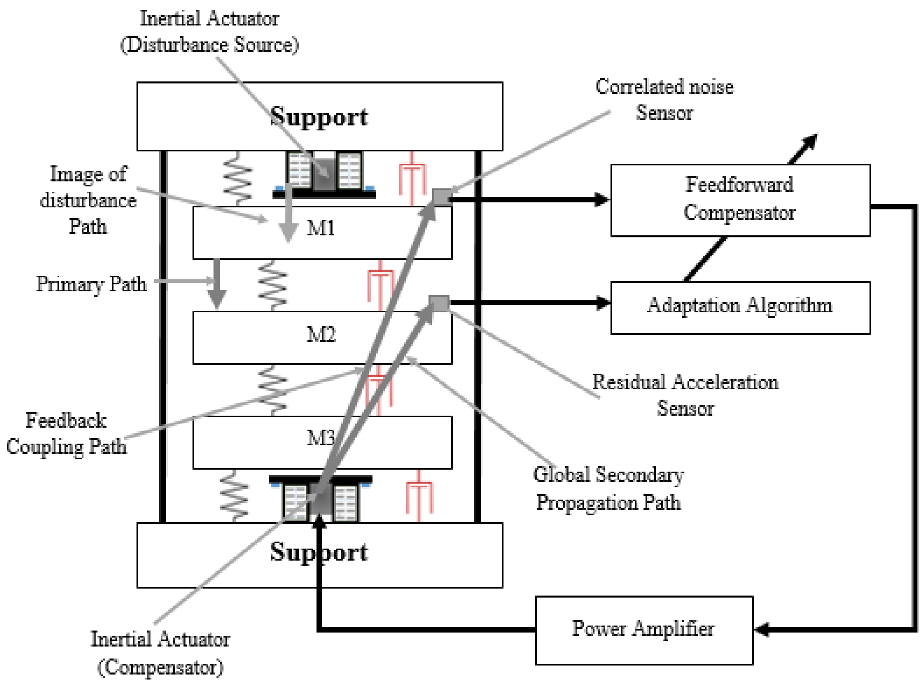

The path between the disturbance (in this case, generated by the inertial actuator on the top of the structure) and the residual acceleration is called the *Global Primary path*. The path between the measure of position M1 (an image of the disturbance) and the residual acceleration (in open loop) is called the *Primary path*, and the path between the inertial actuator for compensation and the residual acceleration is called the *Secondary path*. When the compensator system is active, the actuator acts upon the residual acceleration, but also on the measurement of the image of the disturbance (a positive feedback).

The disturbance is the pressure wave of the inertial actuator (see figure 24) located on top of the structure. The output of the compensator system is the pressure wave of the inertial actuator located at the bottom of the structure. The parameters of the filter are estimated to minimize the measurement of the residual acceleration. The block diagram of the AVC system can be observed in Figure 8. The $\boldsymbol{W_{dist}}(\boldsymbol{z})$ filter is emulating the band limiter filter and the power amplifier. The perturbation source is white noise filtered by $\boldsymbol{W_{dist}}(\boldsymbol{z})$ to obtain $\boldsymbol{d_s}(\boldsymbol{t})$. The filter $\boldsymbol{P_G}$ emulates the global primary path which contains the disturbance inertial actuator and the mechanical path between pressure wave and the residual acceleration. The filter $\boldsymbol{P_C}$ characterizes the dynamics of the disturbance source and the image of the disturbance (inertial actuator + dynamics of the mechanical system). The compensation actuator is modeled by the transfer function $\boldsymbol{Act}$ with the control signal as input and the pressure wave as output (power amplifier + the compensation inertial actuator).

The secondary path is represented by $\boldsymbol{S}$ block which models the dynamics of the travel of the pressure wave from the compensation inertial actuator to the residual acceleration in the absence of the disturbance. $\boldsymbol{Fc}$ is the block that emulates the mechanical path between the inertial compensator actuator and the correlated disturbance. The feedforward compensator is the $\boldsymbol{K_{adaptive}}$ block with $\ddot{\boldsymbol{X}}_{\boldsymbol{1}}$ as the correlated noise and the residual acceleration (the desired signal) as inputs and the output $\hat{\boldsymbol{u}}(\boldsymbol{t})$ is the control signal. The value of $\ddot{\boldsymbol{X}}_{\boldsymbol{1}}$ is the sum of the correlated disturbance measurement $\ddot{\boldsymbol{X}}_{\boldsymbol{1}_{\boldsymbol{p}}}$ obtained in the absence of the feedforward compensation (see figure 25(a)) and the effect of the actuator used for compensation.

Figure 25. Block diagram of the plant of the AVC system a) open loop b) with the feedforward compensator

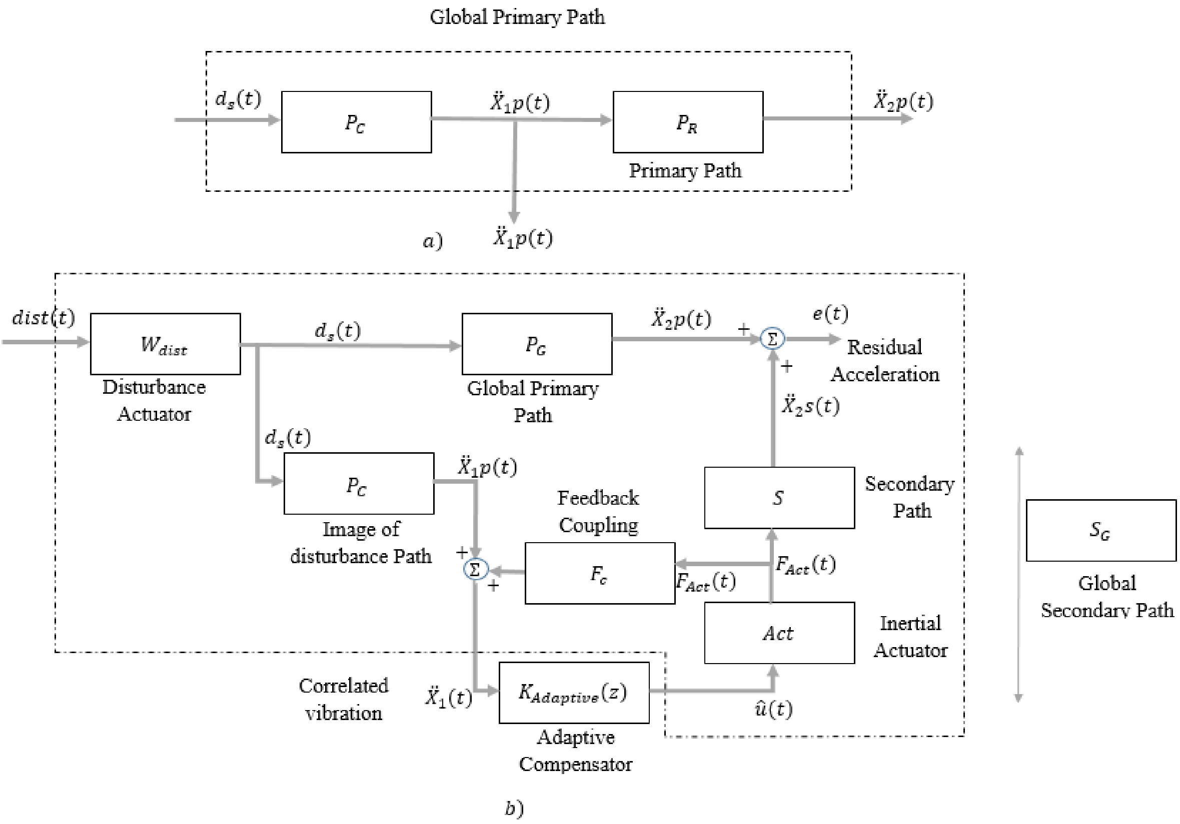

5.2. SYSTEM IDENTIFICATION OF THE PROPAGATION PATHS

A System Identification process was implemented to estimate the impulse response of the four propagation paths in the AVC system. The models obtained consider the Unmodeled Dynamics inherent to the simplification of the Plant. The SI process applied an Adaptive Filter with Normalized LMS algorithm to adapt the impulse response of the Unknown System (Nominal plant + uncertainties + the measurement error) injecting band limited noise to both i.e. the Adaptive Identification System and the Unknown System and comparing theirs responses, see Figure 26 (a)

Figure 26. Block Diagram of the System Identification Using the NLMS Adaptive Filter

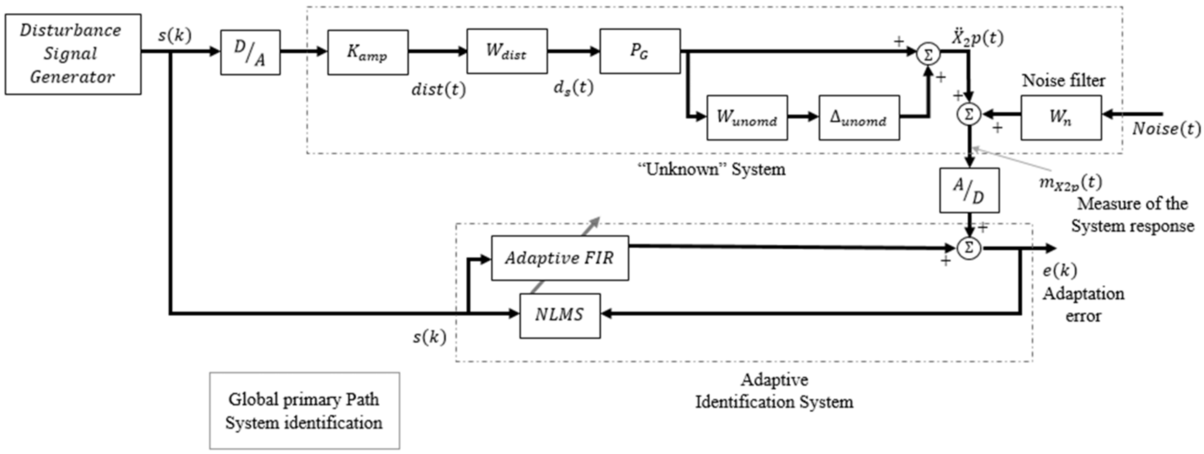

a)

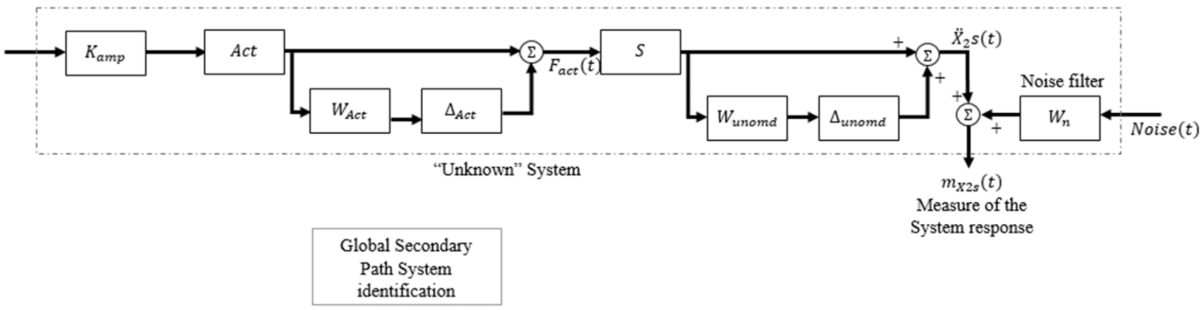

b)

The initial coefficients of the Adaptive Filters, that identify each system, are taken as the coefficients of a FIR filter. This filter emulates the impulse response obtained initially for each propagation path. The FIR filter obtained has a response time of 10 ms. the identification process of the filter is shown in Figure 27. The main characteristic of this new filter is the length of the secondary path filter estimated since it is not as long as the actual secondary path and does not need to be like so that the control is adequate in most cases. The excitation signal used to identify the different paths of the system was a broad band white noise signal, and then used an impulse response to verify the accuracy of the estimation.

Figure 27. Primary path SI Using the NLMS Adaptive Filter with 1000 Filter order

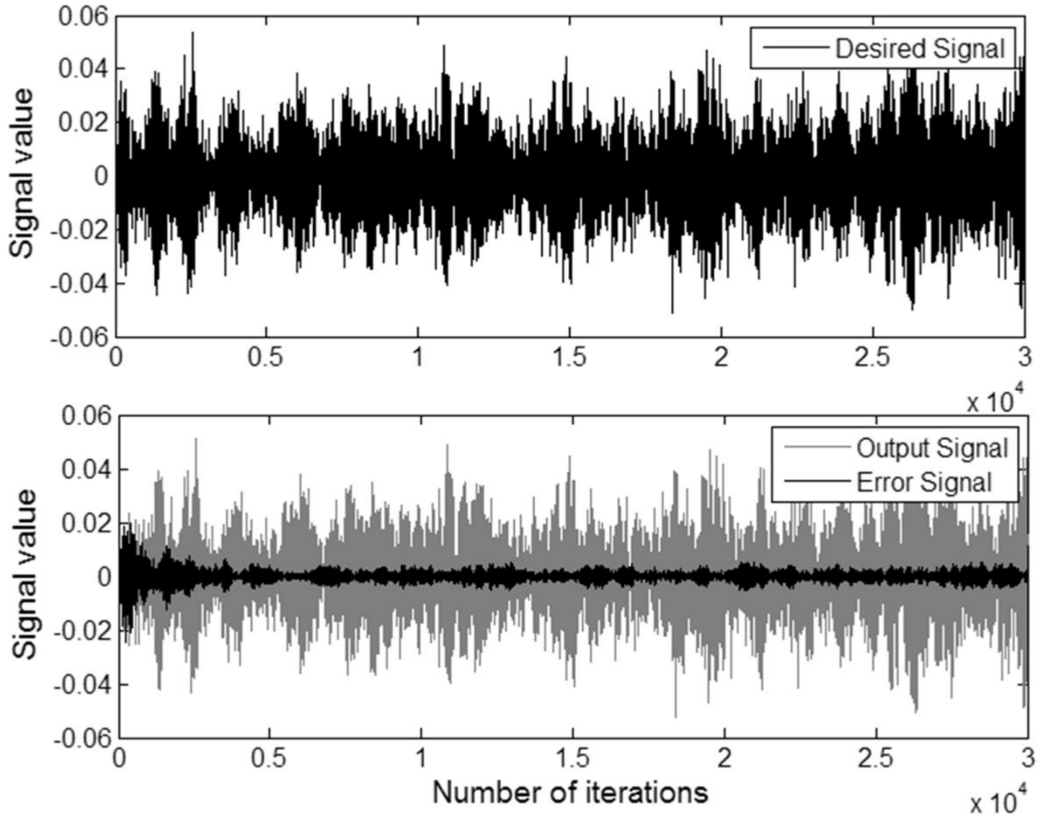

The same Identification was applied using a 500 Filter order.

Figure 30 shows the behavior of the estimated secondary path impulse response and the comparison with the real path.

Figure 28. Primary path Impulse response identification

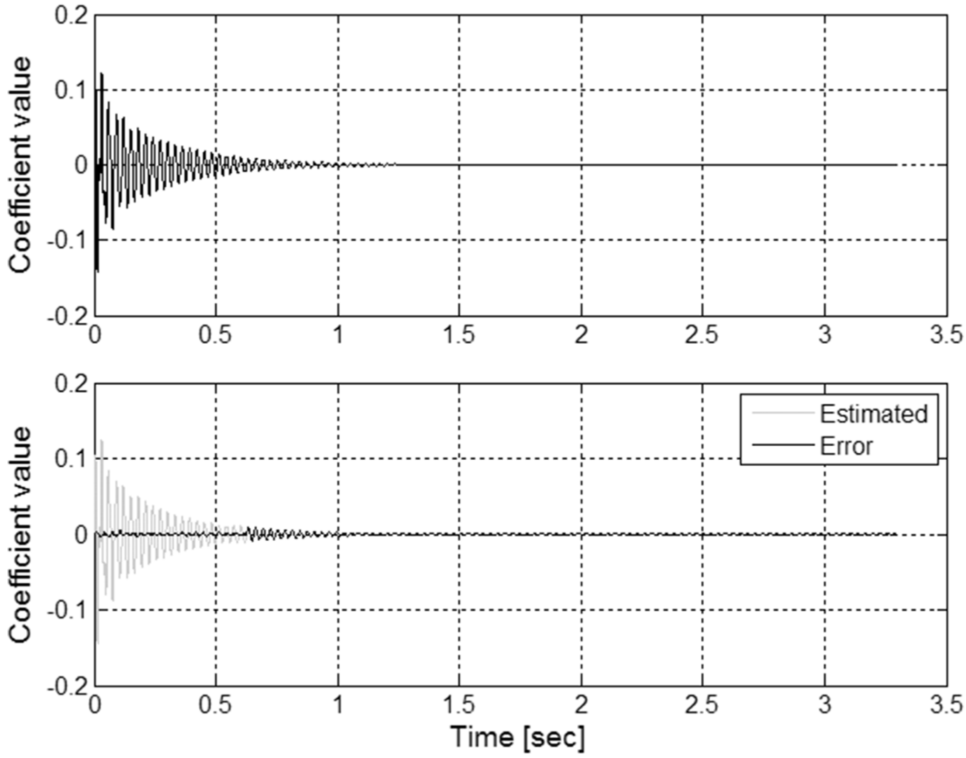

Figure 29. Primary path SI Using the NLMS Adaptive Filter with 500 Filter order

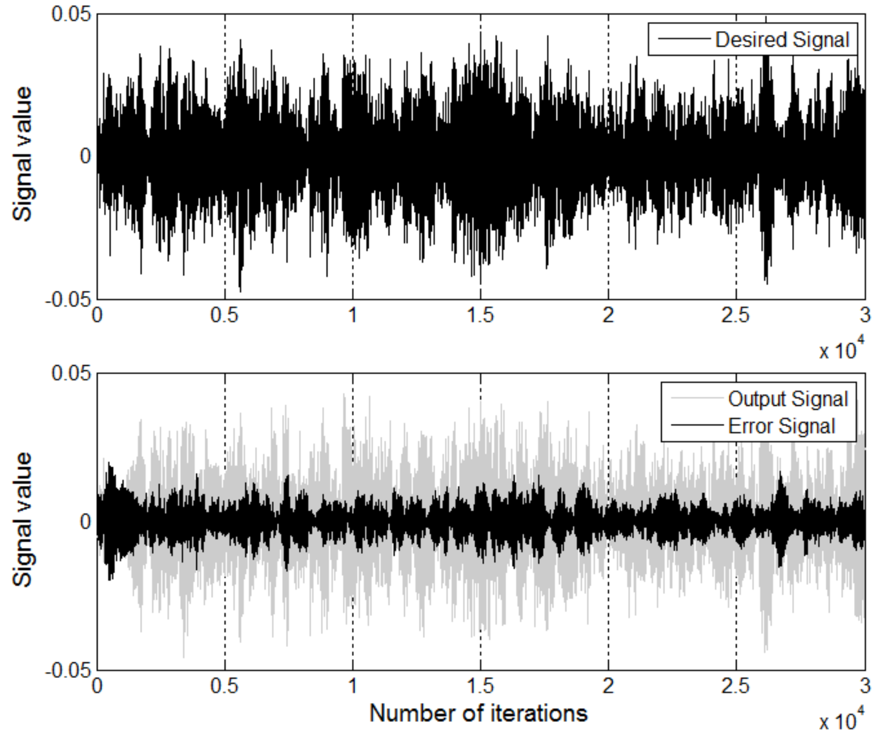

The accuracy of the 500 FIR filter is low. The performance in the estimation of the true impulse response tail is poor and affects significantly the operation of the AVC system during its operation in the chosen task. After matching the two results it is concluded that the ideal size of the FIR filters for the System Identification spans between this two values. 800 Filter order was chosen because of its performance in contrast to its computational cost.

SI was performed independently from Vibration Control; however, it is part of this as a separate function that can be used each time the error of the disturbance rejection is very large, or cannot be reduced by the action of the controller due to drastic changes of operating point. In other words, it is a way to generalize the control solution.

The FIR filters that emulate the propagation paths of the Studied Plant are presented in Figure 30. For the purposes of studying adaptive filters, these filters are not changed and the input signals of the system will be kept in the same range. The frequency characteristics of the various paths are shown in Figure 31.

Figure 30. Frequency characteristics of the primary, secondary and reverse paths

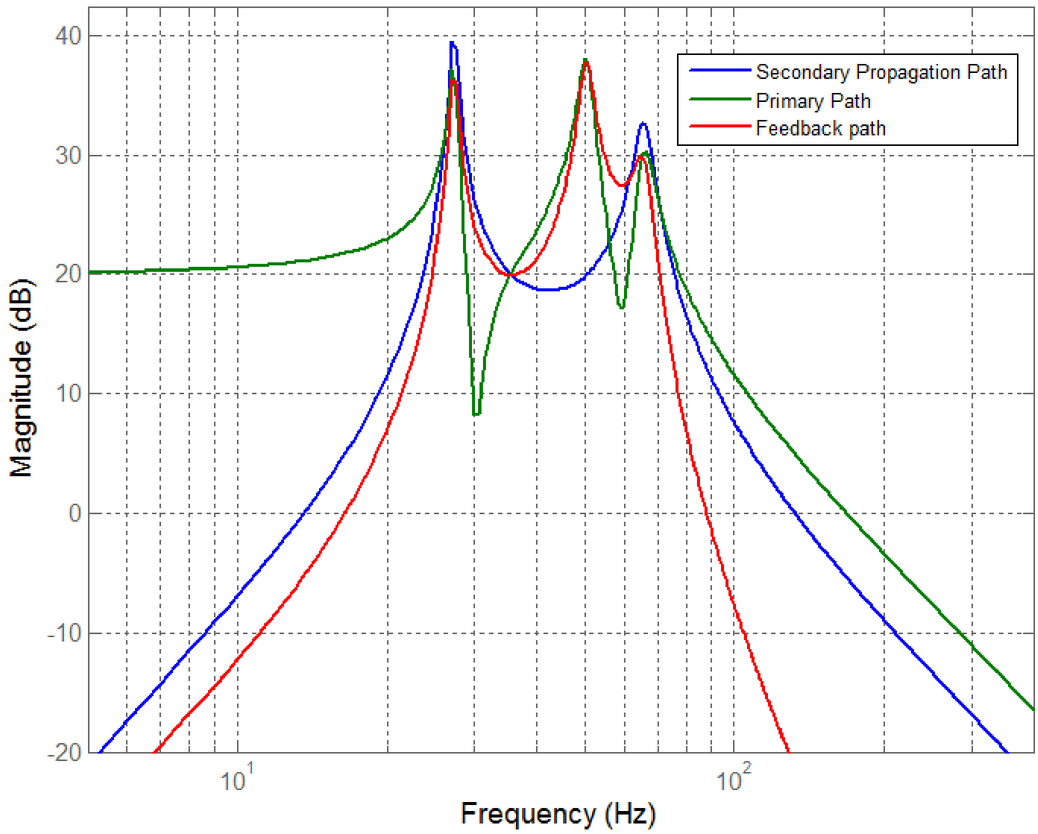

5.2.1. SI Global Primary Path FIR Filter

The primary propagation path $\boldsymbol{P_C}$ is modeled by a linear filter. This Filter was obtained in absence of compensation and by observing the correlated accelerometer signal after an impulse disturbance was applied. The coefficients of the FIR impulse response filter represent the response of the entire global primary path.

Figure 31. SI of Global Primary path using the NLMS Adaptive Filter. a) Estimation Error b) Magnitude response of the FIR filter

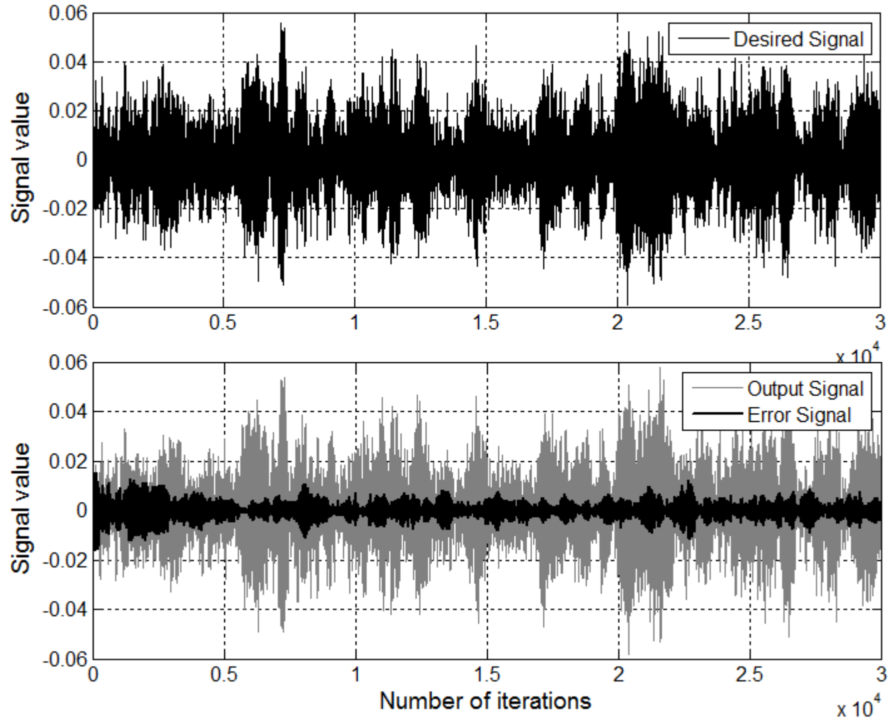

a)

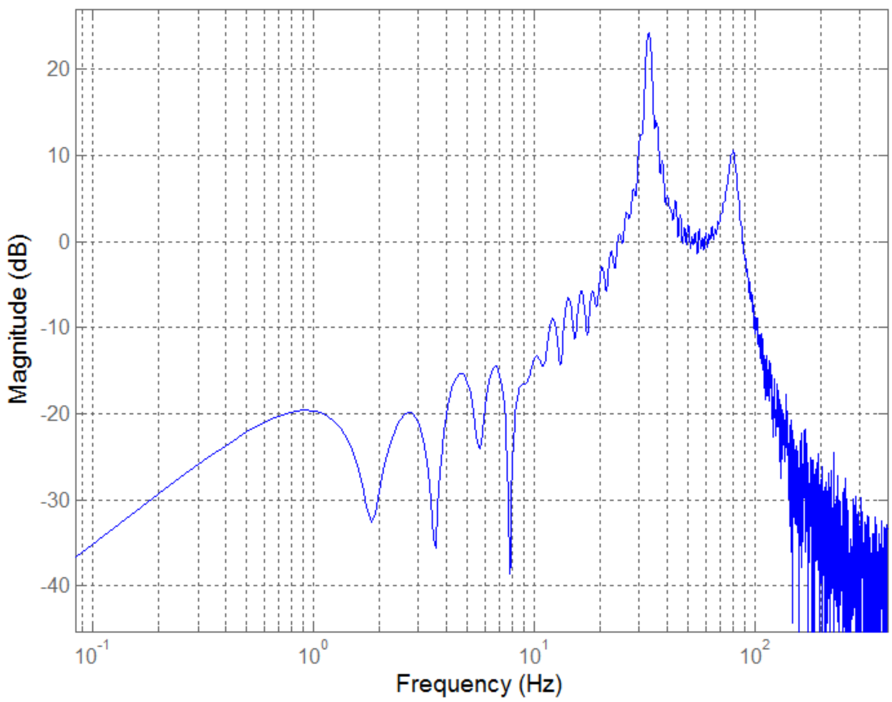

b)

5.2.2. Feedback Coupling Propagation Path Identification

The Propagation path of the “Additive” Feedback Coupling is the effect of the compensation inertial actuator over the correlated accelerometers in the absence of perturbation.

Figure 32. SI of the Feedback Coupling path, using the NLMS Adaptive Filter. a) Estimation Error b) Magnitude response of the FIR filter

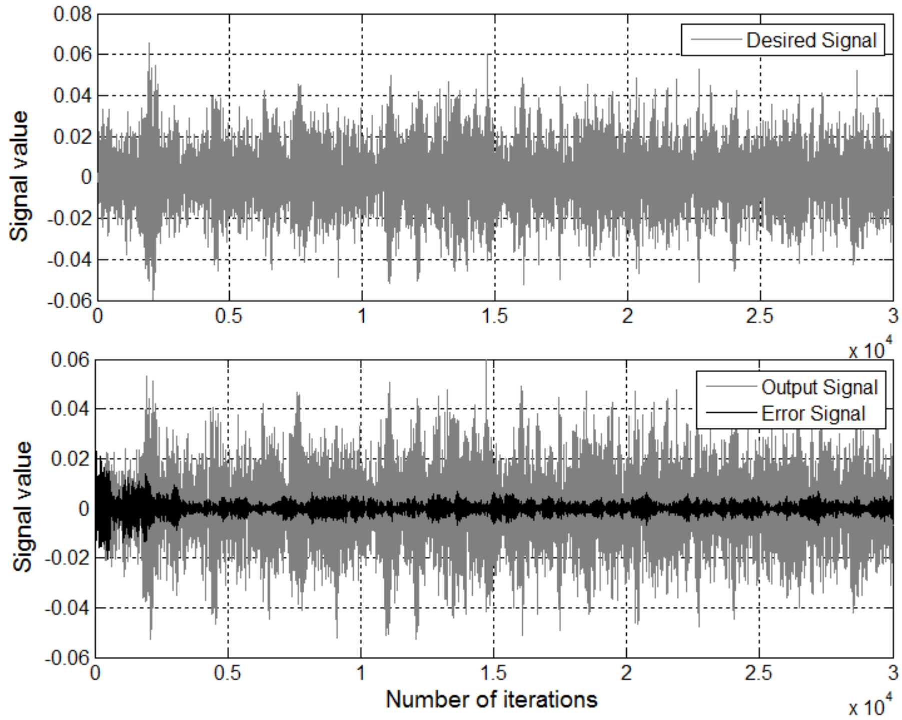

a)

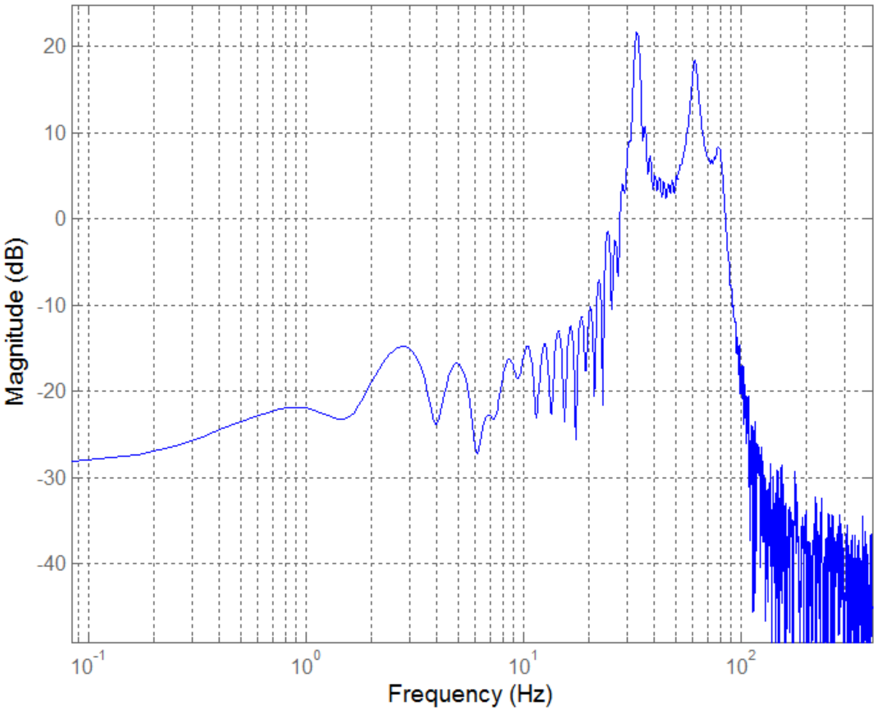

b)

5.2.3. Image of the Disturbance Path

Image of the Disturbance Path is the effect of the disturbance inertial actuator over the correlated accelerometers in the absence of compensation or disturbance rejection.

Figure 33. Image of the disturbance path Identification Using the NLMS Adaptive Filter. a) Estimation Error b) Magnitude response of the FIR filter

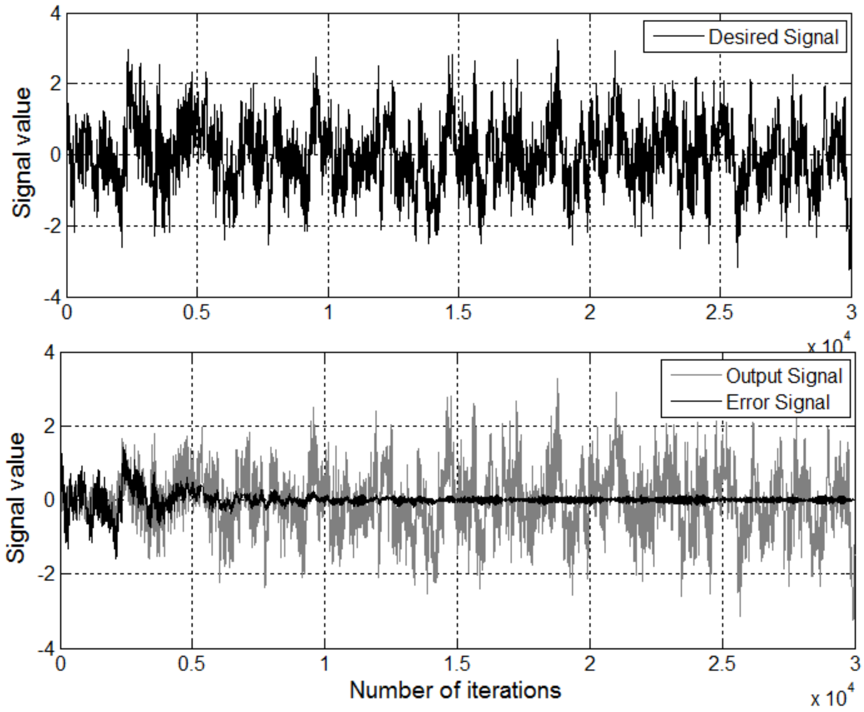

a)

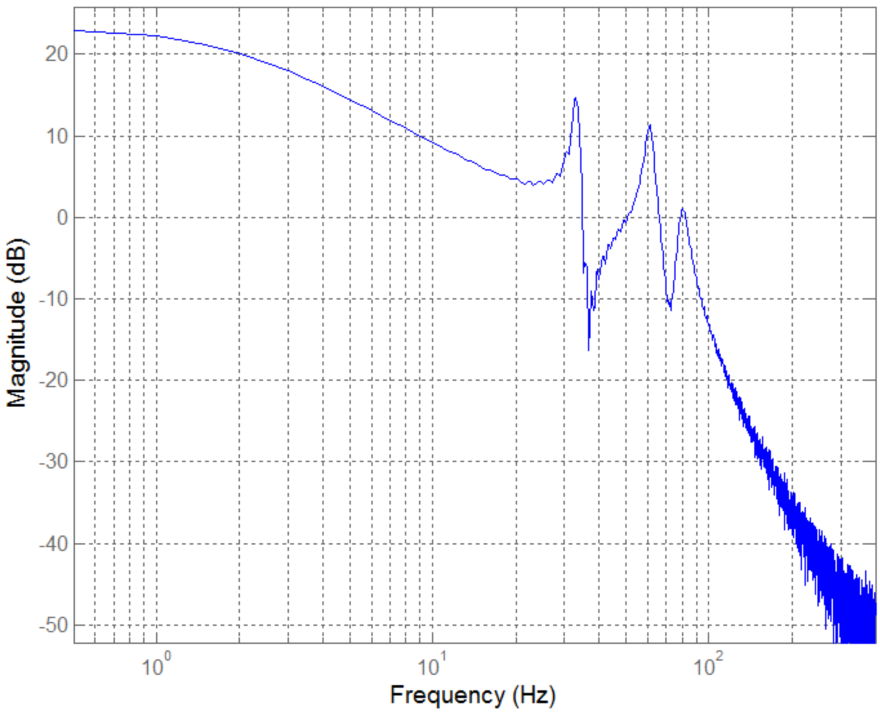

b)

5.2.4. SI Secondary Path

System Identification of the secondary path was applied when there was absence of disturbance and white noise was applied through the compensator inertial actuator.

Figure 34. Secondary Path Identification Using the NLMS Adaptive Filter. a) Estimation Error b)Magnitude response of the FIR filter

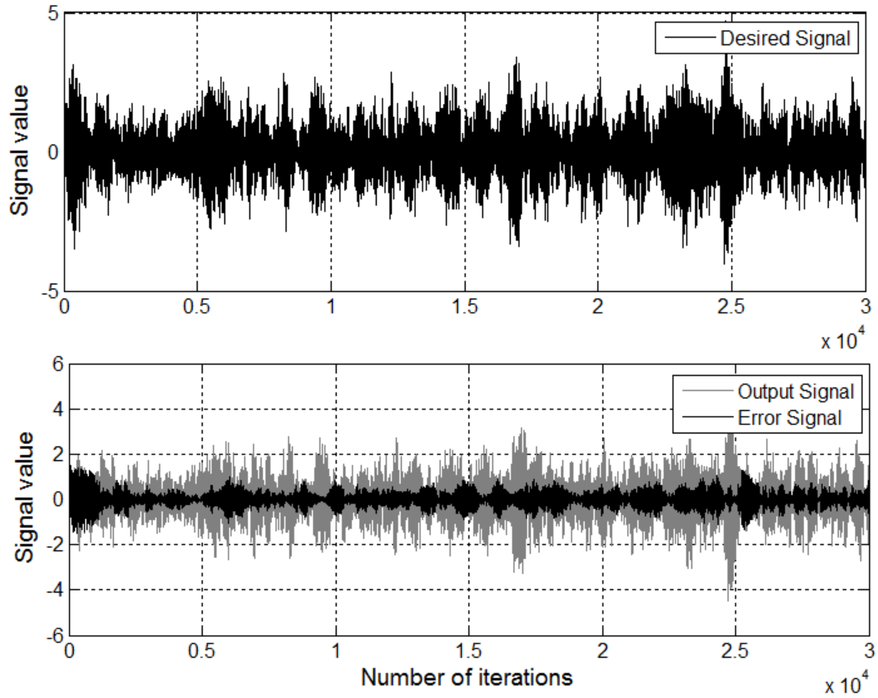

a)

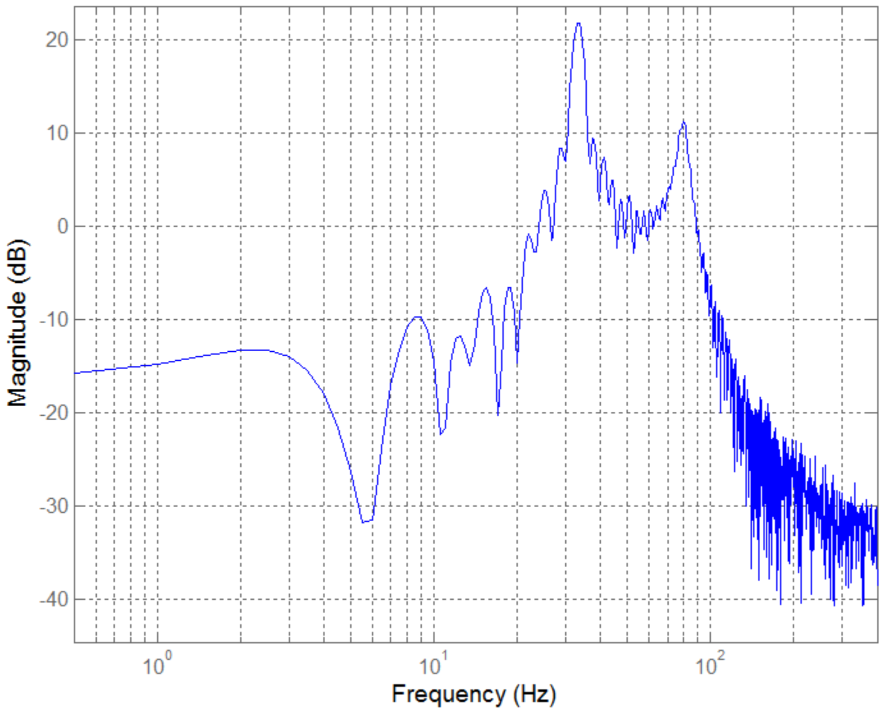

b)

5.3. AVC USING FILTERED-X LMS FIR ADAPTIVE FILTER

In the design of the FIR Adaptive Filter using the filtered-x LMS algorithm was not considered the additive feedback coupling. The correlated noise is the measure of the image of the perturbation (See Figure 35), $\ddot{X}_1(t)$ and the desired signal is $\ddot{X}_2(t)$. The Adaptive Compensator is a Feedforward controller with a step size of 0.01.

Figure 35. a) Schematic arrangement of Feedforward AVC system with FxLMS

b) Block Diagram

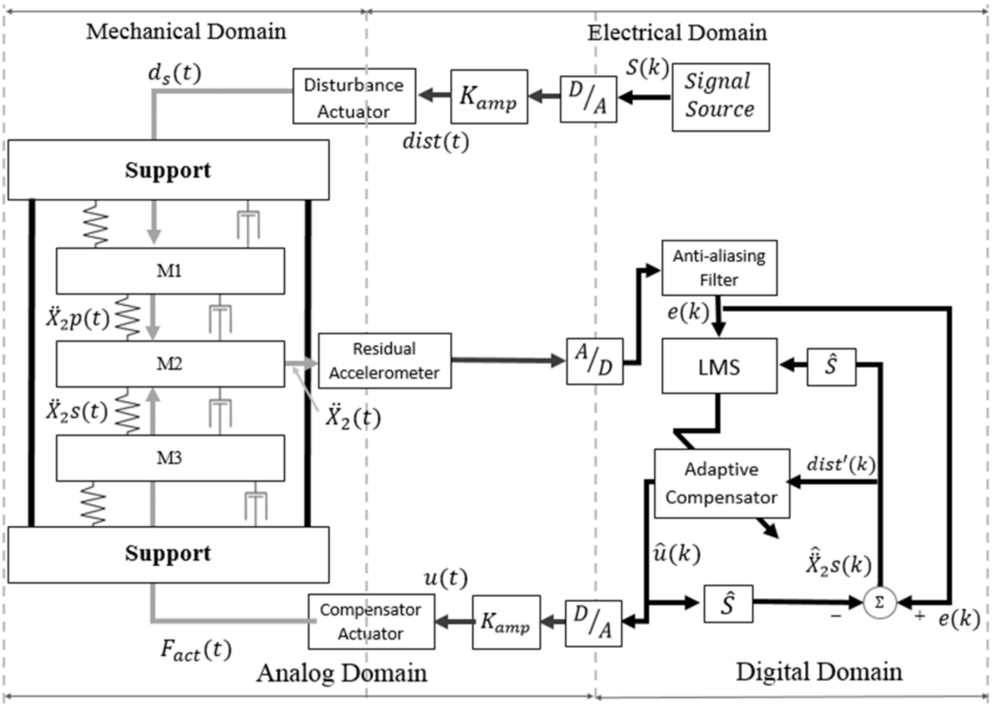

a)

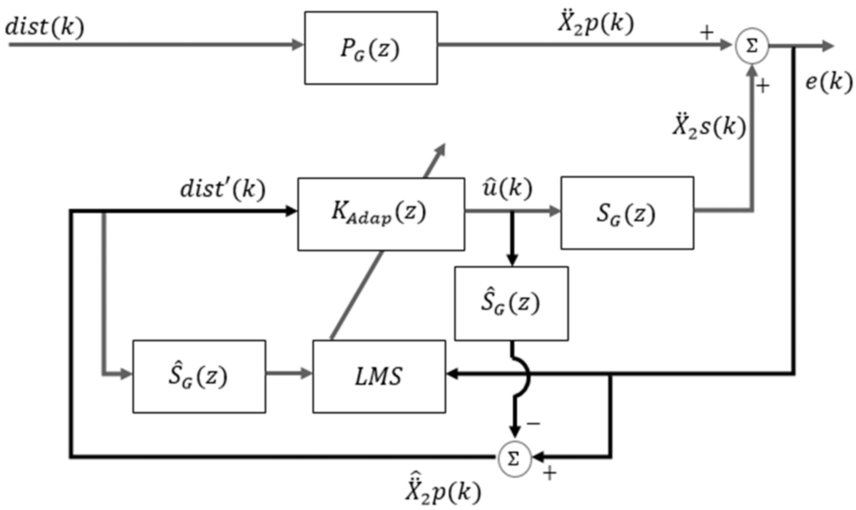

b)

The experiments had been carried out by first applying the disturbance in open loop during 30 seconds and after that by closing the loop with the adaptive Feedforward-Feedback algorithms. Time domain results obtained in open loop and with the compensator (using Adaptive Feedforward compensation algorithm) on the AVC system are shown in Figure 35. The filter for algorithm had been computed based on the parameter estimation obtained from the SI process. The band limited disturbance frequencies source emulates the bandwidth attribute of the rotating machinery vibration. Specifically, generated noise might come from a typical electric servomotor.

The Figure 36 shows the resulting power spectral of the residual acceleration. Channel 1 is the residual accelerometer without compensation and channel 2 is the residual acceleration with compensation. In Figure 36, channel 2, it is observed frequencies of 21 and 50 Hz. The higher components of the disturbance are attenuated below -40 dB. On the other hand, a decrease in the compensation performance at components of 34 and 36 Hz is observed. These components are partially ignored by the compensator algorithm and give the maximum amplitude value of the error signal.

Figure 37 shows the disturbance rejection of the system using Feedback FxLMS Algorithm.

Figure 36. Power spectral of AVC of the Filtered-x LMS

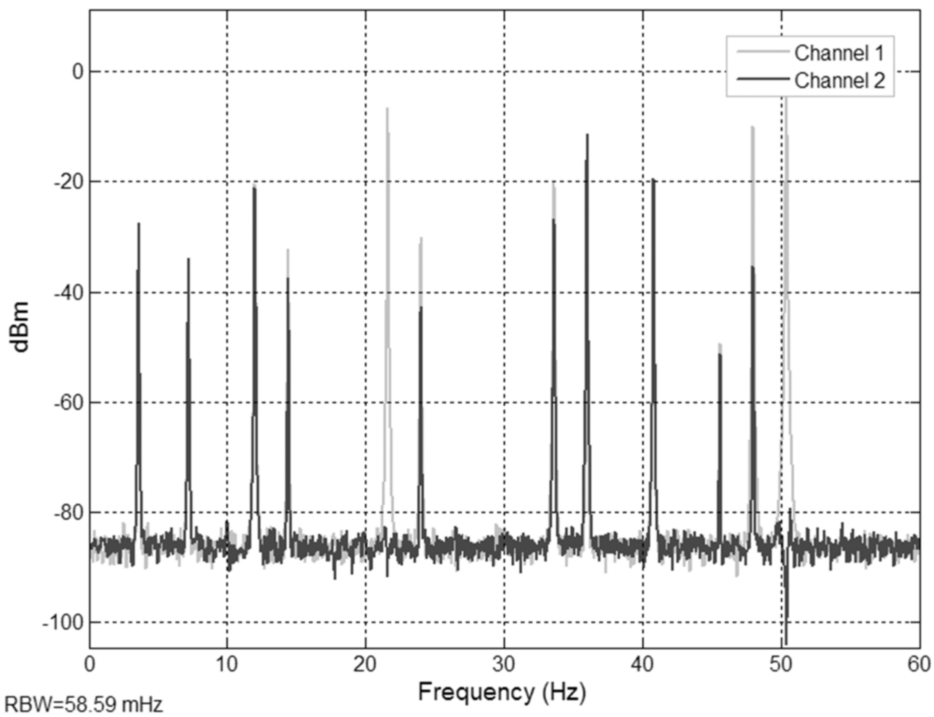

Figure 37. Disturbance rejection of the feedback Filtered-x LMS

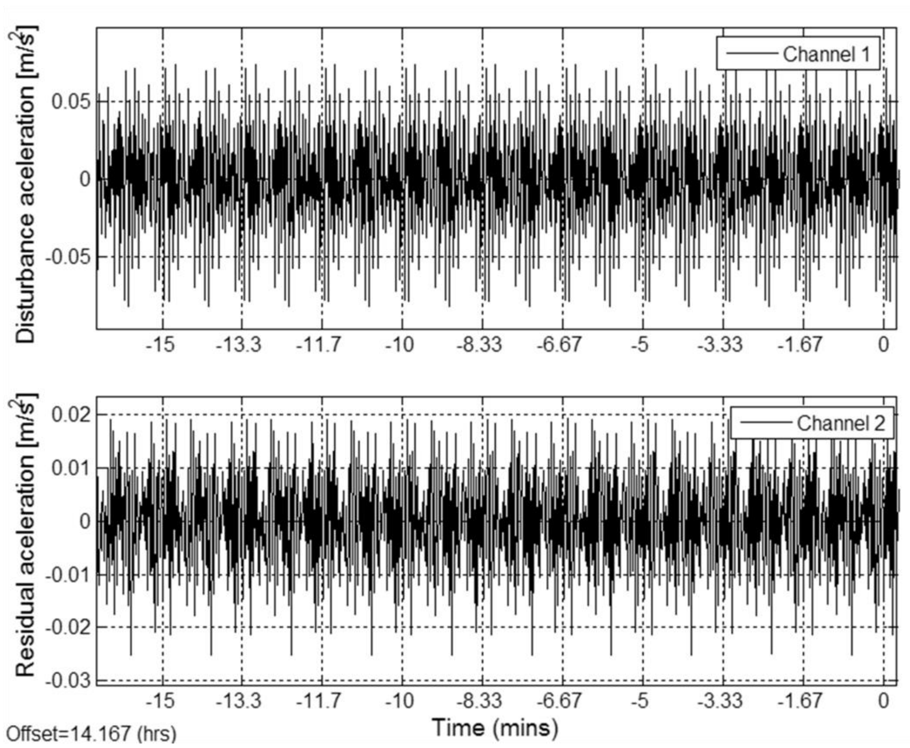

The results are shown as a plot of the residual acceleration measured by the residual accelerometer $[m/s^2]$ seen in Figure 38 and they are quantified as the variance of the history of the residual force (error) in mass 2. The variance of the residual error with the Feedforward compensator is: $var(e(t)) = 0.0019(16.40dB)$, with a reduction of $(26.40dB)$ compared with the open loop Plant.

5.4. ADAPTIVE FEEDBACK AVC USING FxLMS ALGORITHM

A new approach was proposed to improve the attenuation of the disturbance: the Feedback Control scheme using FxLMS algorithm. The Figure 38 shows the scheme of the Adaptive Feedback AVC System. The system synthesizes or regenerates its own reference signal, using an estimated path and the Adaptive Filter output and the error signal. The advantage of this scheme is the use of only one accelerometer. The reference signal or primary noise is expressed in Z-Domain as $Dist'(z) = E(z) + \hat{S}_G(z)y(z)$ where$\hat{S}_G(z)$ is the estimated secondary propagation path, and $E(z)$ the error signal. $y(z)$ is the secondary signal produced by the Adaptive Filter.

Figure 38. Schematic arrangement of feedback AVC system with FxLMS b) Block Diagram

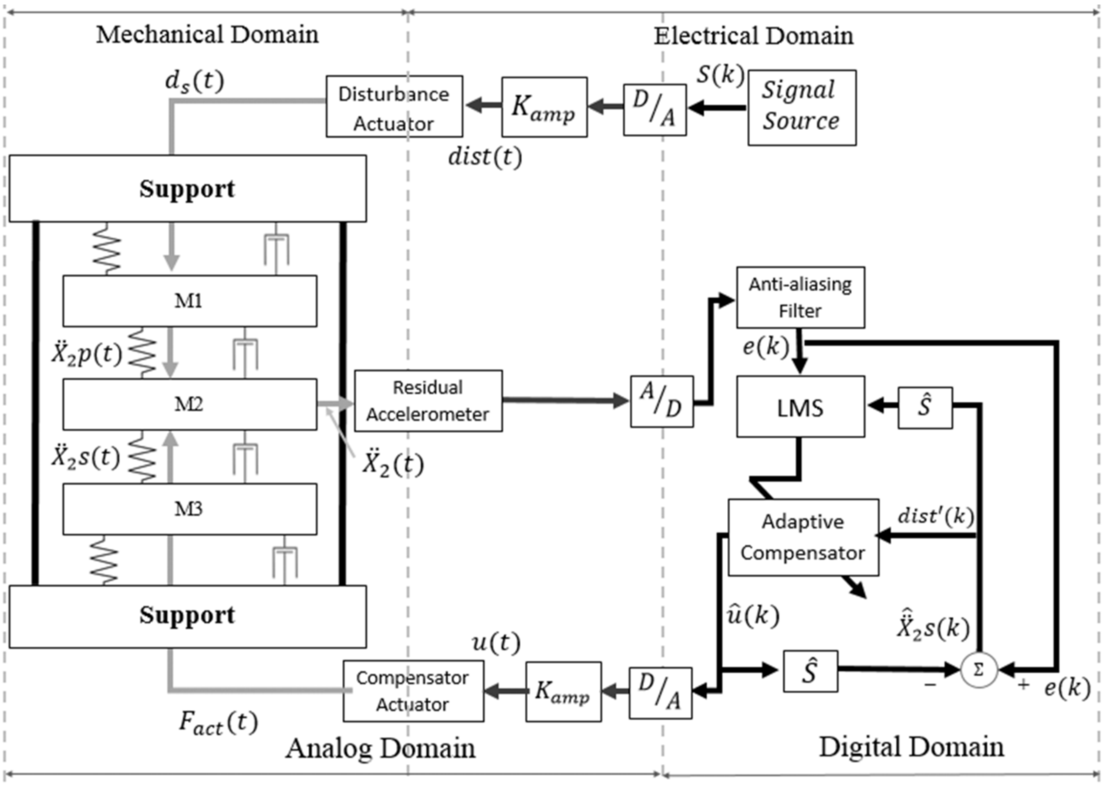

a)

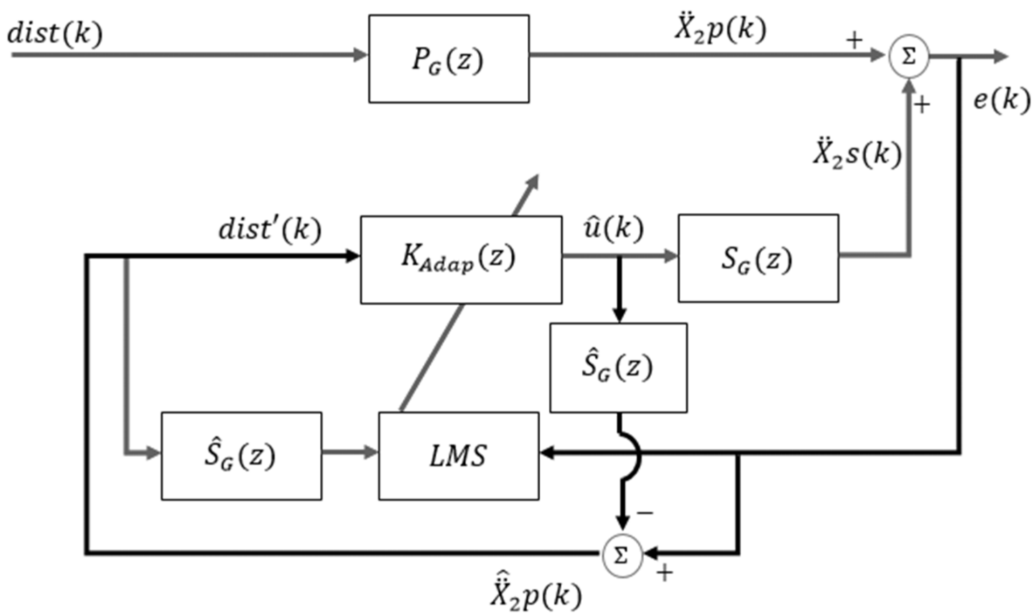

b)

When comparing Figures 37 to Figure 39 can be noted a decrease in performance of the compensation when the Adaptive Feedback FxLMS was implemented. The lack of compensation performance is attributed to the SI process because, although, the correlation between the desired signal and the correlated signal is 1, the system was incapable to fully identify specific values of frequencies.

Figure 39. Disturbance rejection of the AVC using feedback FxLMS

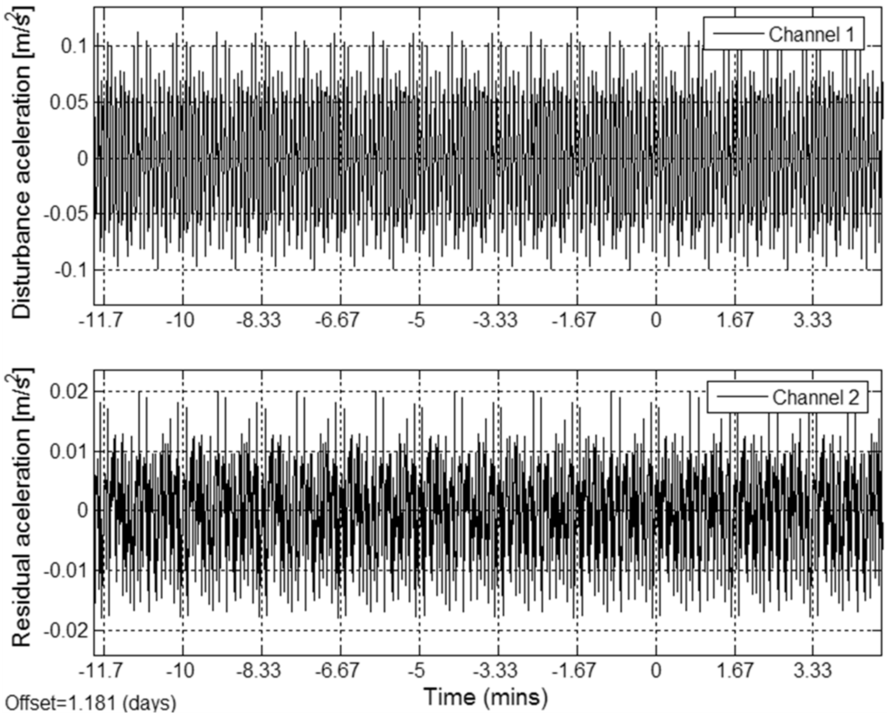

The Figure 40 shows frequency spectrum of the closed-loop system. The higher peaks to attenuate at 21 and 50 Hz can be observed in Channel 1. The Feedback FxLMS AVC has a higher computational cost due to the calculation of the reference disturbance signal. The Feedback Compensator has less time than Feedforward compensators to minimize the residual error, making the value of the cost function higher or in this case for the same cost a lower performance of the disturbance rejection.

The AVC system feedback has a lower performance in rejecting the disturbance than the compensator in Feedforward. This is because the reference signal is disturbed by the modeling propagation paths by filtering part of the information about which frequencies must be rejected. This gap of information on the reference signal, the non-rejected frequencies, occurs in the digital domain where the reference signal is calculated, and is affected by the order of the FIR modeler filters. Actual Plant dynamics do not lessen these frequencies, so to make a decision; the compensator misses attenuated frequencies in the calculation. Therefore, the compensator does not attenuate these frequencies, as it does not take action on them.

Figure 40. Power spectral of the AVC system using feedback FxLMS

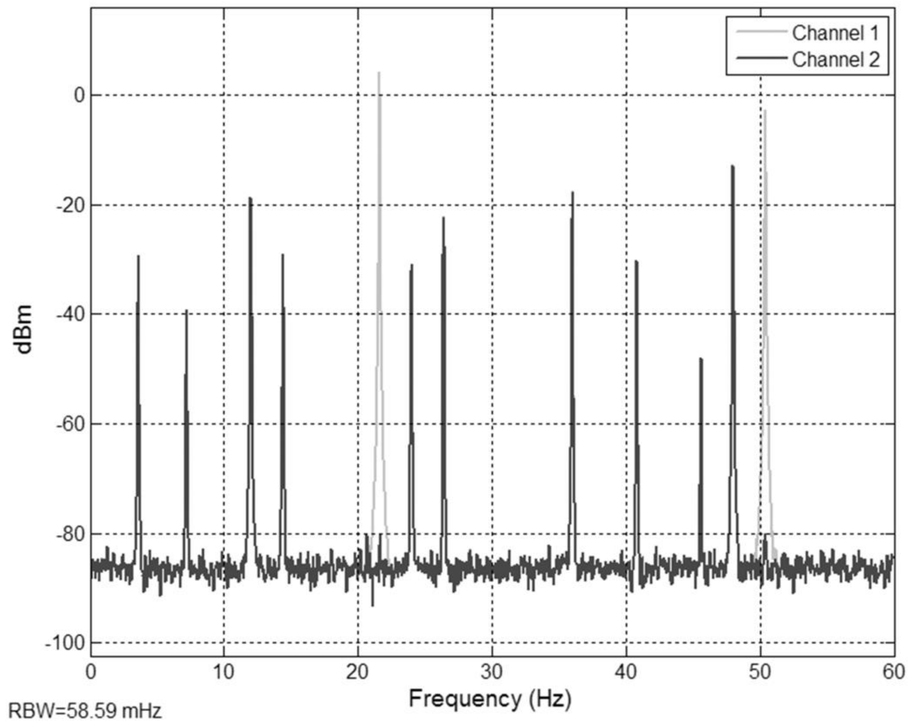

For an algorithm of minimization like the LMS, linear error alone is not robust enough to counteract this disturbance in the reference signal.

When the feedback controller is active, the variance of the residual acceleration is: $var\big(e(t)\big) = 0.02(16dB)$ with a disturbance rejection of $(20dB)$.

A reasonable length (300) of adaptive filter order is used because the augmentation of this value can affect the real response of the system caused by the extra calculation of the order. In this study, the FxLMS algorithm and the RLS algorithm were selected due to their simplicity, deriving in low computational cost. On the other hand, many other control applications complement the compensation of this controller with an extra reasonable computational cost, less than trying to augment the length or order of the applied compensator.

5.5. ADAPTIVE FEEDFORWARD AVC USING RLS ALGORITHM WITH FEEDBACK COUPLING

A new control scheme was proposed in order to improve the performance observed in the Feedforward FxLMS. The new compensator considered the Feedback Coupling caused by the compensator actuator affecting the correlated disturbance as shown in Figure 25. The performance of the new control scheme can be noted in Figure 41. In this Figure is presented the frequency response of the residual acceleration with and without compensation in Channel 2 and Channel 1 respectively:

The peaks observed in the spectrum of channel 2, Figure 41, are the frequencies applied as the disturbance source. The attenuation of the highest peaks on channel 1 at 18Hz, 30Hz and 42 Hz is observed. The maximum value of the attenuated signal in this new scheme is at 42 Hz frequency as noted in the FxLMS scheme. Therefore, the RLS algorithm is capable of identify and compensate this frequency value.

Figure 42 shows the residual acceleration of the Plant with and without compensation to attenuate the disturbance.

Figure 41. Power Spectrum of AVC System using RLS algorithm with Feedback Coupling

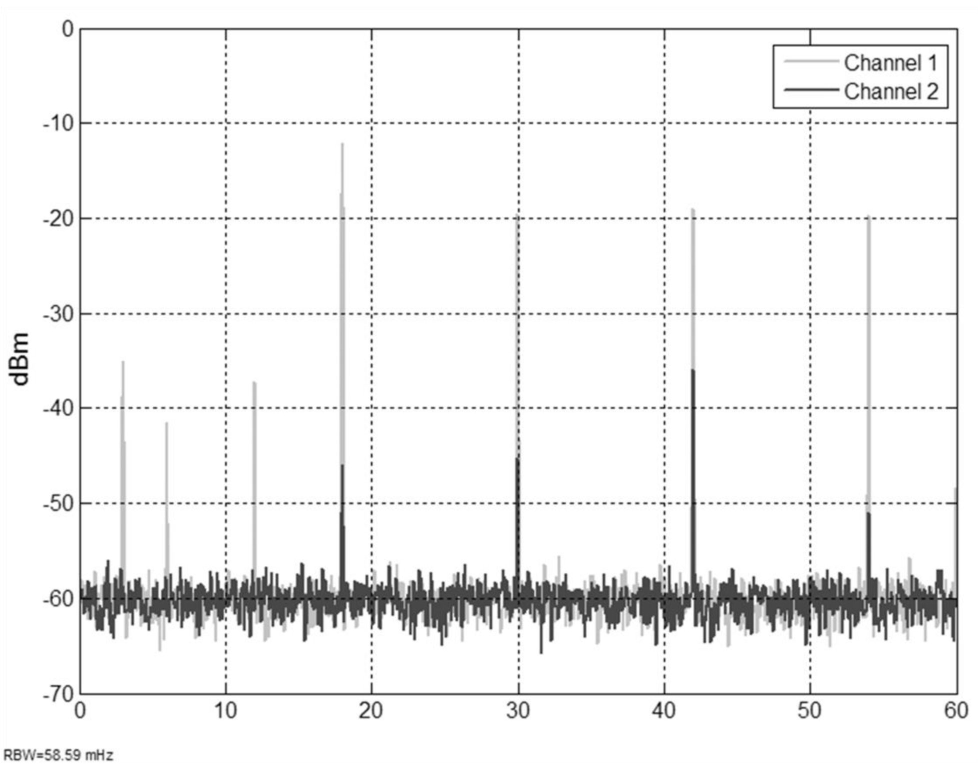

When using only adaptive feedforward compensation RLS, the variance of the residual acceleration is $var(e(t)) = 0.003(36dB)$ with a reduction of $(39.2dB)$. Clearly, RLS scheme brings a significant improvement in performance in respect to the other schemes offering adaptation capabilities to the disturbance characteristics.

Figure 42. Disturbance rejection of the AVC using RLS algorithm with feedback coupling

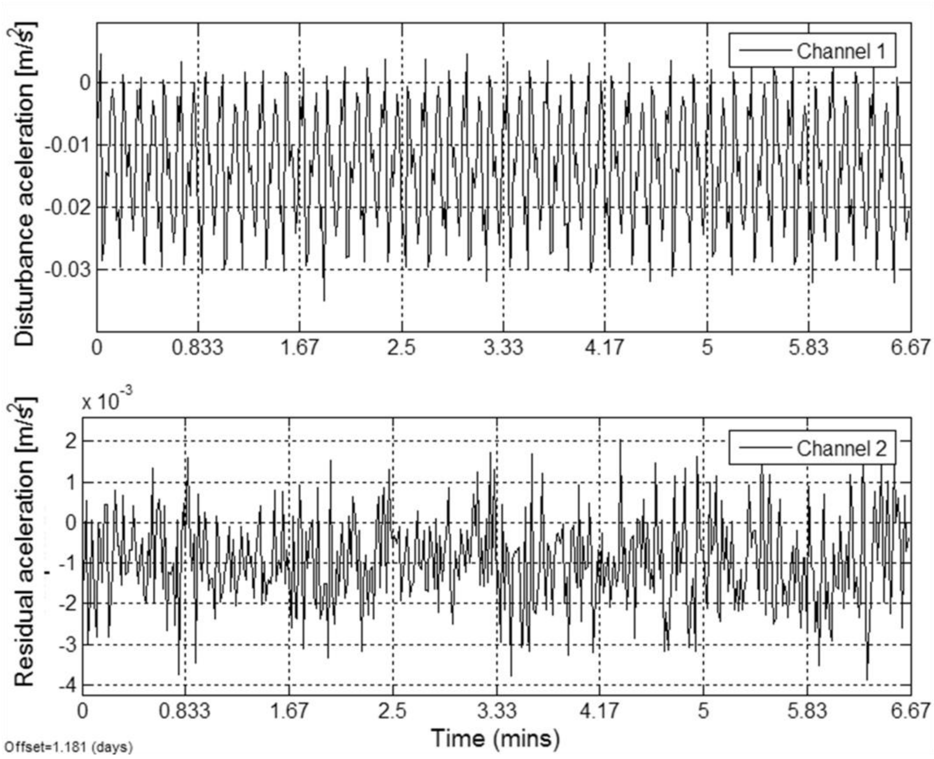

5.6 PRELIMINARY CONCLUSIONS

Present study took three different designs of Adaptive Filter with FxLMS algorithm and RLS algorithm applied to periodical disturbances rejection.

- The attenuation of the FxLMS Feedforward AVC System uses a reasonable amount of effort to find the opposite form of the perturbation to attenuate the disturbance. There are not many operations out of the block algorithm. This is a reliable form to attenuate the perturbation.

- There are frequencies that are ignored in the adaptation algorithm within the compensation of the Feedforward AVC systems due to extra calculation added in the simulation. These frequencies are the reason of the maximum amplitude value of the residual acceleration.
- To perform the attenuation of the disturbance the design of the Feedback AVC System using the FxLMS is developed. Although, the correlation between the two input signals of the adaptive filter is high. The algorithm does not attenuate all the frequency response of the residual acceleration. This is caused by corrupted signal due to the extra calculation added to extracted the reference signal.
- Using the Feedforward AVC system with RLS algorithm and considering the Feedback Coupling showed improved results in the attenuation of the disturbance. Although, the Feedback Coupling may cause instability when the wrong adaptation step is used. This happens because of its offset sum of the Feedback Coupling plus the image of the disturbance.
- Implementing AVC with "The Feedback from Compensation" instead of using the estimated secondary path filters, is closer to the real propagation path model, and hence the real Plant dynamics.

6. COMPARATIVE ANALYSIS

The difference between Robust Control and Adaptive Control is the way the lack of knowledge we have about the Plant to be controlled can be compensated.

Robust Control carries out an investigation on the life of the Plant, trying to find all the uncertainties that could lead to model the System. Under this investigation we found these uncertainties during: the design and construction of the System to find the uncertainty in the constants (parameters) of the model; the relationship between the Plant with surroundings to understand the uncertainties that may affect the normal behavior of the model; and the Plant operation to understand the possible changes in control operating points, all in order to convert these uncertainties in part of the model of the Generalized Plant. Thus, find a “worst-case” situation to design the controller. Following this idea, we cannot say that there is an ideal Driver situation, but the suboptimal or optimal Driver for the model that attempts to emulate the Plant. The more the model approaches the actual Plant, the most optimal the driver would be. But more effort is needed to design it. When designing the controller, the determining factor is not necessarily to find the closest model to reality but the most suitable to the specific application.

Adaptive Control seeks to compensate the uncertainties on the Plant lifetime. This is achieved by focusing on increasing the response capacity of the controller to a set of possible responses of the Machine. The bigger and more varied the set of answers to control; much more great must be the capacity for decision, making your controller a generalized design. Also, the computational cost is increased, becoming it a trade-off relationship. The controller may compensate for uncertainties, recognizing and cataloging them, whether, they are inherent to the lack of accuracy of the design or the operation of the plant, staggering the phases of adjustment or increasing the number of adaptive filters.

6.1. RLS ADAPTIVE FILTER

Figure 43. Disturbance rejection using RLS algorithm Feedforward Compensator: Residual Acceleration

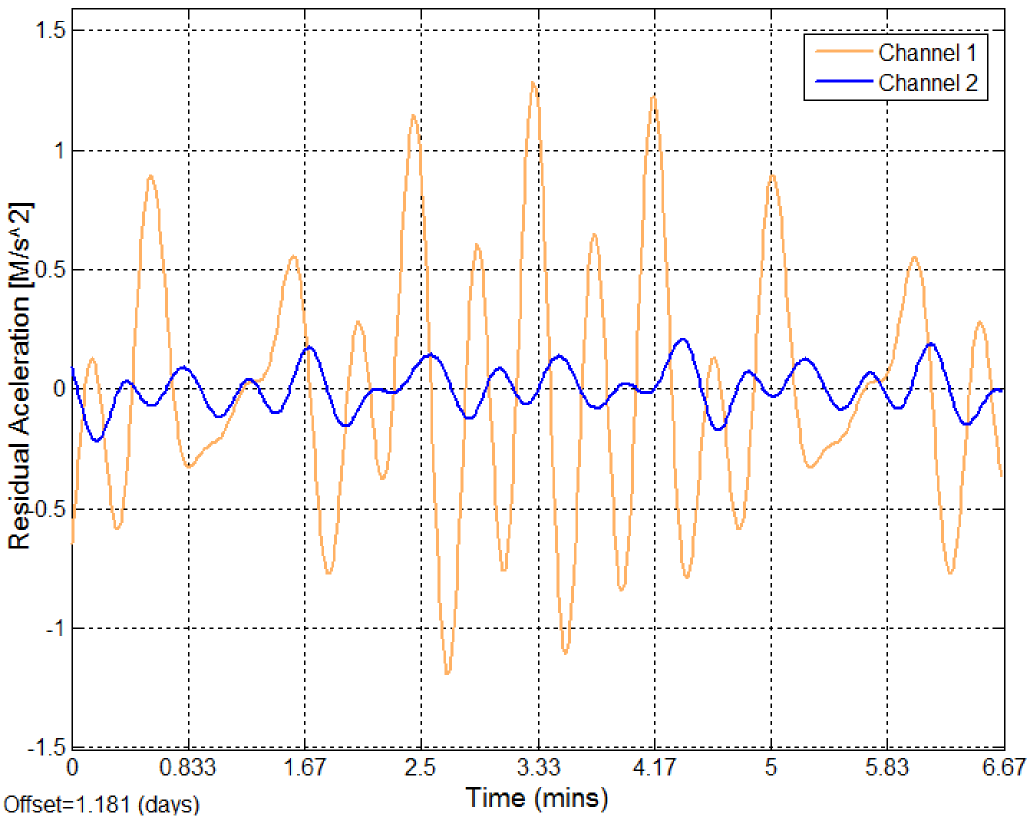

Adaptive Filter using the RLS algorithm with positive feedback for the design of the filter had a reduction of almost 40 dB of its original value when the disturbance is a sum of periodic noise.

But, due to this algorithm to reduce the error of the residual acceleration is simple; the filter cannot anticipate actions to eliminate non-periodical noise. By increasing the data buffer of the filter the error can be minimized. However, in the cost-benefit ratio it is unjustifiable an increased computational cost to increase the filter performance

Adaptive Filters may reject periodic disturbance characteristics of rotating machines, better than the Robust Control, and more widespread because of its SI of the Plant with reasonable computational cost. The noise injected to compare the Adaptive Control is a mixture of 12 sinusoidal signals that emulate different sources of periodic type of disturbance, typical from servo positioning systems. The amplitude of the signals depends on the proximity between the source and the AVC system. Frequencies and the offset between the signals are random, but the frequencies are between a bandwidth of 0 to 150 Hz. The simulation of the AVC rejection is presented in figure 44.

The amplitudes of the frequency response of the Global Primary Path propagation is affected by the frequency response of the plant, according to its form, since the response of the propagation path as the sum of the latter and the disturbing signal is counted.

Figure 44. Disturbance rejection using RLS algorithm Feedforward Compensator Magnitude Response

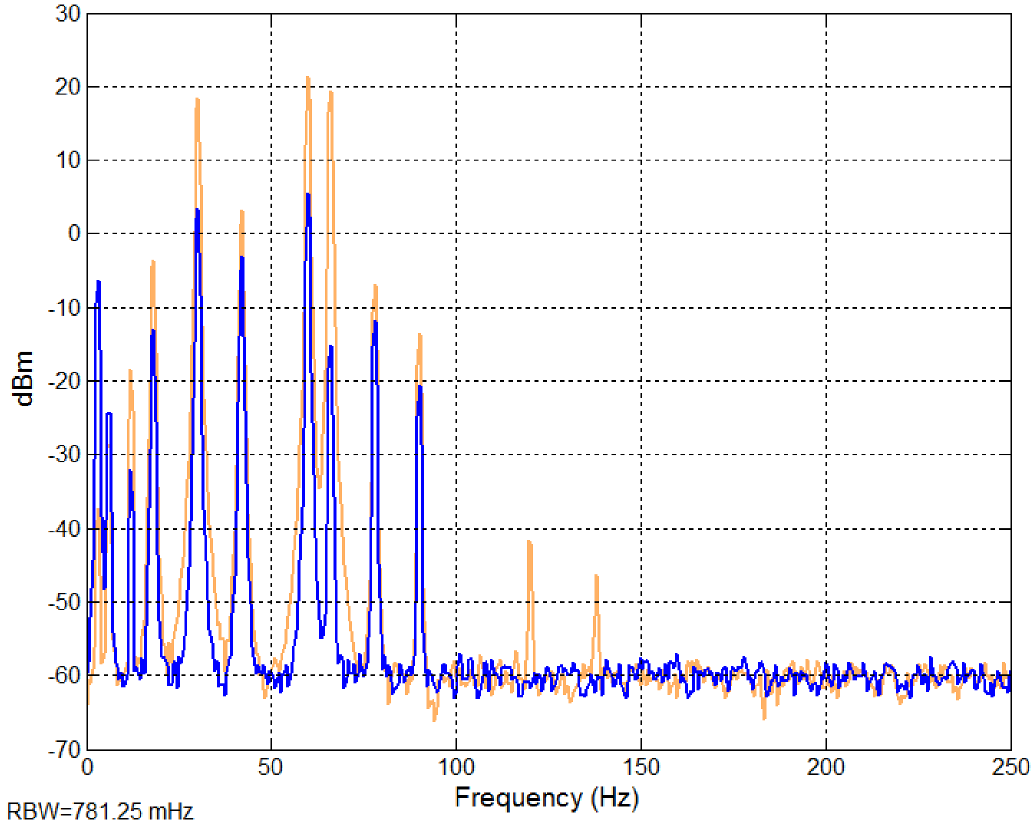

6.2. MIXED-μ ROBUST CONTROLLER

Applied to Active Vibration Control (AVC), Robust Control has its best application for the mixed-mu controller (which allows scaling to give the real and imaginary values separated by the minimization of the computational cost of the controller designed) improving the robustness with the worst possible scenario. The rejection of the disturbance as white noise is performed up to 10% of its original value in the worst case, when the maximum possible control is applied.

Figure 45. Disturbance rejection using Mixed-μ Robust Controller: Frequency response

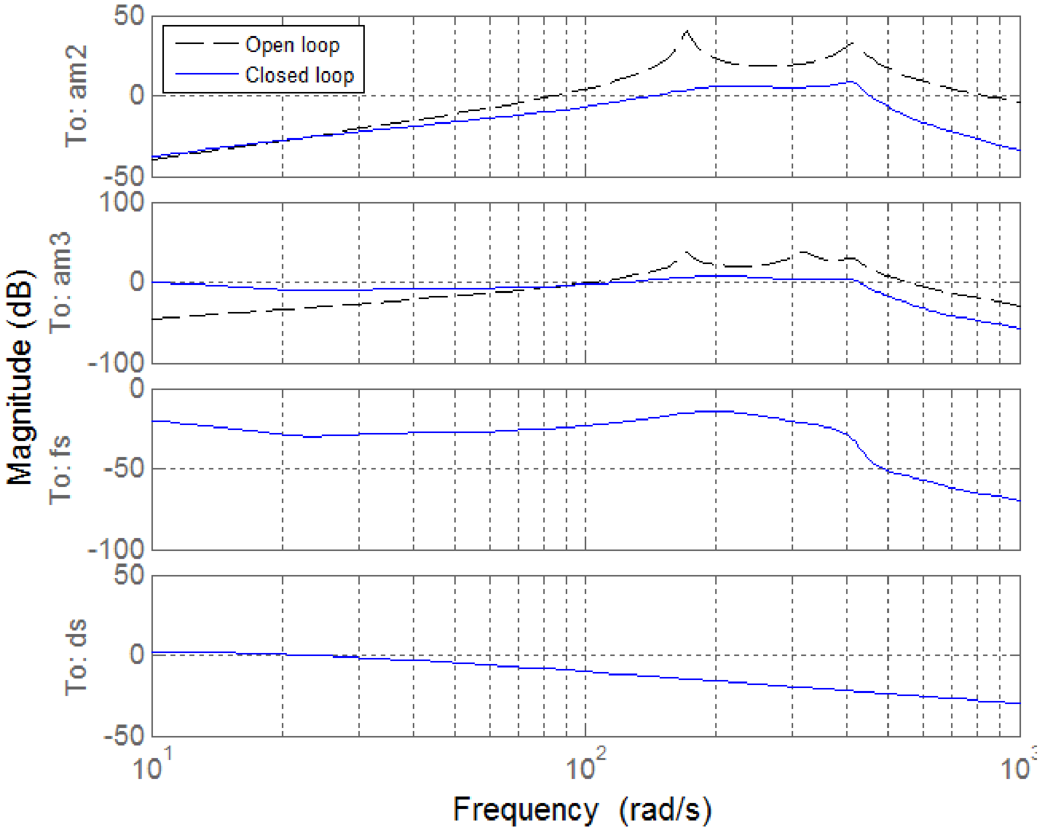

The Robust Controller is capable of reject the unknown disturbance modeled as Pseudo-random white noise, with a robust performance of mu = 0, 85. The resulting controller has a 20 order. The figure 45 shows the resulting controller in action. The disturbance is colored noise applied to the Studied Plant and the closed loop.

Figure 46. Disturbance rejection using Mixed-μ Robust Controller: Residual Acceleration

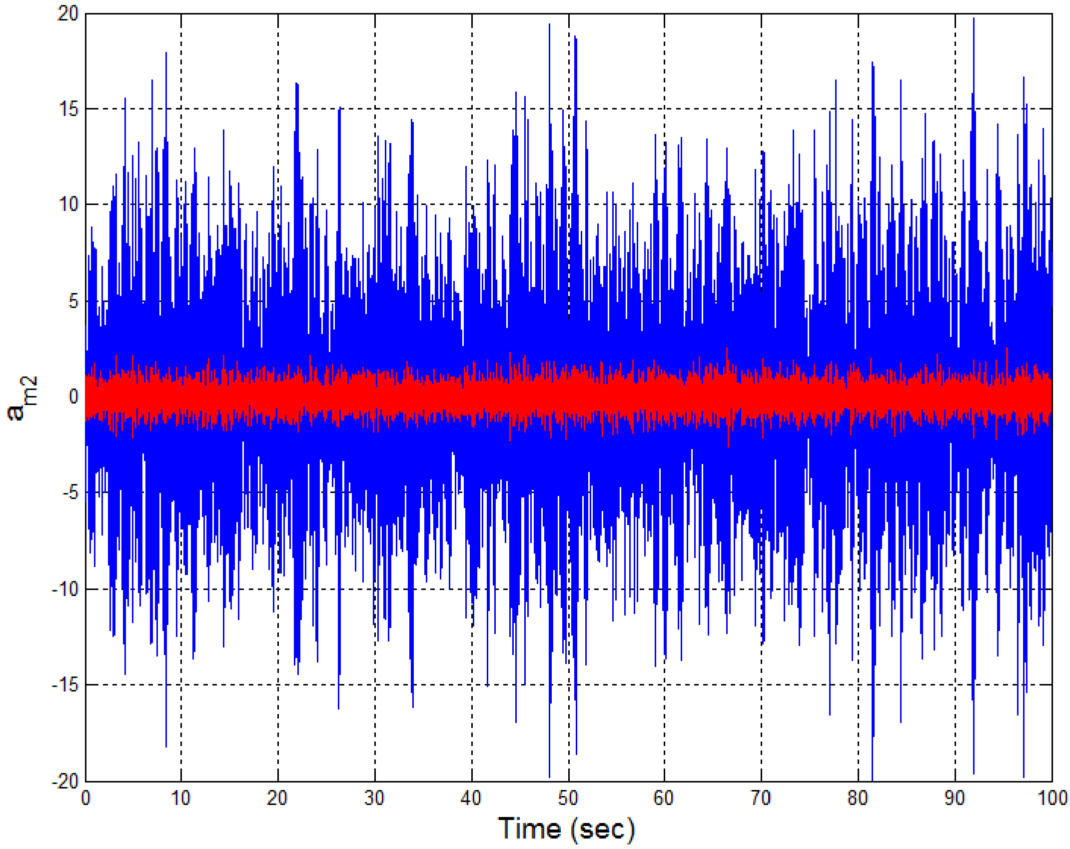

7. CONCLUSIONS

The comparative study between the techniques of control, Robust and Adaptive, took place through applying them to Active Vibration Control (AVC) in the Studied Plant, concluding:

Considering that the bigger and more varied the set of answers to control, much greater must be the capacity for decision making the controller-generalized design, but also increasing their computational cost, becoming a trade-off relationship.

- When the disturbance is a sum of periodic noise, due to its algorithm is simple, the filter cannot anticipate actions to eliminate non-periodic noise. Increasing the data buffer of the filter may help further minimize the error but in the cost benefit-ratio it is unjustifiable an increased computational cost to increase the filter performance.
- The Robust Controller has a better performance by eliminating non-periodic disturbances. Its advantage lies on the ability to model a family of systems with similar dynamic responses within a specified range. While the disturbances do not exceed the range of uncertainties, their performance is greater than the Adaptive Filters. Another advantage is minimizing the computational cost and the use of control.
- SI not only generalizes the answer of the Adaptive AVC problem but also improves the disturbance rejection by making fewer filters to model the plant. By reducing the number of modeler filters, the lower the disturbance

between the measures of the disturbing signal and the image of them. With less disruption of signals is greater the effectiveness of the linear error reduction algorithms.

- From the viewpoint of the applicability of the proposed controller and its possible final output in industry, the best solution to the AVC problem is the mixed mu-Synthesis. Despite having a lower generalization, in respect to the other proposals and due to the extra effort, to study in detail all the possible uncertainties and the need for a good designer criterion for weights of each uncertainty, mu-Synthesis is able to reject non-periodic disturbances much better than the Adaptive Filters.
- On the other hand, the Adaptive Filter is much more general in the solution. The generalization can be increased by augmenting the length of the filter and the ability to recognize disturbances near the dynamic response of the nominal Plant. In general, the proposed solution is able to recognize any type of modified time response with the dynamic response of the Plant that controls. However, the filter does it one at a time between identifications of the system. In addition, you need to implement an SI in the Plant. At the same time, the designer should be very careful not to disturb the image of the disturbance causing the least amount of digital signal processing, which is unlikely to control complex systems.

8 RECOMMENDATIONS

Based on the conclusions, Robust Control can reject non-periodic disturbances within a small range with a reasonable computational cost and the use of Adaptive Filters to model and control the Plant.

Only under the influence of periodic disturbances the following is recommended:

- When making a design of an AVC system, constrain the types of disturbances which the plant will be under control.
- If the designer needs to remove all signs listed in this research, it is recommended to use both controllers in a complementary way to reduce each of the disturbances, by first applying the Robust Controller, the Synthesized Mixed-MU Controller, in closed loop with Feedback, to eliminate non-periodical disturbances and then the Feedforward Adaptive Filter with the RLS algorithm.

.

BIBLIOGRAPHY

[1] AHMAD, M. A., MOHAMED, Z., ISHAK, H. and Nasir A. N. K. Vibration suppression techniques in feedback control of a very flexible robot manipulator. In *Modeling Simulation, AICMS 08. Second Asia International Conference on,* pages 469-474, May 2008.

[2] ALMA, M., LANDAU, I. D., MARTÍNEZ, J.-J. And AIRIMITOAIE, T.-B. Hybrid adaptive feedforward-feedback compensation algorithms for active vibration control systems. In *IEEE Conference on Decision and Control and European Control Conference*, pages 6771-6776. IEEE, Dec. 2011.

[3] ALMA, M., MARTÍNEZ, J.-J., LANDAU, I. D., BUCHE, G. Design and tuning of reduced order h-infinity feedforward compensators for active vibration control. *IEEE Transactions on Control Systems Technology*, 20(2): pages 554-561, March 2012.

[4] AMARA, F. B., KABAMBA, P. T. and ULSOY, A. G. Adaptive sinusoidal disturbance rejection in linear discrete-time systems - part i: Theory. *Journal of Dynamic Systems, Measurement and Control, Transactions of the ASME*, 121(4): pages 648-654, 1999.

[5] AMARA, F. B., KABAMBA, P. T. and ULSOY, A. G. Adaptive sinusoidal disturbance rejection in linear discrete-time systems - part ii: Experiments. *Journal of Dynamic Systems, Measurement and Control, Transactions of the ASME,* 121(4): pages 655-659, 1999.

[6] ARDEKANI, I. T., ABDULLA, W. H. Theoretical framework for stochastic modeling of fxlms-based active noise control dynamics. In *2012 Conference Handbook-Asia-Pacific Signal and Information Processing Association Annual Summit and Conference, APSIPA ASC,* 2012.

[7] ARDEKANI, I. T., ABDULLA, W. H. Stochastic modelling and analysis of filtered-x Least-Mean-Square adaptation algorithm. *IET Signal Processing*, 7(6):pages 486- 496, August 2013.

[8] BALAS, G., CHIANG, R., PACKARD, A., SAFONOV, M. Robust Control Toolbox User's guide. Mathworks Inc., 3 ed. 2005.

[9] BARROS, D., FEKRI, S., ATHANS, M. Robust mixed-mu synthesis performance for mass-spring system with stiffness uncertainty. In *Intelligent Control. Proceedings of the 2005 IEEE International Symposium on, Mediterrean Conference on Control and Automation*, pages 743- 748, June 2005.

[10] BURL, J. B. Linear Optimal Control: H2 and H∞. Addison-Wesley Longman, Inc., 1999.

[11] ELLIOTT, S. J., NELSON, P. A. Active Noise Control. Signal Processing Magazine, IEEE, 10(4): pages 12-35, 1993.

[12] ELLIOTT, S. J. Down with noise [active noise control]. Spectrum, IEEE, 36(6): pages 54-61,Jun 1999.

[13] ELLIOTT, S. J., REX, J. Adaptive algorithms for underdetermined active control problems. *In Acoustics, Speech, and Signal Processing, 1992. ICASSP-92., 1992 IEEE International Conference on*, vol. 2, pages 237-240, Mar 1992.

[14] ELLIOTT, S. J., STOTHERS, I., NELSON, P.A. A multiple error LMS algorithm and its application to the active control of sound and vibration. *Acoustics, Speech and signal Processing, IEEE Transactions on*, 35(10), pages: 1423-1434, Oct 1987.

[15] ELLIOTT, S. J., SUTTON, T.J. Performance of feedforward and feedback systems for active control. *Speech and Audio Processing, IEEE Transactions on*, 4(3), pages: 214-223, May 1996.

[16] FEKRI, S., ATHANS, M., PASCOAL, A. A two-input two-output robust multiple model adaptive control (RMMAC) case study. *In American Control Conference*, pages 8 pp.-, June 2006.

[17] KOUHI, Y:, LABIBI, B., FATEHI, A:, ADLGOSTAR, R. H-infinity and QFT robust control designs for level control plant. In *India Conference. INDICON 2008. Annual IEEE*, vol. 2, pages 388-393, Dec 2008.

[18] KUO, S: M., MORGAN, D. R. Review of DSP algorithms for active noise control. In *IEEE Conference on Control Applications - Proceedings*, vol. 1, pages 243-248, 2000.

[19] KUO, S: M., MORGAN, D. R. Active noise control: a tutorial review. *Proceedings of the IEEE*, 87(6), pages: 943-975, Jun 1999.

[20], LANDAU, I. D., ALMA M., MARTÍNEZ, J.-J., BUCHE, G. Adaptive suppression of multiple time-varying unknown vibrations using an inertial actuator. *IEEE Transactions on Control Systems Technology*, 19(6) pages: 1327-1338, Nov. 2011.

[21] LIU, S.-J., LIU, D.-l., Zhang, J.-q., Zeng, Y. Extraction of fetal electrocardiogram using Recursive Least Squares and Normalized Least Mean Squares algorithms. In *2011 3rd International Conference on Advanced Computer Control*, pages: 333-336. IEEE, Jan. 2011.

[22] MATHWORKS. DSP System Toolbox: User's Guide. 2014.

[23] MOSER, A N. Designing controllers for flexible structures with h-∞ μ-synthesis. Control Systems, IEEE, 13(2), pages: 79-89, April 1993.

[24] TOKHI, M. O., VERES, S. M. Active sound and vibration control: theory and applications. Num. 62. Iet, 2002.

[25] WANG, T., GAN, W.-S. Stochastic analysis of FxLMS-based internal model control feedback active noise control systems. *Signal Processing*, 101, pages: 121-133, Aug. 2014.

ANNEXES

ANNEX A. PROGRAMMING OF THE ROBUST CONTROL

```
% Program to model, to analyze and to control a nominal plant using Robust Control. The nominal plant consists of a flexible structure of 3 masses connected by springs. The mass 1 is disturbed by a pressure wave. The plant is controllable from the mass 3. An inertial actuator is located on the mass 3 to reduce the disturbance on the mass 2 transmitted from the mass 1.

% This program is part of the master in mechanical engineering project by Efrain Guillermo Mariotte Parra; A COMPARATIVE STUDY OF LINEAR TECHNIQUES AVC H-INFINITY AND STRUCTURE ADAPTIVE FILTERS FLEXIBLE ONE DEGREE OF FREEDOM

% Bucaramanga April 14 of 2014
clear all
close all
clc

%% PROBLEM IDENTIFICATION

% Flexible structure of 3 masses conected by springs
% Primary path of the disturbance of one degree of freedom

% System Constant

m1 = 1;            % 1kg
m2 = 1;            % kg
m3 = 1;            % kg

%% Parametric uncertainties modeling

k = ureal('k',2,'range',[1.5,2.5]);

k1 = k;            % N/m
k2 = k;
k3 = k;
k4 = k;

b = ureal('b',0.01,'range',[0.008,0.012]);
b1 = b;
b2 = b;
b3 = b;
b4 = b;

%% Modeling of the uncertainty by the actuators delay.
% delay's model between the actuator's force and the mass 1, the maximum delay is about 0,05 seconds, if the delay isn't considered, the model error will be of exp(-s*tau)-1. This error can be modeled as an uncertainty due to it is missed in the Space-State representation of the Plant. A highpass filter that limited the magnitude of the frequency response of the nominal plant models this delay Wunmod = 2.1*s/(s+40)

Wunmod = 2.1*tf([1 0],[1 40]);
tau = ss(1,'inputdelay',0.05);
bodemag(tau-1,Wunmod,logspace(0,3,200));
title('Multiplicative Time-Delay Error: Actual vs. Bound')
legend('Actual','Bound','Location','NorthWest')
grid on

% Space-State Representation of the nominal plant

A11 = zeros(3,3);
A12 = eye(3,3);
A21 = [-(k1+k2)/m1 k2/m1 0;k2/m2 -(k2+k3)/m2 k3/m2; 0 k3/m3 -(k3+k4)/m3];
A22 = [-(b1+b2)/m1 b2/m1 0;b2/m2 -(b2+b3)/m2 b3/m2; 0 b3/m3 -(b3+b4)/m3];

B1 = zeros(3,2);
B2 = [0 1/m1; 0 0 ; 1/m3 0];

%D11 = [0; 0]; D12 = zeros(2,3); D21 = zeros(2,1); D22 = C1;

A =[A11 A12; A21 A22];
B = [B1;B2];
```

```
C = [0 1 0 0 0 0;
A(5,:);A(6,:)];
D = zeros(3,2); %[D11 D12; D21
D22];

Planta = ss(A,B,C,D);
Planta.statename =
{'x1','x2','x3','v1','v2','v3'};
Planta.outputname =
{'xm2','am2','am3'};

%% Transport delay between the
control force and the
acceleration of the mass 1
addition

deltaT =
ultidyn('deltaT',[1,1],'bound',0
.4);
Planta =
Planta*append(1+deltaT*Wunmod,1)
;
Planta.inputname = {'fs','ds'};
figure
bode(Planta.Nominal(1,1),'r+',Pl
anta(1,1),'b',{0.1,10}); grid on
legend('Nominal Plant','Family
of Plant with
uncertainty','location','southwe
st')
title('Bode Plot for nominal and
20 samples of uncertainties')
%% Poles analysis of the Studied
system
tzero(Planta({'am2'},{'fs'}))
zero(Planta({'xm2'},{'fs'}))
%% Bode diagram of the Plant and
its uncertainties

figure
bodemag(Planta.Nominal({'xm2','a
m2','am3'},'ds'),'r',{0.1,10});
grid on
legend('Perturbation
ds','location','southwest');
title(['Gain from external
disturbance (ds)'...
    'to displasment m2 and Body
aceleration 2 and 3'])

%% Model of the inertial
actuator

ActNom = tf(1,[1/50 1]);
Wunc = makeweight(0.4,2,1.5);
unc =
ultidyn('unc',[1,1],'bound',0.35
,'samplestatedim',5);
Act = ActNom*(1 + Wunc*unc);
Act.inputname = 'u';
Act.outputname = 'fs';

%% Bode diagram of the Actuator
and its uncertainty


 figure

bode(Act,'b',Act.Nominalvalue,'r
o',logspace(-1,3,120));grid on
 title('Nominal and 20 random
actuator models')

%% Normalization of the nominal
plant signals.
% The actuator is penalized by a
factor of 1 at low frequencies
and by a factor of 10 at high
frequencies with a cut frequency
of 100 Hz.

Wu = 15*tf([1 50],[1 500]);
Wu.u = 'u';
Wu.y = 'e1';

% the function to color the
noise, is a first order filter
Wdist
% The disturbance has a pole at
0.25 rad/s

Wdist = tf(0.25, [1 0.25]);
Wdist.u = 'dist'; Wdist.y =
'ds';
bodemag(Wdist,Wu);
grid on

% The target is to reduce the
disturbance on the mass 2 by a
factor of 80 and below the 0.1
rad/s

WP = 1/0.28 * tf([1 0.15],[1
16]);
Wacc3 = 1/70 * tf([1 20],[1
0.15]);
targets = [WP;0;Wacc3];
WP.u = 'am2'; WP.y = 'e2';
Wacc3.u = 'am3'; Wacc3.y = 'e3';

% the controller measures the
displacement of the mass 2 with
the noise of the sensor and
applies the control with the
```

```
force F1, the sensor noise is
modeled as a constant 0.001

wn1 = tf(0.001);
wn1.u = 'noise'; wn1.y= 'nu1';

wn2 = tf(0.05);
wn2.u = 'noise'; wn2.y= 'nu2';

% Closed loop target

figure
bodemag(Planta.NominalValue({'am
2','xm2','am3'},'ds')*Wdist,'b',
targets,'r--',{0.5,10});
grid on
title('Response to disturbance')
legend('Open-loop','Closed-loop
target','location','southwest')

%% Connections between the
nominal plant, the actuator and
the weight matrices

x2meas = sumblk('m1 = am2 +
nu1');
x3meas = sumblk('m2 = am3 +
nu2');

ICinputs = {'dist';'noise';'u'};
ICoutputs =
{'e1';'e2';'e3';'m1';'m2'};
Plantaic=connect(Planta(2:3,:),A
ct,WP,Wacc3,Wu,Wdist,wn1,wn2,...

x2meas,x3meas,ICinputs,ICoutputs
);

get(Plantaic)

%% nominal H-infinity synthesis

ncont = 1;
nmeas = 2;

[K,~,gamma,info]=hinfsyn(Plantai
c,nmeas,ncont);

info %#ok<NOPTS>
gamma  %#ok<NOPTS>

K.u = {'am2','am3'}; K.y = 'u';
CL=connect(Planta.nominal,Act.no
minal,K,Wdist,'dist',{'xm2';'am2
';'am3';'fs'});

figure
bodemag(Planta.Nominal(:,'ds'),'
k:',CL(:,:,1),'b--',{0.5,10});
grid on
legend('Open      loop','Close
loop','location','southwest');
title('Plant deformation');

%% Robust Stability analysis

SIMK                                  =
connect(Planta,Act,K,Wdist,'dist
',{'xm2';'am2';'am3';'fs'});

ropt                                  =
robustperfOptions('Sensitivity',
'off');
[rpcmarg,rpcunc,rpcreport]       =
robustperf(SIMK,ropt);
rpcreport %#ok<NOPTS>

%% Robust Design mu

% Using the D-K iteration to
obtain a robust controller

[Krob,~,RPmuval,dkinfo]          =
dksyn(Plantaic(:,:),nmeas,ncont)
;

% Examination of the mu-
Synthesis controller
size(Krob)
RPmuval %#ok<NOPTS>

%% Closed loop system with the
robust controller connection

Krob.u = {'am2','am3'};
Krob.y = 'u';
SIMKrob                               =
connect(Planta,Act,Krob,Wdist,'d
ist',{'xm2';'am2';'am3';'fs';'ds
'});

ropt                                  =
robustperfOptions('Sensitivity',
'off');

[rpcmargrob,rpcuncrob,rpcreportr
ob] = robustperf(SIMKrob,ropt);
rpcreportrob %#ok<NOPTS>

figure
```

```
bodemag(Planta.Nominal(:,'ds'),'k:',SIMKrob.nominal(:,:,1),'b--',{0.5,10});
grid on
legend('Open loop','Closed loop','location','southwest');
title('Plant deformation');

%% Mixed mu

opt = dksynOptions('MixedMU','on','AutoScalingOrder',[5 6]);
[Km,gm,mu_m]=dksyn(Plantaic,nmeas,ncont,opt);

% mu value when treating k1 as real:
mu_m %#ok<NOPTS>

Km.u = {'am2','am3'}; Km.y = 'u';
clsimKm = connect(Planta,Act,Km,Wdist,'dist',{'xm2','am2','am3','fs','ds'});

figure
bodemag(Planta.Nominal(:,'ds'),'k:',clsimKm.nominal(:,:,1),'b--',{0.1,10});
grid on
legend('Open loop','Closed loop','location','southwest');
title('Plant deformation');

%% Worst case analysis

om = logspace(-1,3,100);
clpKred = ufrd(SIMK,om);
clpKrob = ufrd(SIMKrob,om);
clpKm = ufrd(clsimKm,om);
wopt = wcgainOptions('sensitivity','off');
[maxgainK,badpertK]=
wcgain(clpKred,wopt);
maxgainK %#ok<NOPTS>

[maxgainKrob,badpertKrob]=
wcgain(clpKrob,wopt);
maxgainKrob %#ok<NOPTS>

[maxgainKm,badpertKm]=
wcgain(clpKm,wopt);
maxgainKm %#ok<NOPTS>

%% Disturbance Rejection Simulations

t = 0:.01:100;
dist = randn(size(t));
yKred = lsim(SIMKrob.Nominal,dist,t);
yKm = lsim(clsimKm.Nominal,dist,t);

% Plot
figure
subplot(311)
plot(t,yKred(:,2),'b',t,yKm(:,2),'r')
title('Nominal Disturbance Rejection Response')
ylabel('Xm2')
grid
subplot(312)
plot(t,yKred(:,4),'b',t,yKm(:,4),'r')
ylabel('fs (control)')
legend('Krob','Km','Location','NorthWest')
grid
subplot(313)
plot(t,yKred(:,5),'k')
ylabel('ds (disturbance)')
xlabel('Time (sec)')
grid

%% Worst Case

clsimKrob_wc = usubs(SIMKrob,badpertKrob);
clsimKm_wc = usubs(clsimKm,badpertKm);
yKc_wc = lsim(clsimKrob_wc,dist,t);
yKm_wc = lsim(clsimKm_wc,dist,t);

figure
subplot(211)
plot(t,yKc_wc(:,2),'b',t,yKm_wc(:,2),'r')
title('Worse-Case Disturbance Rejection Response')
ylabel('Xm2')
grid
subplot(212)
plot(t,yKc_wc(:,4),'b',t,yKm_wc(:,4),'r')
ylabel('fs (control)')
legend('Krob','Km','Location','NorthWest')
grid
```

```
%% Controller Simplification

%To create a controller matrix with the reduced order
NS = order(Km);
StateOrders = 1:NS;
Kred = reduce(Km,StateOrders);

% To calculate the performance margin of each reduced controller

CLP = lft(Plantaic(:,:,1),Kred);
%Linear Fractional Transformation Reduce Closed loop
ropt = robustperfOptions('Sensitivity','off','Display','off','Mussv','a');
PM = robustperf(CLP,ropt);

% Comparison between the performance of every reduced controller and the synthetized controller.

%% Graphics order controller vs performance
figure

plot(StateOrders,[PM.LowerBound],'b-o',...
    StateOrders,repmat(1/mu_m,[1 NS]),'r');
title('Robust performance as a function of controller order')
legend('reduced order','Controller MU')
grid on

%% Controller reduced

Krob8 = Kred(:,:,8);

Krob8.u = {'am2','am3'};
Krob8.y = 'u';
CLredK = connect(Planta,Act,Krob8,Wdist,'dist',{'xm2','am2','am3','fs','ds'});

yKred = lsim(CLredK.Nominal,dist,t);

% Plot
figure
subplot(311)
plot(t,yKred(:,2),'b',t,yKm(:,2),'r')
title('Nominal Disturbance Rejection Response')
ylabel('Xm2')
grid
subplot(312)
plot(t,yKred(:,4),'b',t,yKm(:,4),'r')
ylabel('fs (control)')
legend('Krob','Km','Location','NorthWest')
grid
subplot(313)
plot(t,yKred(:,5),'k')
ylabel('ds (disturbance)')
xlabel('Time (sec)')
grid

om = logspace(-1,3,100);
clpKred = ufrd(CLredK,om);
wopt = wcgainOptions('sensitivity','off');
[maxgainKred,badpertKred]= wcgain(clpKred,wopt);
maxgainKred          %#ok<NOPTS>
```

ANNEX B. PROGRAMING OF SYSTEM IDENTIFICATION

ANNEX B1: PROGRAMING OF THE SYSTEM IDENTIFICATION OF THE GLOBAL SECONDARY PATH

```
function [SNLMS,n,dS,yS,eS]= IdentifySP()

clear all
close all
clc

%% PROBLEM IDENTIFICATION

% Flexible Structure of 3 masses connected by mechanical elements (Springs)
% Disturbance secondary Path of one degree of freedom

% System Constants

m1 = 0.1;           % 1kg
m2 = 0.1;           % kg
m3 = 0.1;           % kg

%% Modeling of the parametric uncertainty

k = 5000;
k1 = k;           % N/m
k2 = k;
k3 = k;
k4 = k;

b = 1;
b1 = b;
b2 = b;
b3 = b;
b4 = b;

%% Modeling of the uncertainty due the Actuator's delay
% Model of the delay between actuator force and the mass 1
% maximum delay is about 0.05 seconds.

Wunmod = 2.1*tf([1 0],[1 40]);

% State-Space Representation of the nominal plant

A11 = zeros(3,3);
A12 = eye(3,3);
A21 = [-(k1+k2)/m1 k2/m1 0;k2/m2 -(k2+k3)/m2 k3/m2; 0 k3/m3 -(k3+k4)/m3];
A22 = [-(b1+b2)/m1 b2/m1 0;b2/m2 -(b2+b3)/m2 b3/m2; 0 b3/m3 -(b3+b4)/m3];

B1 = zeros(3,2);
B2 = [0 1/m1; 0 0 ; 1/m3 0];

A =[A11 A12; A21 A22];
B = [B1;B2];
C = [A(5,:);A(4,:)];
D = zeros(2,2);

Planta = ss(A,B,C,D);
Planta.statename={'x1','x2','x3','v1','v2','v3'};
Planta.outputname = {'am2','am1'};
Planta.inputname = {'fs','ds'};

%% Inertial actuator's model

ActNom = tf(100,[1 80]);
Wunc = makeweight(0.50,2,10);
unc=ultidyn('unc',[1,1],'type','gainbound','bound',0.25,'samplestatedim',7);
Act = ActNom*(1 + Wunc*unc);
Act.inputname = 'u';
Act.outputname = 'fs';

%% Noise
wn1 = tf(0.001);
wn1.u = 'noise'; wn1.y= 'nu1';

%% Global secondary Path disturbance propagation

[numS,denS]=ss2tf(Planta.a,Planta.b,Planta.c,Planta.d,1);
S = tf(numS(1,:),denS);
S.y = 'x2s';

% disturbance addition on the global secondary path

deltaT=ultidyn('deltaT',[1,1],'bound',0.25);
S = S*(1+deltaT*Wunmod);
```

```
S.u = 'fs' ;
x1meas = sumblk('m1 = x2s + nu1');

%% Secondary Path interconnection

ICinputs = {'u';'noise'};
ICoutputs = {'m1'};
Secondaryic=connect(S,Act,wn1,x1meas,ICinputs,ICoutputs);
get(Secondaryic)
figure
bodemag(Secondaryic,{0.5 1600});
grid on

%% Secondary Path Identification

Ts = 4;
sigman = 0.0001;
[x2s] = impulse(Secondaryic,Ts);
x2s = x2s(:,1)/norm(x2s(:,1));
figure
plot(x2s);
grid on

ntrS = 30000;
s = randn(ntrS,1); % Synthetic random signal to be played
x2sfir=dsp.FIRFilter('Numerator',x2s.');
dS = step(x2sfir,s) + ... % random signal propagated through secondary path
    sigman*randn(ntrS,1); % measurement noise at the acelerometer

%% Design the Secondary Path Estimate

M = 800;  %900
muGp = 0.3; %1
SEstLMS=dsp.LMSFilter('Method','Normalized LMS','StepSize', muGp,...
    'Length', M);
[yS,eS,SEst] = step(SEstLMS,s,dS);

n = 1:ntrS;
figure
subplot(2,1,1)
plot(n,dS);
grid on
ylabel('Signal value');
legend('Desired Signal');
subplot(2,1,2)
plot(n,yS,n,eS);
xlabel('Number of iterations');
ylabel('Signal value');
title('Secondary Path System Identification Using the NLMS Adaptive Filter');
legend('Output Signal','Error Signal');

%% Accuracy of the secondary path

Fs = 1600;
[N,min]=size(x2s);
t = (1:N)/Fs;
figure
subplot(2,1,1)
plot(t,x2s,'k');
xlabel('Time [sec]');
ylabel('Coefficient value');
title('True Secondary Path Impulse Response');
grid on
subplot(2,1,2)
plot(t(1:M),SEst,'c',t,[x2s(1:M)-SEst(1:M); x2s(M+1:N)],'k');
xlabel('Time [sec]');
ylabel('Coefficient value');
title('Secondary Path Impulse Response Estimation');
legend('Estimated','Error');
grid on

%% Design of the FIR filter

SNLMS=dsp.FIRFilter('Numerator',SEst.');
W = linspace(0,400,800);
fvtool(SNLMS,'Fs',1600,'FrequencyRange','Specify freq. vector',...
    'FrequencyVector',W);

save('Secondary','SNLMS','n','dS','yS','eS');

end
```

ANNEX B2: PROGRAMING OF THE GLOBAL SECONDARY PATH SYSTEM IDENTIFICATION

```
function[PgNLMS,n,dS,yGp,eGp]=
IdentifyGP()

clear all
close all
clc

%% PROBLEM IDENTIFICATION

% Flexible Structure of 3 masses
connected by mechanical elements
(Springs)
% Disturbance secondary Path of
one degree of freedom

% System Constants

m1 = 0.1;               % 1kg
m2 = 0.1;             % kg
m3 = 0.1;               % kg

%% Modeling of the parametric
uncertainty

k = 5000;
k1 = k;             % N/m
k2 = k;
k3 = k;
k4 = k;

b = 1;
b1 = b;
b2 = b;
b3 = b;
b4 = b;

%% Modeling of the uncertainty
due the Actuator's delay
% Model of the delay between
actuator force and the mass 1
% maximum delay is about 0.05
seconds.

Wunmod = 2.1*tf([1 0],[1 40]);

% State-Space Representation of
the nominal plant

A11 = zeros(3,3);
A12 = eye(3,3);
A21 = [-(k1+k2)/m1 k2/m1 0;k2/m2
-(k2+k3)/m2 k3/m2; 0 k3/m3 -
(k3+k4)/m3];
A22 = [-(b1+b2)/m1 b2/m1 0;b2/m2
-(b2+b3)/m2 b3/m2; 0 b3/m3 -
(b3+b4)/m3];

B1 = zeros(3,2);
B2 = [0 1/m1; 0 0 ; 1/m3 0];

A =[A11 A12; A21 A22];
B = [B1;B2];
C = [A(5,:);A(4,:)];
D = zeros(2,2);

Planta = ss(A,B,C,D);
Planta.statename =
{'x1','x2','x3','v1','v2','v3'};
Planta.outputname =
{'am2','am1'};
Planta.inputname = {'fs','ds'};
bodemag(Planta,{1,1600});
grid on

%% Colored noise function is a
first order filter Wdist, the
disturbance has a pole in 0.25
rad/s

Wdist = tf(8, [1 10]);
Wdist.u = 'dist'; Wdist.y =
'ds';

%% Noise
wn1 = tf(0.0005);
wn1.u = 'noise'; wn1.y= 'nu1';

%% Global primary Path
disturbance propagation

[numG,denG] =
ss2tf(Planta.a,Planta.b,Planta.c
,Planta.d,2);
Gp = tf(numG(1,:),denG);
Gp.y = 'x2p';

% disturbance addition on the
global primary path

deltaT =
ultidyn('deltaT',[1,1],'bound',0
.25);
Gp = Gp*(1+deltaT*Wunmod);
Gp.u = 'ds' ;
```

```
x1meas = sumblk('m1 = x2p +
nu1');

%% Primary Path interconnection

ICinputs = {'dist';'noise'};
ICoutputs = {'m1'};
Globalic =
connect(Gp,Wdist,wn1,x1meas,ICin
puts,ICoutputs);
get(Globalic)

bodemag(Globalic,{1,1600})
grid on

%% Primary Path Identification

Ts = 4;
sigman = 0.0001;
[x2p] = impulse(Globalic,Ts);
x2p =x2p(:,1)/norm(x2p(:,1));
ntrS = 30000;
s = 0.015*randn(ntrS,1); %
Synthetic random signal to be
played
Hfir =
dsp.FIRFilter('Numerator',x2p.')
;
dS = step(Hfir,s) + ... % random
signal propagated through
secondary path
    sigman*randn(ntrS,1); %
measurement noise at the
acelerometer

%% Design the primary Path
Estimate

M = 800;  %900
muGp = 0.6; %1
PgEstLMS =
dsp.LMSFilter('Method','Normaliz
ed LMS','StepSize', muGp,...
    'Length', M);
[yGp,eGp,PgEst] =
step(PgEstLMS,s,dS);

figure
n = 1:ntrS;
subplot(2,1,1)
plot(n,dS);
ylabel('Signal value');
legend('Desired Signal');
subplot(2,1,2)
plot(n,yGp,n,eGp);
xlabel('Number of iterations');
ylabel('Signal value');
title('Secondary Identification
Using the NLMS Adaptive
Filter');
legend('Output Signal','Error
Signal');

%% Accuracy of the primary path

Fs = 1600;
[N,min]=size(x2p);
t = (1:N)/Fs;
figure
subplot(2,1,1)
plot(t,x2p,'k');
xlabel('Time [sec]');
ylabel('Coefficient value');
title('True Secondary Path
Impulse Response');
grid on
subplot(2,1,2)
plot(t(1:M),PgEst,'c',t,[x2p(1:M
)-PgEst(1:M); x2p(M+1:N)],'k');
xlabel('Time [sec]');
ylabel('Coefficient value');
title('Secondary Path Impulse
Response Estimation');
legend('Estimated','Error');
grid on

%% Design of the FIR filter

PgNLMS =
dsp.FIRFilter('Numerator',PgEst.
');
W = linspace(0,400,4800);
fvtool(PgNLMS,'Fs',1600,'Frequen
cyRange','Specify freq. vector',
...
    'FrequencyVector',W);

save('GlobalP','PgNLMS','n','dS'
,'yGp','eGp');

end
```

ANNEX B3: PROGRAMING OF FEEDBACK COUPLING SYSTEM IDENTIFICATION

```
function [FCNLMS,n,dS,yFC,eFC] = IdentifyFC()

clear all
close all
clc

%% PROBLEM IDENTIFICATION

% Flexible Structure of 3 masses connected by mechanical elements (Springs)
% Disturbance secondary Path of one degree of freedom

% System Constants

m1 = 0.1;             % 1kg
m2 = 0.1;           % kg
m3 = 0.1;             % kg

%% Modeling of the parametric uncertainty

k = 5000;
k1 = k;           % N/m
k2 = k;
k3 = k;
k4 = k;

b = 1;
b1 = b;
b2 = b;
b3 = b;
b4 = b;

%% Modeling of the uncertainty due the Actuator's delay
% Model of the delay between actuator force and the mass 1
% maximum delay is about 0.05 seconds.

Wunmod = 2.1*tf([1 0],[1 40]);

% State-Space Representation of the nominal plant

A11 = zeros(3,3);
A12 = eye(3,3);
A21 = [-(k1+k2)/m1 k2/m1 0;k2/m2 -(k2+k3)/m2 k3/m2; 0 k3/m3 -(k3+k4)/m3];
A22 = [-(b1+b2)/m1 b2/m1 0;b2/m2 -(b2+b3)/m2 b3/m2; 0 b3/m3 -(b3+b4)/m3];

B1 = zeros(3,2);
B2 = [0 1/m1; 0 0 ; 1/m3 0];

A =[A11 A12; A21 A22];
B = [B1;B2];
C = [A(5,:);A(4,:)];
D = zeros(2,2);

Planta = ss(A,B,C,D);
Planta.statename = {'x1','x2','x3','v1','v2','v3'};
Planta.outputname = {'am2','am1'};
Planta.inputname = {'fs','ds'};

%% Inertial actuator's model

ActNom = tf(100,[1 80]);
Wunc = makeweight(0.50,2,100);
unc = ultidyn('unc',[1,1],'type','gain bound','bound',0.5,'samplestatedim',7);
Act = ActNom*(1 + Wunc*unc);
Act.inputname = 'u';
Act.outputname = 'fs';

%% Noise
wn1 = tf(0.001);
wn1.u = 'noise'; wn1.y= 'nu1';

%% Feedback Coupling Path propagation

[numFc,denFc] = ss2tf(Planta.a,Planta.b,Planta.c,Planta.d,1);
Fc = tf(numFc(2,:),denFc);
Fc.y = 'x1s';

% disturbance addition on the global primary path

deltaT = ultidyn('deltaT',[1,1],'bound',0.1);
Fc = Fc*(1+deltaT*Wunmod);
Fc.u = 'fs' ;
```

```
x1meas = sumblk('m1 = x1s +
nu1');

%% Primary Path interconnection

ICinputs = {'u';'noise'};
ICoutputs = {'m1'};
Reverseic =
connect(Fc,Act,wn1,x1meas,ICinpu
ts,ICoutputs);
get(Reverseic)
bodemag(Reverseic,{1,1600});
grid on

%% Primary Path Identification

Ts = 4;
[x1s] = impulse(Reverseic,Ts);
x1s = x1s(:,1)/norm(x1s(:,1));
figure
plot(x1s);
grid on

ntrS = 30000;
s = 0.015*randn(ntrS,1); %
Synthetic random signal to be
played
x1sfir =
dsp.FIRFilter('Numerator',x1s.')
;
dS = step(x1sfir,s) + ... %
random signal propagated through
secondary path
    0.0001*randn(ntrS,1); %
measurement noise at the
acelerometer

%% Design the Secondary Path
Estimate

M = 800;  %900
muGp = 0.6; %1
FCEstLMS =
dsp.LMSFilter('Method','Normaliz
ed LMS','StepSize', muGp,...
    'Length', M);
[yFC,eFC,FCEst] =
step(FCEstLMS,s,dS);

figure
n = 1:ntrS;
subplot(2,1,1)
plot(n,dS);
grid on
ylabel('Signal value');
legend('Desired Signal')
subplot(2,1,2)
plot(n,yFC,n,eFC);
xlabel('Number of iterations');
ylabel('Signal value');
title('Secondary Identification
Using the NLMS Adaptive
Filter');
legend('Output Signal','Error
Signal');
grid on
%% Accuracy of the secondary
path

Fs = 1600;
[N,min]=size(x1s);
t = (1:N)/Fs;
figure
subplot(2,1,1)
plot(t,x1s,'k');
xlabel('Time [sec]');
ylabel('Coefficient value');
title('True Secondary Path
Impulse Response');
grid on
subplot(2,1,2)
plot(t(1:M),FCEst,'c',t,[x1s(1:M
)-FCEst(1:M); x1s(M+1:N)],'k');
xlabel('Time [sec]');
ylabel('Coefficient value');
title('Secondary Path Impulse
Response Estimation');
legend('Estimated','Error');
grid on

%% Design of the FIR filter

FCNLMS =
dsp.FIRFilter('Numerator',FCEst.
');
W = linspace(0,400,4800);
fvtool(FCNLMS,'Fs',1600,'Frequen
cyRange','Specify freq. vector',
...
    'FrequencyVector',W);
save('Feedback','FCNLMS','n','dS
','yFC','eFC');

end
```

ANNEX C. PROGRAMING OF ADAPTIVE FILTERS

ANNEX C1: PROGRAMMING FOR ADAPTIVE DISTURBANCE REJECTION USING FLMS ALGORITHM

```
clear all
close all
clc

%% Loading Transfer Function of the Disturbance Propagation Paths

load('GlobalP.mat'); % Global Primary path
load('Secondary.mat'); % Global secondary propgation path
load('ds2x1p'); % Image of the disturbance propagation path

%% High pass disturbance filter

delayW = 15;
Flow   = 145; % Lower band-edge: 79 Hz
Fhigh  = 150; % Upper band-edge: 80 Hz
Astop  = 15;  % 10 dB stopband attenuation
Apass  = 5;  % Filter order
N = 160;
fd =1600;

d = fdesign.highpass('Fst,Fp,Ast,Ap',Flow,Fhigh,Astop,Apass,fd);
Hd = design(d, 'cheby2','SystemObject',true);

% Filter noise to generate impulse response
G1 = step(Hd,[zeros(delayW,1); log(0.99*rand(N-delayW,1)+0.01).*...
    sign(randn(N-delayW,1)).*exp(-0.01*(1:N-delayW)')]);
G1 = G1/norm(G1);

% FIR Filter to be used to model primary propagation path
Hfir1 = dsp.FIRFilter('Numerator',G1.');

%% Estimation noise

SigmaN_Sim = 0.001;
sigman = 0.001; accelerometer noise variance

%% Actuator response and secondary path to the disturbance signal

delayW = 6;
N = 1000;

% Filter noise to generate impulse response
Simp = step(SNLMS,[zeros(delayW,1); log(0.99*rand(N-delayW,1)+0.01).*...
    sign(randn(N-delayW,1)).*exp(-0.01*(1:N-delayW)')]);

Simp = Simp/norm(Simp);

ntrS = 30000;
s = randn(ntrS,1); % Synthetic random signal to be played
Shatfir = dsp.FIRFilter('Numerator',Simp.');
x2hats = step(Shatfir,s) + ... % random signal propagated through Global primary path
    SigmaN_Sim*randn(ntrS,1); % measurement noise at the accelerometer

L=900;
Mu = 0.6;
SdigLMS = dsp.LMSFilter('Method','Normalized LMS','StepSize', Mu,...
    'Length', L);
[yShat,eShat,ShatLMS] = step(SdigLMS,s,x2hats);
Shat = dsp.FIRFilter('Numerator',ShatLMS.');

%% adaptive filtered-LMS: reduce noise
```

```
L = 500; %700
MuW = 0.00000025; %0.01
Hfx =
dsp.FilteredXLMSFilter('Length',
L,'StepSize',MuW,...

'SecondaryPathCoefficients',Shat
LMS);


%% Generator of the sinusoidal
signal to create asymptotically
the noise
Fs = 1600;
A = ones(1,24);
F0 = 5; k = 1:24 ; Lk =
length(k);
F = F0*k; phase = randn(1,Lk);
Hsin =
dsp.SineWave('Amplitude',A,'Freq
uency',F,'PhaseOffset',phase,...

'SamplesPerFrame',512,'SampleRat
e',Fs);

Hts =
dsp.TimeScope('TimeSpan',1000,'Y
Limits',...
    [-
0.1,0.1],'NumInputPorts',2,'Posi
tion',[10 10 750 750]
,'ShowGrid',...
    true,'ShowLegend',true);

% Spectrum analyzer to show
original and attenuated noise
Hsa =
dsp.SpectrumAnalyzer('SampleRate
',Fs,'OverlapPercent',80,...

'SpectralAverages',20,'PlotAsTwo
SidedSpectrum',false,...
    'ShowGrid',true);
```

```
%% Simulation of the adaptive
control using Filtered-LMS

for m = 1:200
    s = step(Hsin); % Generate
sine waves with random phase
    x = sum(s,2);   % Generate
synthetic noise by adding all
sine waves
    xp =randn (size(x));
    sign1 = step(Hfir1,xp);
    x2p = step(PgNLMS,xp) + ...
% Propagate noise through
primary path
        sigman*randn(size(x)); %
Add measurement noise
    if m <= 100
        % No noise control for
first 200 iterations
        e = x2p;
        uhat = zeros(size(x));
        y = zeros(size(x));
    else
        % Enable active noise
control after 200 iterations
        x2hats = step(Shat,y);
        uhat = step(WNLMS,xp) +
sigman*randn(size(x));       %+
x2hats;
        [y,e] =
step(Hfx,uhat,x2p);
    end
    step(Hts,x2p,e);   % Show
spectrum of original (Channel 1)
                        % and
attenuated noise (Channel 2)
    step(Hsa,[x2p,e]);  % Show
the spectrum analyzer
end

corrcoef(uhat,x2p)
release(Hts); % Release spectrum
analyzer
```

ANNEX C2: PROGRAMMING FOR ADAPTIVE DISTURBANCE REJECTION USING FEEDBACK FXLMS ALGORITHM

```
clear all
close all
clc

load('GlobalP.mat');
load('Secondary.mat');
```

```
%% Secondary path and inverse
primary path estimation

% Estimation noise
SigmaN_Sim = 0.001;
sigman = 0.001;
```

```
%% Actuator response and secondary path to the disturbance signal

delayW = 6;
N = 1000;
Fs = 1600;

% Filter noise to generate impulse response
Simp = step(SNLMS,[zeros(delayW,1); log(0.99*rand(N-delayW,1)+0.01).*...
    sign(randn(N-delayW,1)).*exp(-0.01*(1:N-delayW)')]);

Simp = Simp/norm(Simp);

ntrS = 30000;
s = randn(ntrS,1); % Synthetic random signal to be played
Shatfir = dsp.FIRFilter('Numerator',Simp.');
x2hats = step(Shatfir,s) + ... % random signal propagated through Global primary path
    SigmaN_Sim*randn(ntrS,1); % measurement noise at the accelerometer

L=900;
Mu = 0.6;
SdigLMS = dsp.LMSFilter('Method','Normalized LMS','StepSize', Mu,...
    'Length', L);
[yShat,eShat,ShatLMS] = step(SdigLMS,s,x2hats);
Shat = dsp.FIRFilter('Numerator',ShatLMS.');

% n = 1:ntrS;
% plot(n,x2hats,n,yShat,n,eShat);
% xlabel('Number of iterations');
% ylabel('Signal value');
% title('Secondary Identification Using the NLMS Adaptive Filter');
% legend('Desired Signal', 'Output Signal', 'Error Signal');
```

```
%% adaptive filtered-LMS: reduce noise

L = 800;
MuW = 0.00000018;
Hfx = dsp.FilteredXLMSFilter('Length', L,'StepSize',MuW,...
    'LeakageFactor',1,'SecondaryPathCoefficients',ShatLMS);

%% Generator of the sinusoidal signal to create asymptotically the noise

Fs = 1600;
A = [0.9 0.8 0.75 0.5 0.4 0.2];
F0 = 5; LA = length(A);
F = [10 15 20 30 50 60] ; phase = randn(1,LA);

Hsin = dsp.SineWave('Amplitude',A,'Frequency',F,'PhaseOffset',phase,...
    'SamplesPerFrame',512,'SampleRate',1600);

Hts = dsp.TimeScope('TimeSpan',500,'YLimits',...
    [-1,1],'NumInputPorts',2,'Position',[1 1 750 750] ,'ShowGrid',...
    true,'ShowLegend',true);

% Spectrum analyzer to show original and attenuated noise
Hsa = dsp.SpectrumAnalyzer('SampleRate',Fs,'OverlapPercent',80,...
    'SpectralAverages',20,'PlotAsTwoSidedSpectrum',false,...
    'ShowGrid',true);

%% Simulation of the adaptive control using Filtered-LMS

for m = 1:200
    s = step(Hsin); % Generate sine waves with random phase
```

```
    x = sum(s,2);     % Generate synthetic noise by adding all sine waves
    %xp = randn(size(x));
    x2 = step(PgNLMS,x) + ... % Propagate noise through primary path
    sigman*randn(size(x));     % Add measurement noise
    if m <= 100
        % No noise control for first 200 iterations
        e = x2;
        y = zeros(size(x));
        x2phat = zeros(size(x));
    else
        % Enable active noise control after 200 iterations
        if m == 101
            x2phat = x2;
        end
            [y,e] = step(Hfx,x2phat,x2);
            x2shat = step(Shat,y);
            x2phat = e - x2shat;
    end
    step(Hts,x2,e);    % Show spectrum of original (Channel 1)
                       % and attenuated noise (Channel 2)
    step(Hsa,[x2,e])
end
corrcoef(x2,x2phat)
release(Hts); % Release spectrum analyzer
```

ANNEX C3: PROGRAMMING FOR ADAPTIVE DISTURBANCE REJECTION USING FEEDFORWARD RLS ALGORITHM WITH FEEDBACK COUPLING

```
clear all
close all
clc

%% Loading Transfer Function of the Disturbance Propaation Paths

load('GlobalP.mat');     % Global Primary Path
load('Secondary.mat');   % Global Secondary propagation path
load('ds2x1p');          % Image of the disturbance propagation path
load('Feedback');        % compensation feedback to the correlation accelerometer propagation path
load('PrimaryPath');     % Primary Path

% Variance of the White noise inherent to the sensor

sigman = 0.001;

%% Generator of the sinusoidal signal to create asymptotically the noise

Fs = 1600;
A = [0.6 0.5 0.45 0.3 0.2 0.1];
F0 = 5; LA = length(A);
F = [10 15 20 30 50 60] ;
phase = randn(1,LA);

Hsin = dsp.SineWave('Amplitude',A,'Frequency',F,'PhaseOffset',phase,...

'SamplesPerFrame',512,'SampleRate',Fs);

%% Setting the RLS filter

M      = 70;                     % Filter order
delta  = 50000000;               % Initial input covariance estimate
P0     = (1/delta)*eye(M,M);     % Initial setting for the P matrix
Hadapt = dsp.RLSFilter(M,'Method','Conventional RLS','ForgettingFactor',1,'InitialInverseCovariance',P0);

Hts = dsp.TimeScope('TimeSpan',1000,'YLimits',...
    [-1,1],'NumInputPorts',2,'Position',[1 1 750 750] ,'ShowGrid',...
    true,'ShowLegend',true);
```

```
% Spectrum analyzer to show original and attenuated noise
Fs = 1600;
Hsa = dsp.SpectrumAnalyzer('SampleRate',Fs,'OverlapPercent',80,...
    'SpectralAverages',20,'PlotAsTwoSidedSpectrum',false,...
    'ShowGrid',true);


for k = 1:200
    s = step(Hsin); % Generate sine waves with random phase
    x = sum(s,2);   % Generate synthetic noise by adding all sine waves

    x2p = step(PgNLMS,x) + ... % Propagate noise through primary path
    sigman*randn(size(x)); % Add measurement noise % Noise

    if k == 1
        x1 = step(WNLMS,x);
        mx1 = x1 + sigman*randn(size(x));
    end
    x2 = step(PNLMS,x1);
    mx2 = x2 + sigman*randn(size(x));

    if k <= 100
        % No noise control for first 100 iterations
        y=zeros(size(x));
        e = x2p;
        x1 = step(WNLMS,x) + step(FCNLMS,y);
        mx1 = x1 + sigman*randn(size(x));
    else
        x1 = step(WNLMS,x) + step(FCNLMS,y);
        mx1 = x1 + sigman*randn(size(x));
        [y,e] = step(Hadapt,mx1,mx2);
        x2s = step(SNLMS,y); % Propagate compensation through secondary path
        e = x2 + x2s;
    end
    step(Hts,x2p,e);
    step(Hsa,[x2p,e]);
end
corrcoef(x1,x2p)
release(Hts)
```